Hydrogeothermal studies in the Albuquerque Basin —a geophysical investigation of ground water flow characteristics

Marshall Reiter

CIRCULAR 211 NEW MEXICO BUREAU OF GEOLOGY AND MINERAL RESOURCES 2003

A DIVISION OF
NEW MEXICO INSTITUTE OF MINING AND TECHNOLOGY

Circular 211

Hydrogeothermal studies in the Albuquerque Basin- a geophysical investigation of ground water flow characteristics

by Marshall Reiter

New Mexico Bureau of Geology and Mineral Resources
New Mexico Institute of Mining and Technology
Socorro, New Mexico 87801

New Mexico Bureau of Geology and Mineral Resources

A Division of New Mexico Institute of Mining and Technology

Socorro 2003

Hydrogeothermal studies in the Albuquerque Basin—a geophysical investigation of ground water flow characteristics

The New Mexico Bureau of Geology and Mineral Resources
A Division of New Mexico Institute of Mining and Technology
801 Leroy Place
Socorro, NM 87801
(505) 835-5410
http://geoinfo.nmt.edu

Project Editor
Nancy Gilson

Layout
Nancy Gilson

Cartography
Sandra Azevedo
Leo Gabaldon

Editorial Assistance
Gina D'Ambrosio
Jane A. Calvert Love

Library of Congress Cataloging-in-Publication
Data Reiter, Marshall.
Hydrogeothermal studies in the Albuquerque Basin : a geophysical investigation of ground water flow characteristics / by Marshall Reiter. p. cm. — (Circular ; 211)
Includes bibliographical references.
ISBN 1-883905-19-2
1. Groundwater flow—New Mexico—Albuquerque Region—Mathematical models. 2. Groundwater—Thermal properties—New Mexico—Albuquerque Region—Measurement. I. New Mexico. Bureau of Geology and Mineral Resources. II. Title. III. Circular (New Mexico. Bureau of Geology and Mineral Resources); 211.
GB1197.7.R47 203
551.49'09789'61—dc22

2003016494

Published by authority of the State of New Mexico, NMSA 1953 Sec. 63-1-4 Printed in the United States of America
First Printing

Cover
Above the Rio Grande in the valley south of Albuquerque, New Mexico, looking northwest from north of the Interstate-25 bridge. The Albuquerque volcanoes are on the right horizon in this morning view; photo ©Adriel Heisey.

Summary

Highly sensitive well logs that measure ground water temperature as a function of depth are an important geophysical tool for discerning ground water flow patterns. This study focuses on temperature data from wells in the Albuquerque Basin, including the Albuquerque metropolitan area. These temperature logs can provide insights that are not otherwise available, including the degree to which faults serve as either conduits for or barriers to ground water flow. Temperature data can also be used to identify (both shallow and deep) zones of ground water movement. From the data presented here the author draws some important conclusions regarding the rate at which water from the mountains to the east of the city recharges the basin aquifers, estimating that it can take hundreds to thousands of years for ground water to move from the Sandia Mountains to the Rio Grande. The study will be of interest to hydrologists and geohydrologists throughout the Southwest.

Table of Contents

Figures

Abstract

High precision temperature logs have been made at 30 sites in the Albuquerque Basin; 27 of these logs are at sites in and near to the Albuquerque metropolitan area. These temperature data were taken in piezometers and wells drilled in the Santa Fe Group aquifer. The purpose of the present study is to compare these temperature logs with solutions for models of subsurface temperature-ground water flow interaction and to estimate certain ground water flow characteristics. Although many uncertainties exist as with any models, these data provide fundamental qualitative characteristics concerning the ground water flow pattern in the area. In the upper alluvial aquifer system beneath the inner valley of the Albuquerque Basin and/or near the river channel there is a shallow flow zone, from near the water table to depths 150 m (492 ft), with a cooling horizontal specific discharge, derived from the river, typically of tens to more than a hundred m/yr. A similar shallow cooling flow component is present in the northeastern and east-central part of the study area, and in the western part of the study area near the inner valley (although the flow is typically a good deal less in magnitude than beneath the inner valley). The cooling component of shallow ground water flow in the areas outside the inner valley is also believed to come ultimately from the Rio Grande and associated irrigation. Temperature data indicate a deeper flow zone occurs in the basin-fill aquifer system at many sites along the inner valley and in the bordering eastern and western mesa areas. Data indicate that the deeper flow can have a warming horizontal-flow component less in magnitude than the shallower flow, and at some sites the warm flow comes from higher elevations where the water table is deeper and warmer. It appears that faults act as both conduits for ground water flow or as seals restricting flow. Small specific discharge estimates indicating warm flow beneath some sites in the west mesa are consistent with the location of faults that are sealed, restricting flow from the Rio Grande. Hydraulic conductivity estimates show a statistical difference in the mean horizontal values between sites in the east and west mesa areas, consistent with both faults acting to slow flow west of the Rio Grande and ancestral Rio Grande sediments deposited under the eastern regions of the study area. Regional recharge to the Rio Grande from the bordering eastern highlands is probably modest, taking hundreds to thousands of years to move from the Sandia Mountains to the Rio Grande. Recharge toward the Rio Grande from the eastern highlands along major drainages and transmissive fault zones is probably important.

Introduction

Precision subsurface temperature measurements have the potential to provide valuable information about ground water flow characteristics in a region. The present study applies this geophysical technique to the basin-fill aquifer system of the Albuquerque Basin. Temperature measurements taken in piezometers can provide hydrogeologic information over the entire depth of the piezometer while discriminating flows in zones almost as thin as the depth measurement interval (e.g., a few meters). The measured temperature vs. depth data (T logs) can provide estimates of both the vertical and horizontal components of specific discharge over a given depth interval. Temperature logs can provide information on the direction of ground water flow, both vertically (upward or downward), and horizontally if a number of sites are available. Where piezometric-surface elevations and horizontal temperature gradients are known, calculations of flow rates and flow directions using temperature data are more certain, and estimates of vertical and horizontal hydraulic conductivity can be made. Of course, because T logs are site specific, the data are related to local hydrogeologic conditions, and therefore data from a number of sites are required to provide regionally significant information. In the present study 30 T logs are presented and analyzed; 27 of these sites are in or near the Albuquerque metropolitan area. The data sites are located in the inner valley of the Albuquerque Basin and in the mesa areas bordering the Rio Grande to the east and to the west. The T logs from these piezometer sites provide valuable information regarding the ground water flow characteristics along the Rio Grande valley in the Albuquerque Basin. Because of the many uncertainties in the data and the limited site coverage, the specific flow characterization of any site is not as realistic as the qualitative patterns seen over the study area.

Background theory

Workers in geothermal studies have long recognized that terrestrial heat flow estimates calculated from measurements of geothermal gradients often varied with depth; such variations were attributed to the disturbing effects of climate change and ground water movement (e.g., Bullard, 1939). Over the past several decades the curvature noted in some temperature logs to depths of a hundred meters or more has been related to surface temperature warming occurring largely in the past century, the effect being more prominent in the northern latitudes (e.g., see Pollack and Chapman, 1993). In the Albuquerque Basin, a temperature log in the vadose zone to depths of approximately 100 m (328 ft) does not indicate surface temperature warming during the past century (Reiter, 1999). Consequently non-linear temperature logs below the water table in the area lead one to suspect the influence of ground water flow, although more data need to be collected to fully appreciate the possibility of climate change in the area. Thermal conductivity variations of rock can cause reciprocal changes in temperature gradients; this will be addressed in the section on procedure.

The movement of ground water along faults, fractures, thin layers, and within boreholes is usually indicated by abrupt changes in the T log (e.g., Birch, 1947; Ramey, 1962; Lewis and Beck, 1977; Drury et al., 1984; Ziagos and Blackwell, 1986). Ground water flow along zones on the order of tens of meters and more in thickness typically results in a rather smooth curvature of the temperature-depth data, deviating from the linear profile that characterizes conduction-only conditions. Figure 1 illustrates the effects that vertical and horizontal ground water flow can have on the subsurface temperature profile. In general, downward ground water flow will produce a concave upward temperature profile because of the cooling effect of the shallower water moving downward, whereas upflow bringing heat from depth will cause the temperature profile to be convex upward (Bredehoeft and Papadopulos, 1965; Mansure and Reiter, 1979). The effects of cooling horizontal flow will also produce a temperature profile concave upward because temperatures over the flow zone are cooled from conduction-only conditions where temperatures at the upper and lower boundaries of the flow zone are constant (McCord et al., 1992). Similarly, the effects of warming horizontal flow will cause the temperature profile to be convex upward, analogous to upward

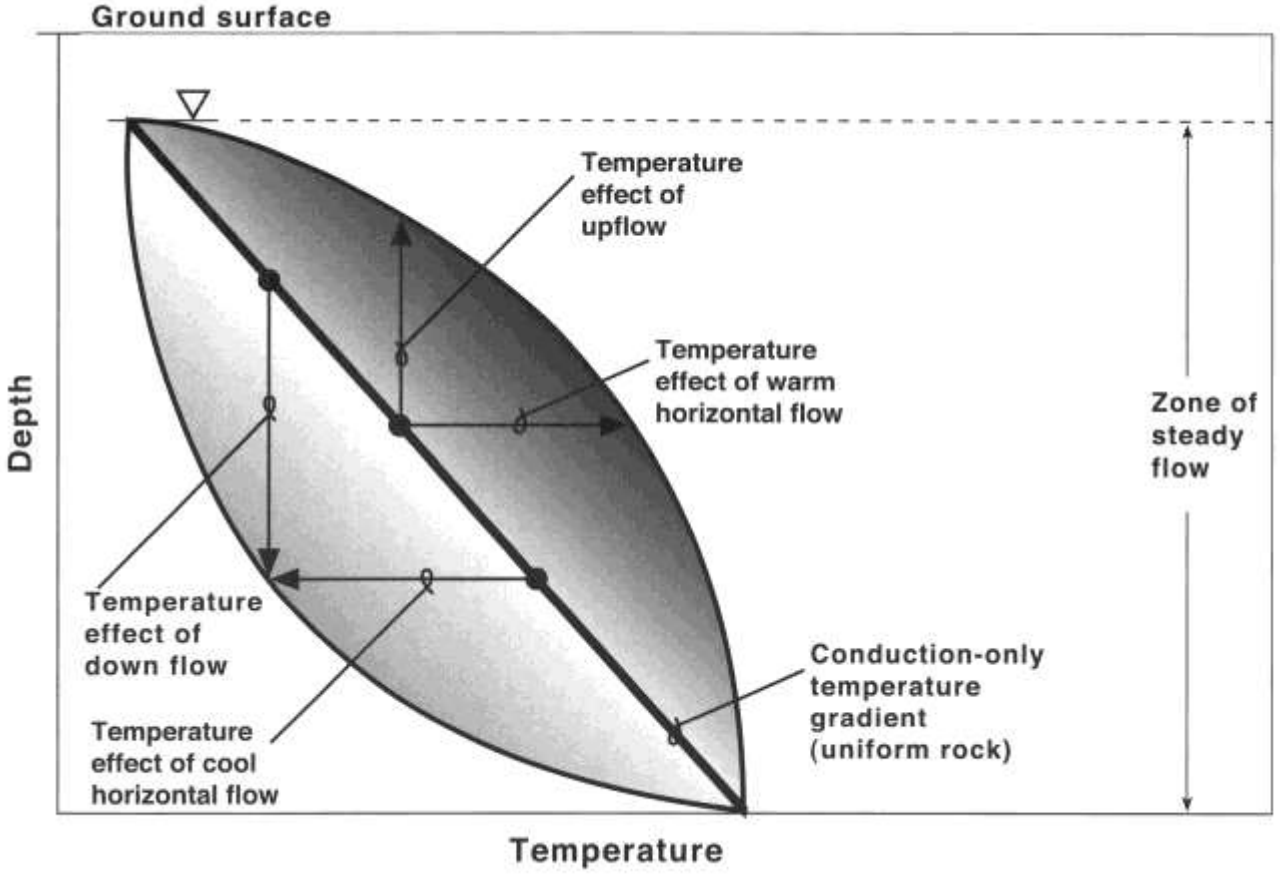

FIGURE 1—Illustration of subsurface temperature effects of steady-state ground water flow across depth interval.

flow. In order to estimate the horizontal and vertical components of ground water flow, the curved surfaces are fitted by expressions representing various models of ground water flow-subsurface temperature interaction, which include the components of ground water flow.

Realizing that subsurface temperature data can provide information on ground water flow, Stallman (1963) uses the general differential equation describing the combined effects of heat conduction and ground water advection to derive a method for estimating the horizontal component of specific discharge. Bredehoeft and Papadopulos (1965) present a solution for estimating the vertical component of specific discharge and suggest that a curve match to site measurements will provide an estimate of the local vertical flow. Mansure and Reiter (1979) show that a plot of the vertical temperature gradient (Tz) vs. temperature can be fitted by a least squares straight line whose slope is related to the vertical component of specific discharge. McCord et al. (1992) show that plots of $_z$ vs. depth can similarly provide estimates of the horizontal component of specific discharge. Lu and Ge (1996) develop a solution for temperature-depth data that couples both the horizontal and vertical flow components of specific discharge. Reiter (2001a) shows that by plotting T_z (vertical temperature gradient) vs. Z (depth) and T (temperature) estimates of both the horizontal and vertical components of specific discharge are possible; quadratic and cubic expressions for temperature vs. depth are also presented for horizontal flow models (quadratic expressions may apply when the statistical fits of the horizontal flow only models to the data are far superior to the other model fits). Reiter (2001a) compares the above techniques for estimating specific discharge in a number of flow intervals for several sites. These techniques are used in the present study to characterize the ground water flow at 30 piezometer sites in the Albuquerque Basin where T logs have been made. It is noted that all of the described solutions for ground water and subsurface temperature interactions are for steady-state conditions. One of the piezometers used in the present study was measured at a six-month interval, another at a four-year interval; both sets of data were without noticeable change. To appreciate longer time dependence, measurements would have to be done over several decades or more; this may be useful in areas where extensive pumping changes water level elevations.

Geologic and hydrogeologic background of the Albuquerque Basin

The piezometers used for the present study are within the Albuquerque Basin (Fig. 2). The Albuquerque Basin is one of the largest and deepest basins along the Rio Grande rift. The basin covers approximately 5,600 km^2 (2,162 mil; Fig. 2) and in places has over 6 km (4 mi) of Tertiary sediments. It is bordered on the east by the Sandia, Manzano, and Los Pinos uplifts, and on the west by the Colorado Plateau. Extensive faulting separates the Albuquerque Basin from the bordering areas; Kelley (1977) presents a tectonic map of the basin showing the fault complexity in the area. More recent geological mapping further details the complex fault structure in the basin (e.g., Hawley and Haase, 1992; Connell, 1997, 1998; Connell et al., 1998a; Maldonado et al., 1999). A gravity map of the area (Keller and Cordell, 1983) shows two large gravity lows in the basin, one in the north and one in the south. Seismic reflection data show extensive syn-rift faulting and support the notion of two subbasins with oppositely dipping beds separated by the Tijeras accommodation zone (Russell and Snelson, 1994). Recent gravity studies in the

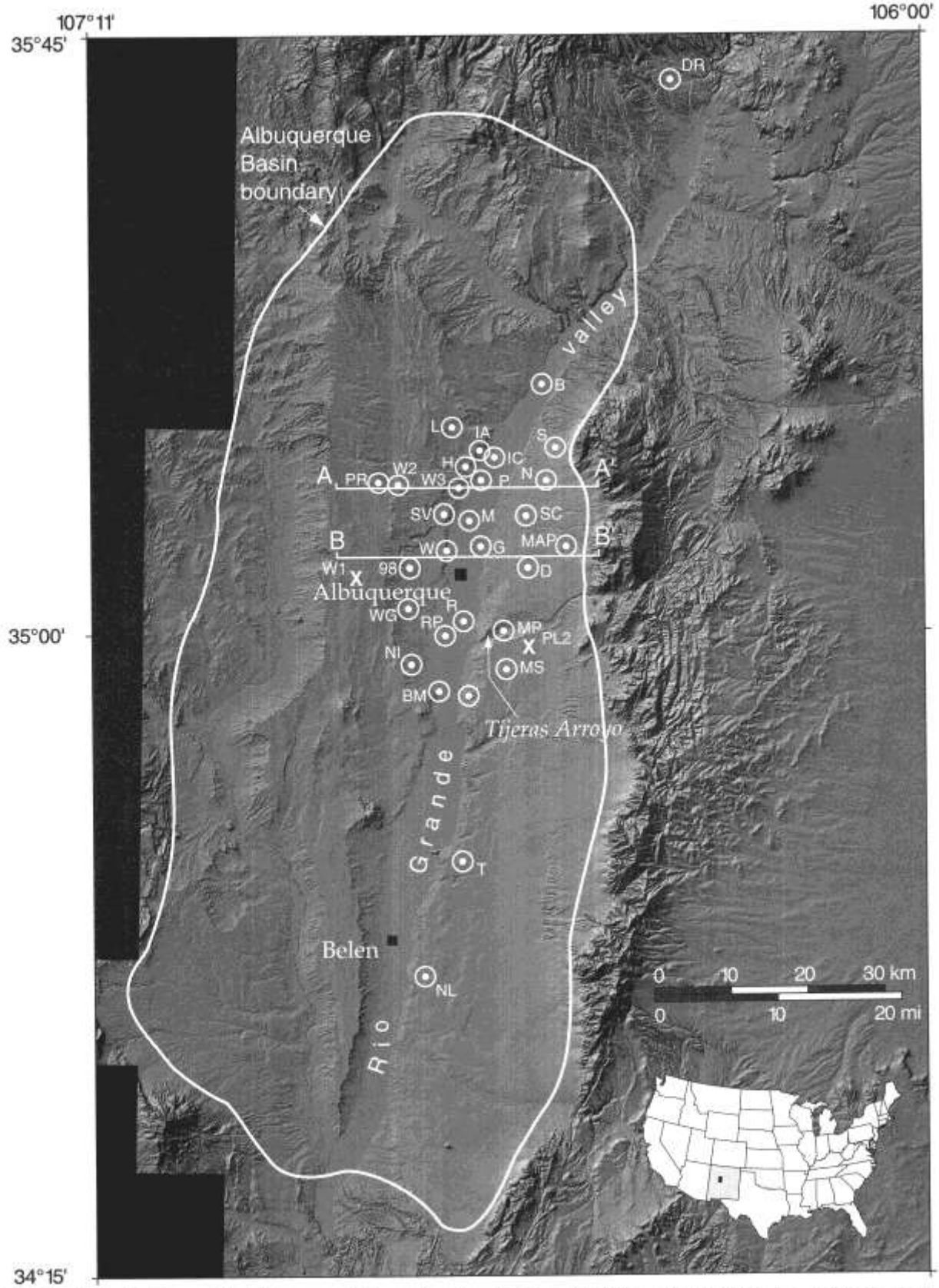

FIGURE 2—Shaded relief map of the Albuquerque Basin and nearby areas. Temperature log sites indicated by ⊙. Sites are: **DR**.—Dome Road, **B**—Bernalillo, **L**—Lincoln Middle School, **IA**—Intel A, **IC**—Intel C, **S**—Sandia Pueblo, **W2**—West Mesa 2, **H**—Hunter Ridge, **PR**—Paradise Road, **W3**—West Mesa 3, **P**—Paseo, **N**—Nor Este, **SV**—Sierra Vista, **M**—Montaño, **SC**—Sister Cities, **98**—98th Street, **WG**—Westgate Heights, **W**—West Bluff, **G**—Garfield Park, **D**—Del Sol Divider, **MAP**—Matheson Park, **RP**—Rio Bravo Park, **R**—Rio Bravo, **NI**—Niese, **MP**—Montesa Park, **BM**—Black Mesa, **I**—Isleta Golf Course, **MS**—Mesa del Sol, **T**—Tomé, **NL**—Nancy Lopez. Other sites used to calculate horizontal temperature gradients indicated by **X**; **W1**—West Mesa 1, **PL2**—Power Line 2. Cross sections **A–A′** and **B–B′** are presented in Figure 8.

Albuquerque Basin suggest a somewhat more complicated picture with several additional subbasins (Grauch et al., 1999). Heat flow data estimated from petroleum bottom hole temperatures indicate that the Albuquerque Basin has intermediate heat flows of about 80 mW /m^2 in the northern part and high heat flows of about 100 mW /m^2 in the southern part approximately coincident with the Tijeras lineament (Reiter et al., 1986).

Hawley et al. (1995) illustrate a hypothetical distribution of lithofacies from the Rio Grande to the eastern uplifts; the lithofacies appear to dip from a few degrees near the eastern boundary to little if any dip in much of the basin floor. Water level data show that water in the alluvial basin aquifer should generally flow from higher bordering eastern areas southwestward toward the Rio Grande, and then southward subparallel to the Rio Grande (Titus, 1961; Bjorklund and Maxwell, 1961; Anderholm, 1988). In addition the present day water elevations are higher along the Rio Grande than in the adjoining areas to the east and west (Connell et al., 1998b). Ground water flow is complicated by variation of hydraulic conductivity both in the varying lithofacies (Hawley et al., 1995) and in the numerous faults that may act as either conduits or seals to ground water flow (e.g., Smith, 1996; Foster and Smith, 1988; Levens et al., 1994; Haneberg, 1995; Reiter, 1999; Sigda et al., 1999).

Recharge to the alluvial basin aquifer occurs along basin margins, arroyo channels, and the Rio Grande. Kernodle et al. (1995) suggest Rio Grande leakage to be a major source of recharge to the alluvial basin aquifer, although more recent estimates from spatial and depth related radiocarbon dates suggest much lower total recharge to the aquifer (Plummer et al., 2000). Subsurface recharge to the alluvial basin aquifer may be limited by basin margin Cretaceous sedimentary rocks and Precambrian crystalline rocks of low permeability to the west and the east of the Albuquerque Basin, respectively (Sawyer, 1999). Estimates of mountain-front recharge along the eastern side of the middle Rio Grande basin are quite variable (Anderholm 1999); estimates of arroyo recharge during spring runoff at Bear Canyon (about 10 km [6 mi] north of Tijeras Arroyo, Fig. 2) vary from 6.6 to 2.6 m /day (22 to 9 ft/day), depending on the year and location in the arroyo (Niswonger and Constantz, 1999). Using temperature measurements from 1 to 15 m (3 to 49 ft) depths at four sites along the Rio Grande, Bartolino and Niswonger (1999) suggest vertically downward flows from the river averaging —2-4 x 10^{-7} m /sec, 6.6-13 x 10^{-7} ft/sec (0.026 m/day; 0.08 ft/day). Chlorofluorocarbons and tritium, which indicate recharge in the past 30-50 yrs, are found in some of the ground water and springs near the basin margins and in the ground water from the upper 60 m (197 ft) of the inner valley (Plummer et al., 1999; see Bexfield and Anderholm, 2000, for location of inner valley in the Albuquerque Basin). The data presented in the present study are related to many of these other investigations.

Procedure

Data acquisition

The temperature data were gathered at sites drilled in the Santa Fe Group aquifer where typically three piezometers were completed at different depths in a single bore hole. The temperature logs were made in the deepest piezometer, which usually had a 1.5-m (5-ft) screen near the bottom. Water level data from these piezometers allowed the vertical flow direction in the thermal models to be constrained and also permitted additional estimates of the horizontal hydraulic gradient between many sites. Unless noted, the method of temperature logging the sites is similar to the continuous logging method described in Reiter et al. (1980). The logging speed in the present study (-6 m/min; —20 ft/min) and the response time of the sensor (-1 sec in water) allow the measured temperature to be depth-representative for present purposes. In stable well zones reproducibility over a period of a week is several thousandths to several hundredths of a degree Kelvin. The absolute accuracy, which is of second order importance to this study, is about several tenths of a degree Kelvin (estimated from ice point calibrations; see also Westgate Heights, Appendix 2-20a). Temperatures are recorded going down the well every meter for continuous logging (or every five meters for the discontinuous logging at the Mesa del Sol site where I waited a few minutes at each depth station). All the data presented are taken in water; T logs begin at 20 m (66 ft) depth (which is below the yearly temperature cycle) or deeper if the water table is deeper.

Comparison of T logs at sites Rio Bravo Park and Mesa del Sol shows no substantial differences over periods of six months to four years and three months (Appendix 2). At present steady-state models are the only analytical solutions available for the analysis of subsurface temperature-ground water flow interaction. Because the thermal response is much slower than the ground water flow response to changing hydraulic conditions and because of the equivalence of time separated data at Rio Bravo Park and Mesa del Sol, it is suggested that the models used are reasonable first order approximations to the thermal regime where data exist.

Data analysis overview

The observational data (T logs) for the sites in the study are tabulated and illustrated in Appendices 1, 2, and 3. Flow zones are typically chosen from the T logs by identifying depth intervals of continuous curvature. Data from these zones are then fitted by several expressions (discussed above) that represent various flow possibilities. In the present study the expressions considered are: 1) exponential and quadratic fits to the temperature data representing only vertical flow (Bredehoeft and Papadopulos, 1965) and only horizontal flow (Reiter, 2001a); 2) the coupled solution for temperatures considering both horizontal and vertical flow components (Lu and Ge, 1996); and 3) the fit to the vertical temperature gradient by Z and T, which also provides estimates of both horizontal and vertical ground water flow components (Reiter, 2001a). The curve matching process is done using commercially available software (TABLE CURVE®, a product of SSOS Inc.). A range of specific discharge is estimated for each flow zone by fitting these possible flow expressions to the data; the resulting values are given in Table 1 of Appendix 1. Fits to the temperature data are typically better statistically than are fits to the vertical temperature gradient data because there are so many more temperature data than gradient data (gradients calculated at 5 m [16 ft] intervals) and because small variations in the temperature measurements will greatly affect the gradient calculations. Good statistical fits to the data can, however, indicate flow directional information that is inconsistent with available hydraulic head data, and therefore the expressions used to fit the data must often be constrained to comply with water level information (Reiter, 2001a). Fits to the temperature data are not considered if they are statistically poorer than the straight line fit as indicated by the F statistic or if they would provide a flow direction contrary to piezometer data. Three-dimensional fits to the gradient data are not considered if the correlation coefficient r^2 is less than 0.8.

The analyses depend upon simplifying assumptions for the model and the hydrogeologic parameters; e.g., the condition of steady-state flow components across a given depth zone (necessary to obtain solutions for specific discharge) is an approximation, as are assumptions of constant specific

heat, water density, and thermal conductivity. Thermal conductivity changes in the rock can cause temperature gradient changes although the resulting gradient change is typically sharp (Reiter et al., 1989) and unlike the smooth temperature curvature characteristic of most ground water flow zones. The thermal conductivity values in the basin alluvial aquifer along the Rio Grande valley do not appear to be significantly depth dependent (Reiter et al., 1986; Wade and Reiter, 1994). Also variations in the geothermal gradient over a flow zone can be a factor of three at some sites in the present study; the only way sediment thermal conductivity could account for such temperature gradient changes is for the porosity and saturation to change by about a factor of three (Woodside and Messmer, 1961) in a uniform and steady manner with depth. The present data are all taken below the water table, and the rock is therefore saturated; it also seems unlikely that the porosity would change uniformly with depth to account for the large (factor of three) gradient changes. Thermal conductivity changes would not account for the negative temperature gradients observed at the top of some cool flow zones, and any phenomena such as compaction with depth increasing thermal conductivity would be inconsistent with higher temperature gradients at the bottom of a cool flow zone. Different conductivity phenomena would be necessary to cause convex upward as opposed to concave upward temperature profiles. The small variations in measured thermal conductivity of the alluvial aquifer system allow the approximation of constant thermal conductivity with depth.

Vertical specific discharge components can be estimated directly from temperatures and/or vertical temperature gradients; however, estimates of horizontal specific discharge components require an estimate of the horizontal temperature gradient (Tx), which is in general difficult to obtain. The model coefficients for horizontal flow involve a linear relation between the horizontal temperature gradient and the horizontal component of specific discharge, the product of these two variables is constant for a given flow zone and model (Reiter, 2001a). Consequently, the smaller the horizontal temperature gradient the larger the calculated horizontal flow for a given model coefficient; if the horizontal temperature gradient is zero, horizontal flow cannot affect in situ temperatures. In the present study, horizontal temperature gradients are typically estimated between wells where flow is likely as indicated by water table contours (Table 1), in a few cases temperature gradients must be estimated between wells where flow seems questionable considering the water table data. If a cooling flow is suggested by the temperature data at a site then another site where cooler temperatures have been measured is sought to estimate the horizontal temperature gradients. The site locations, and therefore ground water flow directions, are chosen to be compatible with water level data when possible. Horizontal temperature gradients between wells are estimated from temperatures at the same depth below the water table in both wells—the depth being the mid-point of the flow zone of interest. To estimate the horizontal temperature gradient at several sites it was necessary to use the data from the Paseo site, where cool temperatures and site location a few tens of meters from the river channel are taken to best represent temperatures at sites along the river (Table 1). Distance to the river for these several sites was approximated along a possible path determined from the water level data map by Bexfield and Anderholm (2000). Although the resulting estimates of horizontal temperature gradients contain many uncertainties they are the only possible estimates that can be made with presently available data coverage. These estimates compare favorably with a generalized horizontal temperature gradient estimate of -3.5×10^{-4} °C/m by Stallman (1963). Horizontal flows are presented in Table 1 using both present estimates of horizontal temperature gradients and the general estimate by Stallman (1963). Typically, horizontal temperature gradients are only a few percent of vertical temperature gradients (Stallman, 1963; present study) and therefore horizontal flow rates must be proportionally larger than vertical flow rates to have similar impact on the T log profile.

Example

In order to demonstrate how the analysis was done in the present study, an example is presented using the T log from the 98th Street site (Fig. 3; Appendix 2-19). This temperature log is chosen as an example because it straightforwardly illustrates a single flow zone over most of the piezometer depth and provides a number of analytical considerations used in the present study. By observing the data one may suggest a rather uniform curvature between depths of 137 m (449 ft) and 396 m (1,299 ft), which suggests a uniform flow condition. The above analysis is applied to this interval. First consider the exponential expression that defines vertical only water flow. Because the log is convex upward (toward the surface), the exponential expression will indicate vertically upward flow, which is, however, contrary to the piezometric data across the interval of interest. Therefore, the exponential solution is discarded in this case. The three-dimensional fit of temperature gradients to depth and temperature yields an r^2 value less than 0.8 and, therefore is also discarded. Both the expressions presented by Lu and Ge (1996) and the quadratic expression for horizontal flow, fit the data in the interval of interest better than a straight line and therefore are included in the analysis (e.g., F statistic for: straight line = 127,747, Lu and Ge (1996) = 793,304, quadratic = 1,987,388). From the coefficients obtained by fitting the expression given by Lu and Ge (1996), constrained to provide downward flow, estimates of the vertical specific discharge are made (Table 1). Likewise from both the expression given by Lu and Ge (1996) and the quadratic, best fit coefficients provide information to estimate horizontal flow; the variability of the resulting estimates is shown in Table 1. The quadratic fit to the data is shown in Figure 3.

At a number of other sites several flow zones are suggested by the temperature data; for example, consider the temperature log at the Bernalillo site (Appendix 2-2). In this log one may notice three different flow zones demonstrating different curvatures in the T log. I've chosen depth zones 20-93 m (66-305 ft), 100-240 m (328-787 ft), and 240-360 m (787-1,181 ft) as having distinctly different T log characteristics and therefore representing different ground water flow regimes. The quantitative analysis of these flow regimes proceeds as discussed above for the example of the 98th Street data.

Presentation of results

Sites in and near the Rio Grande basin inner valley

There are 11 piezometer sites located in the upper alluvial aquifer beneath the Rio Grande basin inner valley or just on the edge of the inner valley and near the river (Fig. 2; Table 1; T logs, Appendices 2 and 3). T logs from these sites typically indicate a shallow zone with relatively large horizontal and vertical components of ground water flow. This shallow zone extends from the water table to depths of from -50 to -150 m (-164 to -492 ft) depending on location. The zone is characterized in many of the T logs by data that are concave upward and /or show a negative temperature-depth gradient at the top of the shallow zone (from Appendix 2-2 to Appendix 2-11). The horizontal component of specific discharge cools the subsurface temperatures as the ground water flows north to south with a horizontal specific dis-

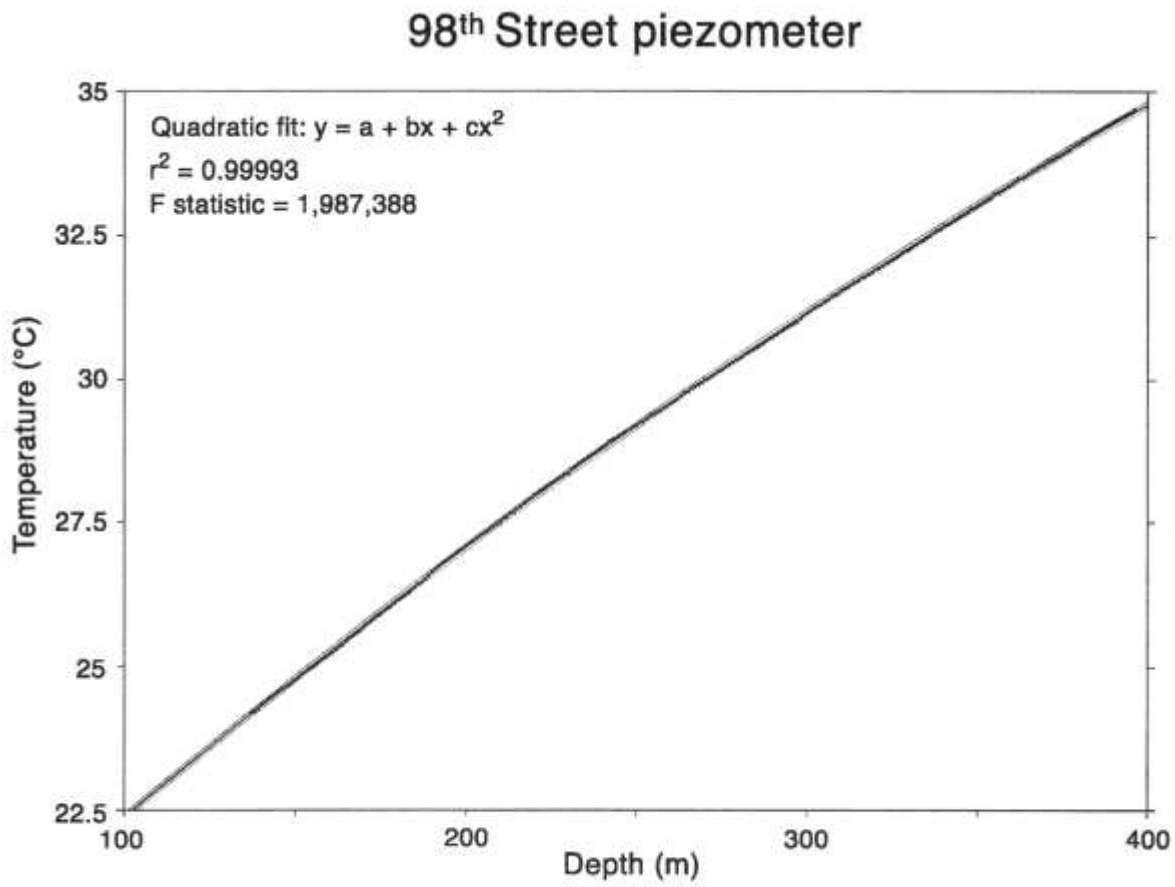

FIGURE 3—Example of temperature data and quadratic fit to data at the 98th Street site. Center line indicates best fit (quadratic); two outside lines indicate 99% confidence.

charge component typically tens of meters per year and sometimes more than a hundred meters per year. The downward vertical component of specific discharge in this shallow zone is generally between 0.02 and 0.50 m/yr (0.07 and 1.6 ft/yr); at a few sites flows of 1-2 m/yr (3-7 ft/yr) downward may be possible. Several notable exceptions to the shallow flow characterization occur just south of 35°N latitude near the southern limits of Albuquerque (Appendix 2-11 and 2-12). Here the shallow flow on the western side of the inner valley is relatively small (V_x <= 8 m/yr 26 ft/yr], V_z -0.07 m/yr [-0.23 ft/yr] ; Black Mesa, Table 1). The flow at a site on the eastern side of the inner valley is quite large but confined to a relatively thin depth zone (e.g., V_x is almost 1,000 m/yr (3,281 ft/yr) between -42 and 50 m (-138 and 164 ft) depth; Isleta Golf Course site, Table 1). The perturbation noticed in the T log at the Isleta Golf Course site might also result from cool ground water moving down a small fault crossing the piezometer.

Below the shallow zone another type of flow occurs at five sites near the river (Bernalillo, Paseo, Montano, West Bluff, and Rio Bravo; Appendix 2-2, 2-4, 2-6, 2-8, and 2-9). This intermediate depth zone appears to be characterized by a warming horizontal flow component with somewhat lower specific discharges than present in the shallow zone (V_x from -4 m/yr to -87 m/yr [-13 ft/yr to -285 ft/yr]; Table 1); the zone extends from the base of the above discussed shallow zone to depths between -130 m and -300 m (427 ft and 984 ft). T logs at other sites in the inner valley, farther away from the river (Intel C, West Mesa 3, Garfield Park, Rio Bravo Park, Black Mesa, and Isleta Golf Course; Appendix 2-3, 2-5, 2-7, 2-10, 2-11, and 2-12) show no indication of a warm horizontal flow component, but instead indicate a cooling horizontal flow component in the intermediate depth zones.

In the deep depth zone of the piezometer at Bernalillo (Appendix 2-2) there is another flow regime characterized by a cooling horizontal flow component (<= 6 m/yr; 20 ft/yr) and a vertically downward flow component (from -0.02 m/yr to 0.03 m/yr [0.06 ft/yr to 0.1 ft/yr]; Table 1). Similar flow characteristics are observed from the T logs in the deep zones at Intel C, West Mesa 3, Garfield Park, and Black Mesa (Table 1; Appendix 2-3, 2-5, 2-7, and 2-11).

Sites west of the Rio Grande inner valley

There are nine piezometer sites west of the inner valley and north of 35°N latitude (Fig. 2). Seven of these piezometers indicate zones of ground water flow with a cooling horizontal flow component and down flow (West Mesa 2, Hunter Ridge, Sierra Vista, Lincoln Middle School, Intel A, Paradise Road, and Niese; Table 1; Appendix 2-13 to 2-18 and 2-21). The horizontal and vertical components of specific discharge are typically less than at sites in the inner valley. T logs from the northwesternmost piezometer (Lincoln Middle School, Appendix 2-16) indicate intervals with cooling horizontal flow components in the upper part of the well. The noticeable cooling perturbation near the screen at -250 m (820 ft) depth may suggest cool ground water flow down a small fault crossing the piezometer as at the Isleta Golf Course site. A modest warming horizontal flow component is suggested over the lower depth interval of the Lincoln Middle School

piezometer (V_x -2 m/yr [-7 ft/yr]; Table 1). The piezometer at the Intel A site shows zones of cooling horizontal flow and downward flow over most of the well depth, with the possibility of a zone of warm horizontal flow near the water table (Table 1; Appendix 2-17). The sites at both 98th Street and Westgate Heights indicate a modest warming horizontal flow component over most of the depth interval below the water table (V_x 11 m/yr 36 ft/yr], $V_{z<=}$ 0.06 m/yr
0.2 ft /yr]; Table 1; Appendix 2-19 and 2-20).

Sites east of the Rio Grande inner valley

All of the piezometers along the eastern side of the Albuquerque Basin, except the Nancy Lopez piezometer site, indicate intervals of ground water flow having a cooling horizontal component at relatively shallow depths below the water table (Table 1; Appendix 2-22 to 2-30). The shallow flow at the eastern sites is from <10 m/yr to >100 m/yr (<33 ft/yr to > 328 ft/yr). Flows <15 m/yr (49 ft/yr) are indicated for the Sister Cities, Matheson Park, Mesa del Sol, and Tome sites over most of the piezometer depth (Table 1). Lesser flow at depth is noticed at the other sites (Sandia Pueblo, Nor Este, Del Sol Divider, and Montesa Park; Table 1). However, at the Sandia Pueblo and Sister Cities sites, noticeable disturbances to the temperature log at deeper depths suggest appreciable flow along faults (Table 1; Appendix 2-22 and 2-24). The deep temperature data along with the water level and hydraulic head information at Sandia Pueblo are interpreted to indicate cool water flow down along a steeply dipping fault that intersects the piezometer at approximately 312 m (1,024 ft). At the Sister Cities site the temperature and hydraulic head data are interpreted to indicate warm flow upward along a zone that intersects the piezometer at 348 m (1,141 ft). Many of the piezometers indicate warm horizontal flow at deeper depths (Nor Este, Del Sol Divider, Matheson Park, Montesa Park, Mesa del Sol, Tome, and Nancy Lopez; Table 1). The data taken at the Montesa Park site initially show a likely disturbance in the deep piezometer probably caused by previous pumping for water samples (compare Appendix 2-27a and 2-27b).

Discussion of specific discharge calculations—relationship to hydrogeology

In the present study (as with most studies) more data would be desirable, especially to estimate the horizontal temperature gradients and the horizontal ground water flow components. Nevertheless, the present data appear to support some interesting interpretations. Figures 4 and 5 indicate general flow directions based on well and piezometer temperature data. If cooling horizontal flow is implied by the temperature log then a cooler well up the hydrologic gradient is sought. In several instances as discussed before (in the data analysis overview) cool temperatures measured at the Paseo piezometer are used at several other sites along the Rio Grande to calculate ground water flow (Intel A and C, Rio Bravo). The flow directions suggested in Figures 4 and 5 are derived from subsurface temperature data and because of the limited number of temperature data sites the flow directions should be viewed as approximations. Flow directions that are incompatible with water table data are indicated with a question mark.

Figure 4 relates to relatively shallow flow approximately 100-150 m (328-492 ft) below the water table. The temperature data at sites within and on the edge of the Albuquerque Basin inner valley, and in the area to the east and northeast of Albuquerque, indicate relatively large values of cooling horizontal flow at shallow depths below the water table in the piezometers (Table 1). Both vertical and horizontal flow are relatively large at the piezometers near the river. This observation is qualitatively consistent with the chlorofluorocarbon and tritium data that indicate ground water recharge in the past 30-50 yrs in the upper 60 m (197 ft) of the inner valley fill (Plummer et al., 1999). From the temperature data it appears that shallow cool flow originates from the Rio Grande as generally shown in Figure 4. The ground water flow at locations east and northeast of Albuquerque may enter the subsurface along the Rio Grande in the northeastern part of the Albuquerque Basin and move southward as shown in Figure 4 (map sites IC to SC to D to MP, and B to S to N). This suggestion is approximately consistent with water table data along flow paths between map sites IC and MP (Titus, 1961; Bexfield and Anderholm, 2000), but there does appear to be some uncertainty between temperature and water table data at map sites N and SC (Fig. 4; to be discussed later). Because there are no temperature data east of map sites B, S, N, and MAP (Fig. 4) potential recharge from the Sandia Mountains cannot be appreciated from subsurface temperatures. Flow from map sites B to S to N is consistent with temperature data but perhaps questionable with regard to water table data. Without data north of map sites PR, W2, and L, in the northwest part of the study area, the flow paths suggested in Figure 4 are similarly ambiguous. The present temperature data shows temperatures typically become cooler going northward and toward the river. The southward flow along the eastern region of the study area appears to be interrupted by or near the Tijeras Arroyo because just to the south of the arroyo the flow is greatly reduced at the Mesa del Sol site. Cooling horizontal flow at sites in the western part of the study area indicates relatively smaller specific discharges compared with sites in the inner valley and in the mesas to the east, possibly due to both faults that are acting to restrict westward flow from the Rio Grande and the more conductive sediments in the Ancestral Rio Grande depositional channel present in the eastern part of the Albuquerque Basin (Hawley et al., 1995). The shallow warm flow noticed on the west mesa at three sites is compatible with ground water contours at West Bluff and Westgate Heights, but not at 98th Street (Fig. 4). This implies that flow to 98th Street has an eastward component or that there is a heat source north or northeast of the 98th Street site.

Figure 5 shows ground water flow directions determined from temperature data, as discussed above, for depth zones typically deeper than 100-150 m (328-492 ft) below the water table. The warming horizontal flow component observed below the shallow flow in the temperature data at some of the piezometers suggests flow zones having a source or path different from zones where cool horizontal flow is implied (compare Figs. 4 and 5). The warming flow zones generally occur at intermediate or deep depths with specific discharges less than those in the shallower, cooling flow zones. Warming trends observed at Paseo, Montano and Del Sol Divider are consistent with warm water moving southwestward from higher elevations to the east (Fig. 5). At Rio Bravo the ground water may be moving southward from West Bluff. Warm flow from 98th Street to Westgate Heights is consistent with water table contours as mentioned above, but the warming noticed at 98th Street and West Bluff may indicate flow with an eastward component or heat sources north of the sites. Subsurface temperatures at a given depth below the water table will generally be greater in the higher eastern and western regions of the basin than in or near the inner valley largely because the depth to the water table is greater at the higher elevations. Some recharge from the east along the Albuquerque Basin is reasonable in terms of the water table slope (Titus, 1961; Bexfield and Anderholm, 2000); however, the temperature data are not deep enough or extensive enough to preclude the possibility of deeper warm water moving upward and horizontally. The warm flows to

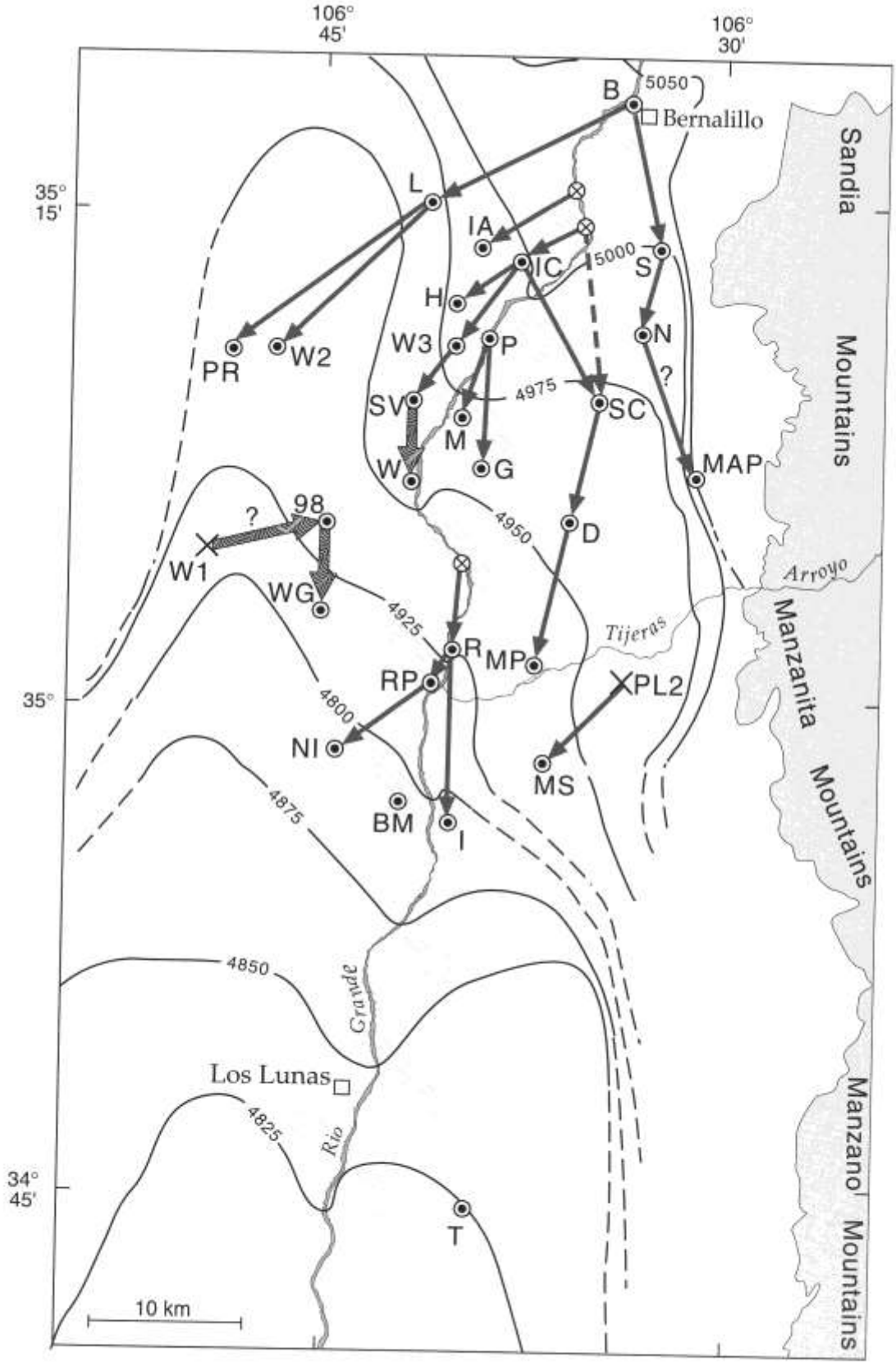

FIGURE 4—Shallow ground water flow directions compatible with temperature measurements at sites in study. Base map and water level contours (ft) from Bexfield and Anderholm (2000). Question mark indicates incompatibility with water contours. Broad arrows indicate warming flow, thin arrows indicate cooling flow, dashed arrow indicates alternative flow path. Piezometer and other sites indicated as in Figure 2; ⊗ indicates sites on Rio Grande where Paseo temperatures were used to calculate horizontal temperature gradients for Intel A, Intel C, and Rio Bravo. Hachured region shows inner valley.

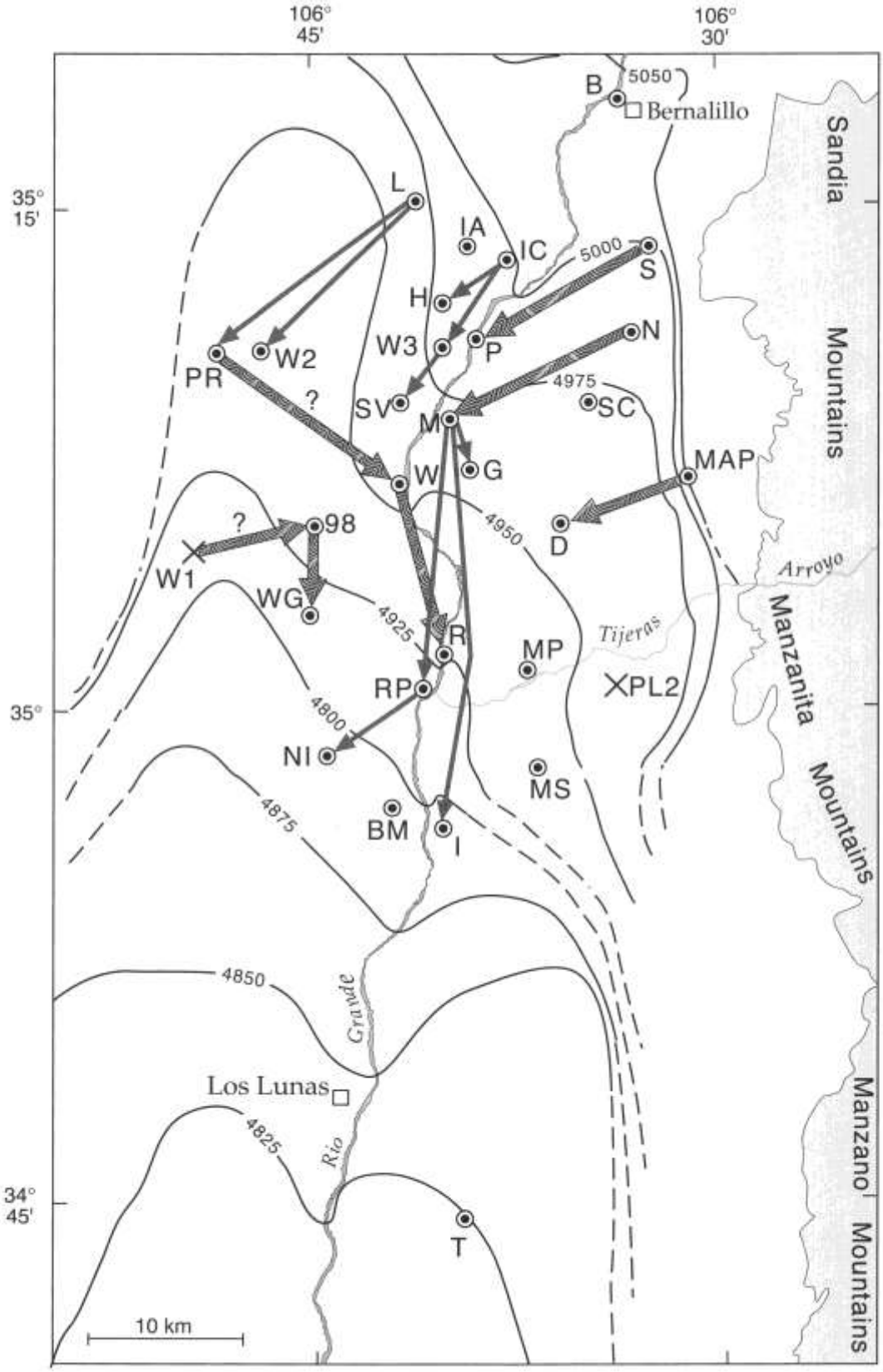

FIGURE 5—Deep ground water flow directions compatible with temperature measurements. Base map and water level contours (ft) from Bexfield and Anderholm (2000). Question marks indicate incompatibility with water contours. Broad arrows indicate warming flow, thin arrows indicate cooling flow. Piezometer and other sites indicated as in Figure 2. Hachured region shows inner valley.

Paseo and Montano from the east mesa are 4-10 m/yr (13-33 ft/yr); at Del Sol Divider approximately 25 m/yr (82 ft/yr). At these rates recharge from the Sandia Mountains would take hundreds to thousands of years to reach the Rio Grande. This relatively small estimated recharge is consistent with the suggestions of Sawyer (1999).

Many of the faults along the eastern margin of the Albuquerque Basin are likely sealed and therefore resistive to ground water flow (Haneberg, 1995; Reiter, 1999); however, at one location where major faults intersect, water seems to flow across fault boundaries (Reiter, 1999). In the present study, a similar situation seems to occur at the Sandia Pueblo site, where largely downward vertical flow is interpreted to occur along a steeply dipping fault crossing the piezometer at approximately 312 m (1,024 ft) depth. This suggestion is consistent with gravity data indicating a large, high angle fault surfacing several hundred meters east of the piezometer (Grauch et al., 1999). The T logs at Nor Este and Sister Cities are also suggestive of a ground water flow zone at approximately 200 m (656 ft) and 350 m (1,148 ft) depth, respectively; warm upward flow is implied from the piezometric data (Appendix 2-23, 2-24). Temperature data from a site at the edge of the inner valley in the northwestern region of the study area also indicate relatively large downward vertical specific discharge estimates; this site is also near probable major faults as indicated on the gravity map of Grauch et al. (1999) (Intel A; Table 1, Appendix 1; Appendix 2-17). From the temperature derived specific discharge estimates at Paseo, Montano, and Del Sol Divider, it appears that recharge to the basin alluvial aquifer from surrounding highlands is modest, possibly occurring with important input along major drainages in the area and across a few locations where faults are transmissive.

The T logs also relate with hydrogeologic studies in the area where faults have been suggested. The background map for Figure 6 is after maps by Hawley and Haase (1992), Connell (1998), Connell et al. (1998a), and Maldonado et al. (1999). Sites west of the Rio Grande but generally east of the fault locations suggested in Figure 6 (H-Hunter's Ridge, W3-West Mesa 3, SV-Sierra Vista and W-West Bluff) indicate cooling ground water flow from the river. Lower horizontal specific discharges estimated at the Sierra Vista and Hunters Ridge sites probably indicate lower hydraulic conductivity sediments. Sites west of the proposed faults in Figure 6 (98-98th Street and WG-Westgate Heights) show a warming ground water flow that implies cool flow from the Rio Grande is not reaching these sites. The Niese site (NI) is located on a proposed fault trace—cool ground water flow from the Rio Grande is suggested at this site. As mentioned previously faults can act as conduits or barriers to ground water flow, and there are several locations in the study area discussed above where temperature data are interpreted to suggest ground water flow along fault zones. The temperature data west of the Rio Grande would complement the fault locations in Figure 6, presuming the faults are acting as ground water flow barriers. Rawling et al. (2001) discuss the Sand Hills fault on the west mesa suggesting that large displacements in poorly lithified sediments may result in zones that greatly restrict ground water flow.

To the east of the Rio Grande the temperature data suggest ground water flow is not occurring from Nor Este to Sister Cities as may be interpreted from water table contours (Figs. 4 and 5). The fault suggested in Figure 6 between the sites may be present and acting as a barrier to ground water flow.

In the southern edge of the Albuquerque metropolitan area it appears that the flow or specific discharge is rather small along the western part of the inner valley at the Black Mesa site (Table 1; Appendix 2-11; V_x 8 m/yr 26 ft/yr) over the well depth). The small ground water flows at Black Mesa may be the result of damming by relatively impermeable dikes that fed the Pliocene basalt flows presently on the surface just a few hundred meters south of the site. Poorly transmissive faults between the site and the Rio Grande, and sediments with lower hydraulic conductivity than sediments to the east, may also cause reduced flow rates. The southward flow at this latitude appears to occur preferentially to the east of Black Mesa; e.g., data at the Isleta Golf Course site indicate appreciable flow at shallow depth along a thin depth interval (Table 1; Appendix 2-12). The southernmost piezometers in the study area (the Tome and Nancy Lopez sites, Fig. 2) are along the eastern bench bordering the Rio Grande inner valley in the southern part of the Albuquerque Basin. The temperature data at Tome indicate a cooling flow probably derived from the Rio Grande over the upper part of the piezometer, and a warming flow across deeper depths in the piezometer perhaps derived from the higher elevation areas where the water table is deeper and warmer (Table 1; Appendix 2-29). Temperature data at Nancy Lopez indicate a warming flow over most of the piezometer depth, which suggests a heat source to the north or flow from higher areas to the east where the water table is deeper and water temperatures are warmer (Table 1; Appendix 2-30; Fig. 2).

Vertical and horizontal hydraulic conductivity estimates

Table 2 (Appendix 1) presents the results of vertical and horizontal hydraulic conductivity estimates of the Santa Fe Group aquifer at most of the piezometer sites in the present study. The values are calculated from vertical and horizontal specific discharge estimates and hydraulic gradients based on piezometric information and/or water level contours using Darcy's Law (Tables 1 and 2; Bexfield and Anderholm, 2000). Vertical hydraulic gradients across a flow zone are estimated using water level information at the site from appropriate screened intervals. When possible horizontal hydraulic gradients are estimated between two appropriate piezometers from water levels representing approximately the same depth below the water table at each site (water levels are in winter months when possible). When such estimates are not possible, water table contours are used to calculate the hydraulic gradient; however, there is uncertainty that these data are valid for zones in the aquifer appreciably below the zone of saturation. Recognizing these uncertainties, at sites where both types of horizontal hydraulic gradient estimates are made, the resulting estimates of horizontal hydraulic conductivity are within a factor of about two to three in all cases except West Mesa 2 (Table 2). The conductivities represent values for the chosen flow zones (Table 1). The values are appropriate for the scale of the flow zone, for K_z a few tens to a hundred or so meters, and for K_x the distance between piezometers, 5-10 km (3-6 mi; Table 2).

Figure 7 shows plots of K_x and K_z (this study) separated regionally; i.e., the Rio Grande inner valley, the west region or mesa, and the east region or mesa, as well as according to depth; i.e., intervals beginning above or below 100 m (328 ft) depth. The only data sets that show statistical differences are: the shallow Rio Grande vs. deep Rio Grande K_x^2 sets, and the deep west mesa vs. the deep east mesa K_x^2 sets (probably of difference >90%, student t test). It is noted that few shallow data exist for the west mesa and east mesa. The difference between shallow and deep horizontal hydraulic conductivities along the Rio Grande inner valley might be expected because of compaction and different rock types (Connell et al., 1998b). The difference between deep horizontal hydraulic conductivities in the east and west mesas may

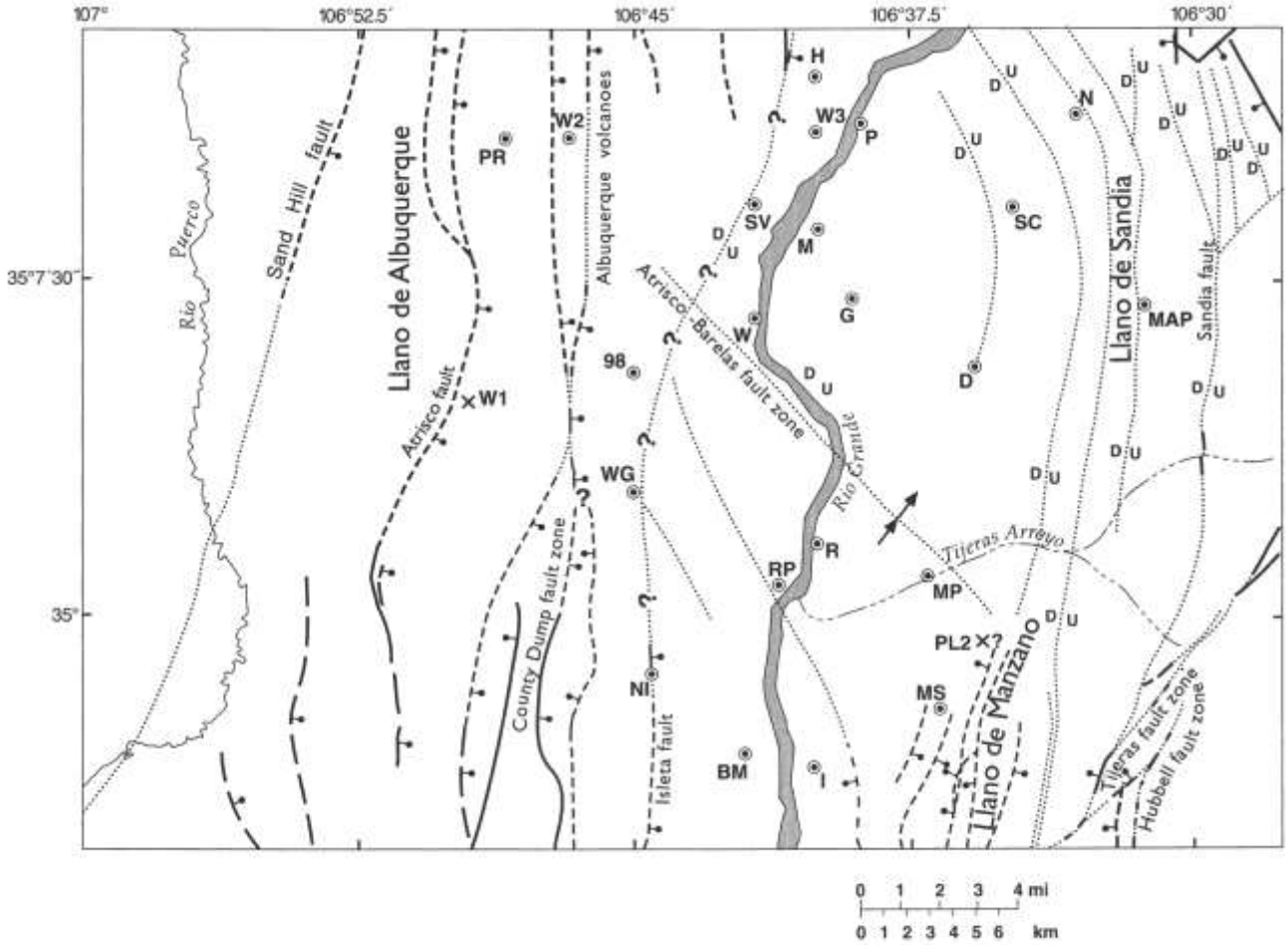

FIGURE 6—Temperature-measured piezometer and well sites (as in Fig. 2) on base map showing proposed faults in the Albuquerque area (from Hawley and Haase, 1992; Connell, 1998; Connell et al., 1998a; Maldonado et al., 1999).

reflect the distribution of poorly transmissive faults preferentially west of the Rio Grande limiting ground water flow and the presence of more conductive ancient Rio Grande deposits along the eastern side of the study area (Hawley et al., 1995). If this is the case, the flow patterns observed in the Albuquerque Basin are significantly influenced by both structural features and sediment deposition.

Also presented in Table 2 are hydraulic conductivity values estimated from air-pressurized slug tests (Thomas and Thorn, 2000). There are 12 zones at eight piezometer sites where hydraulic conductivities were estimated using both temperature methods given in the present study and slug tests. From these data (Table 2) it is noted that across five zones the different estimates agree to within a factor of two to three; across five zones the temperature method yields hydraulic conductivity values approximately an order of magnitude greater than the slug test values; and across two zones the temperature method provides values about an order of magnitude less than the slug test values. Differences in these estimates probably result because of different scales, different measurement dimensionality, and uncertainties in estimating horizontal specific discharges and horizontal temperature gradients.

At 14 sites horizontal hydraulic conductivities across 16 zones are estimated to be of the order of 10^{-3} m/sec in the present study; a thin zone at the Isleta Golf Course site is estimated to have a horizontal hydraulic conductivity of about 10^{-2} m/sec. At two sites (Isleta Golf Course and Lincoln Middle School) the high conductivity zones are very thin and likely represent thin flow channels not characteristic of large depth intervals. The other sites are all along the inner valley or along the flow channel suggested in the eastern part of the study area. Alternatively, aquifer tests suggest the largest horizontal hydraulic conductivity values are approximately 3.5 x 10^{-4} m/sec (-100 ft/day). Such differences appear in other studies; e.g., horizontal hydraulic conductivities estimated from temperature analysis in the San Juan Basin are several orders of magnitude greater than conductivity values obtained from deep and shallow aquifer pumping tests (McCord et al., 1992). The difference between the conductivity estimates of the two techniques has not been investigated but probably results because of differences in scale, direction of measurement, and lithologic inhomogenity and anisotropy. Temperature derived horizontal conductivities in this study are of the order of 5-10 km and therefore likely incorporate many paths of higher conductivity. The temperature derived estimates apply to only one direction, which for the higher values (10^{-3} m/sec) is approximately parallel to the direction of Rio Grande deposition (Davis et al., 1993, have shown there is a two dimensional anisotropy in deposition of Ancestral Rio Grande deposits). Aquifer testing is likely to include the horizontal anisotropy due to depositional processes as well as the vertical anisotropy shown in the present study (vertical hydraulic conductivities being two to four orders of magnitude less than horizontal hydraulic conductivities). Although there are uncertainties in the horizontal conductivity estimates made in the present study, high values associated with directional flow down the Rio Grande depositional channels is qualitatively reasonable.

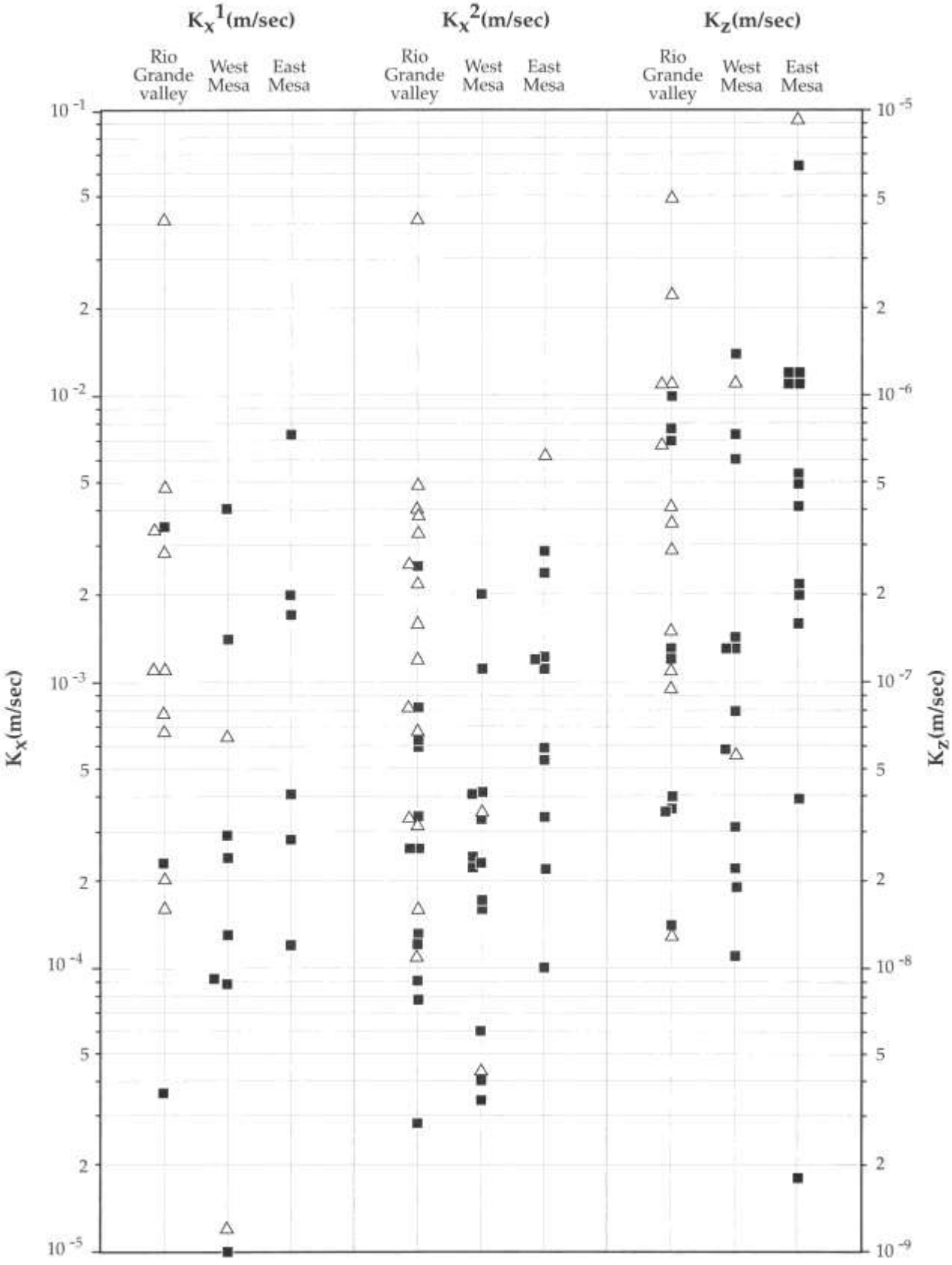

FIGURE 7—Hydraulic conductivities of sediments in the Albuquerque area. Data separated by area and depth interval (beginning at depths greater (■) than or less (Δ) than 100 m). K_x^1 and K_x^2 as in Table 2, Appendix 1.

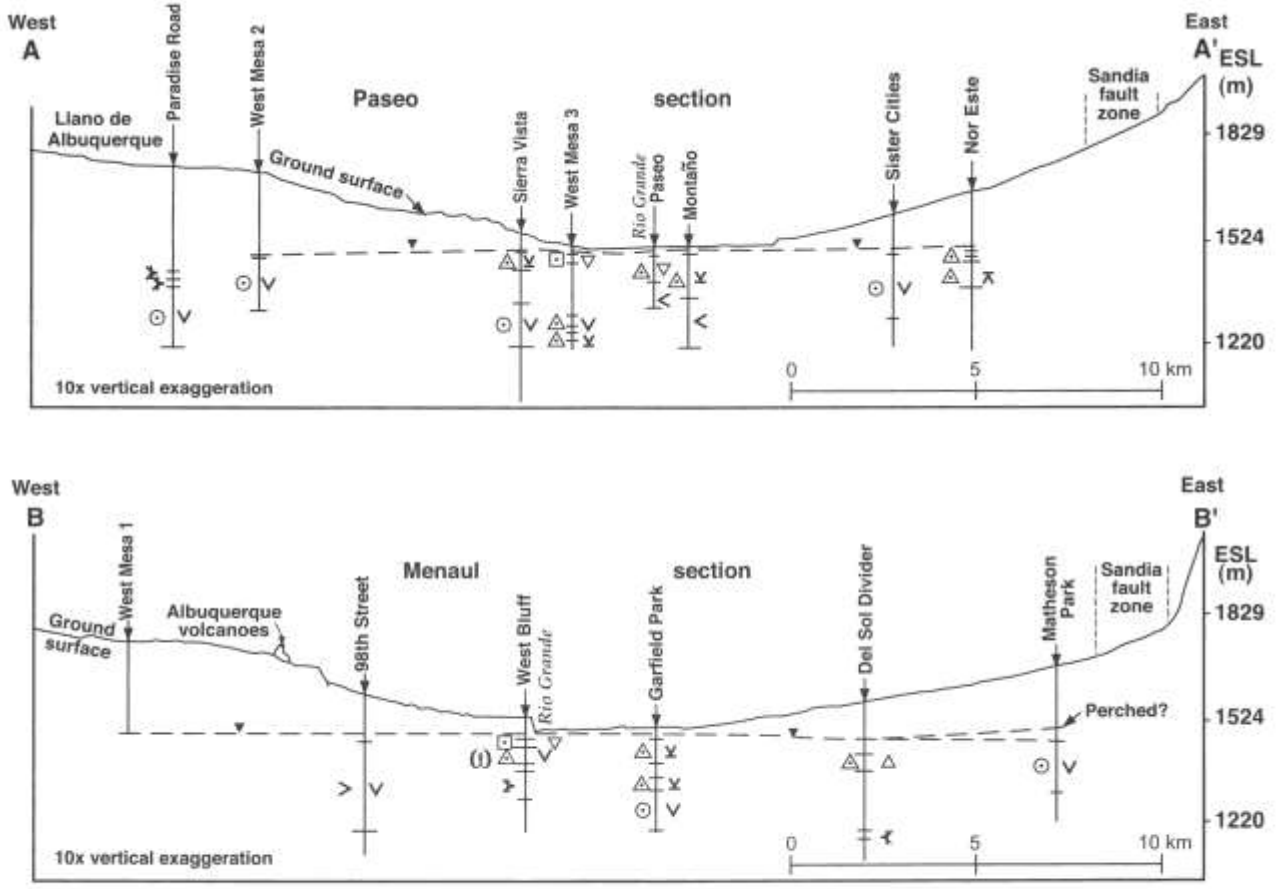

FIGURE 8—Cross sections along **A–A'** (Paseo section) and **B–B'** (Menaul section) indicating flow patterns. See Figure 2 for locations (base section after Hawley in Hawley and Haase, 1992). Symbols ▽, ▽, and ▽ indicate southward horizontal cooling flow of <10, 10–50, >50 m/yr (<33, 33–164, >164 ft/yr), respectively, ϖ implies southward horizontal warming flow (West Bluff site). The symbols >, ⊧, ▷ and <, ⊧, ◁ indicate eastward or westward warming flow of <10, 10–50, > 50 m/yr (< 33, 33–164, >164 ft/yr), respectively. Symbols ▼, ▼, ▽, Λ, Λ̄, Δ indicate downward or upward flow of < 0.10, 0.10–0.25, >0.25 m/yr (<0.33, 0.33–0.82, >0.82 ft/yr), respectively.

Conclusions

Precision temperature logs have provided insight to ground water flow characteristics in the Santa Fe Group aquifer in the Albuquerque Basin; although there are simplification in the ground water flow models used to fit the data (e.g., Reiter, 2001a) and uncertainties in the estimates of specific discharges and hydraulic conductivities. Figure 8 presents a qualitative picture of the ground water flow pattern at two profiles crossing the Albuquerque Basin. The cross sections show some of the following ground water flow characteristics in the basin: 1) generally large to intermediate specific discharges (horizontal and vertical) are noted near the Rio Grande; 2) intermediate specific discharges are also noted in the eastern highlands; and 3) and small specific discharges noted in the western highlands. The warming, deep horizontal flow suggested at Montano, Paseo, and Del Sol Divider are consistent with temperatures and flow from the east mesa. Warming flows observed at West Bluff and 98th Street require warm temperature influences to the west where the water table is deeper and water temperatures are warmer, or a thermal source north of 98th Street (Table 1). Relatively small, horizontal warming flows at Matheson Park (deeper depths) and 98th Street (over the entire depth interval) are consistent with modest basin peripheral recharge.

The complicated hydrogeology in the area results in ground water flow that can be quite different at different locations along the basin; e.g., the small horizontal flows at Black Mesa compared to large horizontal flows at Rio Bravo Park, both sites located along the western part of the inner valley of the Albuquerque Basin approximately 8 km (5 mi) apart. Sealed faults, impermeable volcanic dikes, and low horizontal hydraulic conductivity in the neighborhood of Black Mesa may cause low ground water flow at the site (Fig. 9). Sealed faults along the western part of the Albuquerque Basin appear to restrict flow from the Rio Grande, as indicated by T logs at 98th Street and Westgate Heights; these data also support the location of the faults suggested in Figure 6. Higher specific discharges and larger horizontal hydraulic conductivity estimates along the Rio Grande and in the eastern study area, as contrasted to the western part of the study area, coincide with Rio Grande sediment deposition (Hawley et al.,1995).

Figure 9 locates many of the piezometer sites used in this study on an isostatic residual gravity base map by Grauch et al. (1999). For comparison of temperature data, T logs are presented in Appendix 3 at the same scale. Two elevated temperature regions are indicated inside the hachured lines; one along the southern part of Albuquerque and one around the Nancy Lopez site. Sites in the elevated temperature regions are chosen because of higher temperature-depth gradients and higher temperatures at equivalent depths. The cause of the elevated temperatures is uncertain. Upward moving ground water, below the piezometers, may be migrating from deeper parts of the basin (indicated by the gravity data) regionally or along faults. Alternatively, data from deep petroleum tests indicate a high heat flow along the Tijeras lineament that may be caused by thermal sources

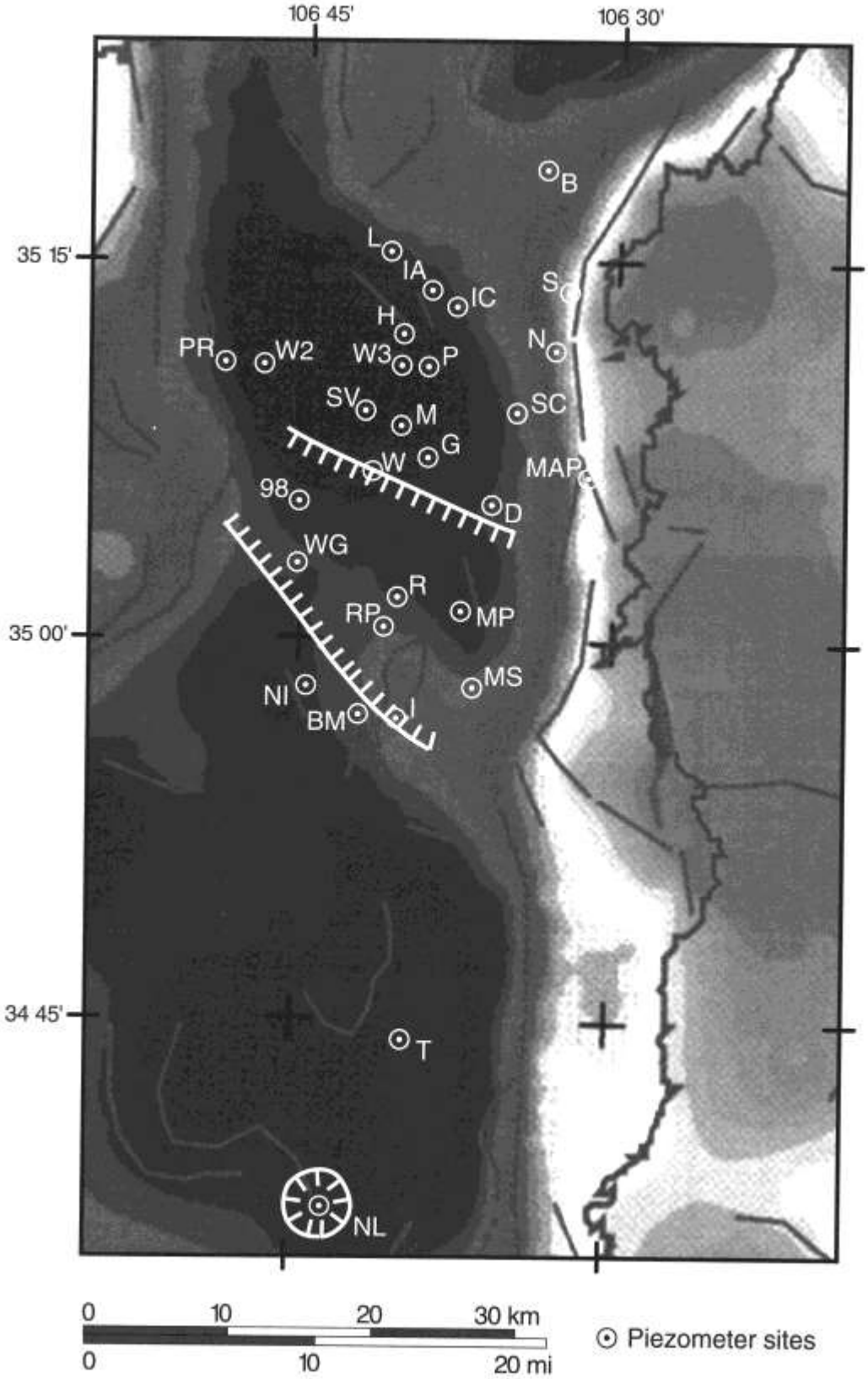

FIGURE 9—T logged piezometer sites (as in Fig. 2) located on isostatic residual gravity base map after Grauch et al. (1999). Areas of high temperatures inside hachured lines; basins and gravity lows indicated by darker areas. Gray lines indicate the steepest gravity gradients found by following the horizontal gradient method of Cordell (1979) to locate steeply dipping faults. The irregular dark gray line on the right is the eastern boundary of the Albuquerque Basin.

originating in the mantle (Reiter et al., 1986). The trend of the elevated temperature region indicated in Figure 9 appears to cross the trend of the Tijeras lineament, but the data coverage is sparse.

Acknowledgments

I thank B. C. Reiter for helping with the temperature measurements in the study. Numerous people with many organizations and governments cooperated with the project: city of Albuquerque, Isleta Pueblo, New Mexico Office of the State Engineer, Sandia Pueblo, Intel, Dunlap Construction, John Shomaker and Associates, U.S. Geological Survey. An equipment contribution from New Mexico Office of the State Engineer helped to develop a computerized temperature logging system. Glen Jones (NMBGMR) and Nathan Reiter (NMSTR) helped program the computerized logging system. Lynne Hemenway typed the manuscript, Sandra Azevedo and Leo Gabaldon drafted the figures. Norton Euart and Floyd Hewett helped assemble the logging equipment. Bruce Allen, Scott Anderholm, Peggy Barroll, Sean Connell, and John Hawley made many helpful suggestions to improve the manuscript.

References

Anderholm, S. K., 1988, Ground water geochemistry of the Albuquerque-Belen Basin, central New Mexico: U.S. Geological Survey, Water-resources Investigation, Report 88-4094, 110 pp.

Anderholm, S. K., 1999, Mountain-front recharge along the eastern side of the middle Rio Grande basin, central New Mexico: U.S. Geological Survey, Open-file Report 99-203, 65 pp.

Bartolino, J. R, and Niswonger, R. G., 1999, Numerical simulation of vertical ground water flux on the Rio Grande from ground water temperature profiles, central New Mexico: U.S. Geological Survey, Water-resources Investigations, Report 99-4212, 34 pp.

Bexfield, L. M., and Anderholm, S. K., 2000, Predevelopment water-level map of the Santa Fe Group aquifer system in the middle Rio Grande basin between Cochiti Lake and San Acacia, New Mexico: U.S. Geological Survey, Water-resources Investigations, Report 00-4249, 1 sheet.

Birch, F., 1947, Temperature and heat flow in a well near Colorado Springs: American Journal of Science, v. 245, no. 12, pp. 733-753.

Bjorklund, L. J., and Maxwell, B. W., 1961, Availability of ground water in the Albuquerque area, Bernalillo and Sandoval Counties, New Mexico: New Mexico State Engineer, Technical Report 21, 117 pp.

Bredehoeft, J. D., and Papadopulos, I. S., 1965, Rates of vertical ground water movement estimated from the earth's thermal profile: Water Resources Research, v. 1, pp. 325-328.

Bullard, E. D., 1939, Heat flow in South Africa: Proceedings of the Royal Society of London, Series A, v. 173, no. 955, pp. 474-502. Connell, S. D., 1997, Geology of the Alameda 7.5 minute quadrangle, Bernalillo County, New Mexico: New Mexico Bureau of Mines and Mineral Resources, Open-file Geologic Map, OF-GM 10, scale 1:24,000.

Connell, S. D., 1998, Geology of Bernalillo 7.5 minute quadrangle, Sandoval County, New Mexico: New Mexico Bureau of Mines and Mineral Resources, Open-file Geologic Map, OF-GM 16, scale 1:24,000, revised February 17, 2000.

Connell, S. D., Allen, B. D., Hawley, J. W., and Shroba, R., 1998a, Geology of the Albuquerque West 7.5 minute quadrangle, Bernalillo County, New Mexico: New Mexico Bureau of Mines and Mineral Resources, Open-file Geologic Map, OF-GM 17, scale 1:24,000.

Connell, S. D., Allen, B. D., and Hawley, J. W., 1998b, Subsurface stratigraphy of the Santa Fe Group from borehole geophysical logs, Albuquerque area, New Mexico: New Mexico Geology, v. 20, no. 1, pp. 2-7.

Cordell, L., 1979, Gravimetric expression of graben in Santa Fe country and the Espanola Basin, New Mexico; *in* Ingersoll, R. V., Woodward, L. A., and James, H. L. (eds.), Santa Fe country: New Mexico Geological Society, Guidebook 30, pp. 59-64.

Davis, J. M., Lohmann, R. C., Phillips, F. W., Wilson, J. L., and Love, D. W., 1993, Architecture of the Sierra Ladrones Formation, central New Mexico-depositional controls on the permeability correlation structure: Geological Society of America, Bulletin, v. 105, no. 8, pp. 998-1007.

Drury, M. J., Jessop, A. M., and Lewis, T. J., 1984, The detection of ground water flow by precise temperature measurements in bore holes: Geothermics, v. 13, no. 3, pp. 163-174.

Foster, C., and Smith, L., 1988, Ground water flow systems in mountainous terrain-2. Controlling factors: Water Resources Research, v. 24, pp. 1011-1023.

Grauch, V. J. S., Gillespie, C. **L.,** and Keller, G. R., 1999, Discussion of new gravity maps for the Albuquerque Basin area; *in* Pazzaglia, F. J., and Lucas, S. G. (eds.), Albuquerque geology: New Mexico Geological Society, Guidebook 50, pp. 119-124.

Haneberg, W. C., 1995, Steady-state ground water flow across idealized faults: Water Resources Research, v. 31, no. 7, pp. 1815-1820. Hawley, J. W., and Haase, C. S. (compilers), 1992, Hydrogeologic framework of the northern Albuquerque Basin: New Mexico Bureau of Mines and Mineral Resources, Open-file Report 387 (Plates 2 and 3).

Hawley, J. W., Haase, C. S., and Lozinsky, R. P., 1995, An underground view of the Albuquerque Basin: New Mexico Water Resources Research Institute, Annual New Mexico Water Conference, 39th proceedings, pp. 37-55.

Keller, G. R., and Cordell, L., 1983, Bouguer gravity anomaly map of New Mexico: Geothermal resources of New Mexico: New Mexico State University Energy Institute, Scientific Map Series.

Kelley, V. C., 1977, Geology of Albuquerque Basin, New Mexico: New Mexico Bureau of Mines and Mineral Resources, Memoir 33, 59 pp.

Kernodle, J. M., McAda, D. P., and Thorn, C. R., 1995, Simulation of ground water flow in the Albuquerque Basin, central New Mexico, 1901-1994, with projections to 2020: U.S. Geological Survey, Water-resources Investigations, Report 94-4251, 114 pp.

Levens, R. L., Williams, R. E., and Ralston, D. R., 1994, Hydrogeologic rate of geologic structures. Part I-the paradigm: Journal of Hydrology, v. 156, pp. 227-243.

Lewis, T. **J.,** and Beck, A. E., 1977, Analysis of heat flow data-detailed observations in many holes in a small area: Tectonophysics, v. 41, no. 1-3, pp. 41-59.

Lu, N., and Ge, S., 1996, Effects of horizontal heat and fluid flow on the vertical temperature distribution of a semiconfining layer: Water Resources Research, v. 32, no. 5, pp. 1449-1453.

Maldonado, F., Connell, S. D., Love, D. W., Grauch, V. J. S., Slate, J. L., McIntosh, W. C., Jackson, P. B., and Byers, F. M., Jr., 1999, Neogene geology of the Isleta Reservation and vicinity, Albuquerque Basin, New Mexico; *in* Pazzaglia, F. J., and Lucas, S. G. (eds.), Albuquerque geology: New Mexico Geological Society, Guidebook 50, pp. 175-188.

Mansure, A. J., and Reiter, M., 1979, A vertical ground water movement correction for heat flow: Journal of Geophysical Research, v. 84, no. B7, pp. 3490-3496.

McCord, J., Reiter, M., and Phillips, F., 1992, Heat flow data suggest large ground water fluxes through Fruitland coals of the northern San Juan Basin, Colorado-New Mexico: Geology, v. 20, no. 5, pp. 419-422.

Niswonger, R. G., and Constantz, J., 1999, Using heat as a tracer to estimate mountain-front recharge at Bear Canyon, Sandia Mountains, New Mexico: U.S. Geological Survey, Open-file Report, 99-203, pp. 71-72.

Plummer, L. N., Bexfield, L. M., Anderholm, S. K., Sanford, W. E., and Busenberg, E., 2000, Geochemical characterization of the ground water flow in parts of the Santa Fe Group aquifer system, middle Rio Grande basin, New Mexico: U.S. Geological Survey, Middle Rio Grande basin study, Open-file report 00-488, pp. 7-10.

Plummer, L. N., Sanford, W. E., Busenberg, E., Bexfield, L. M., Anderholm, S. K., and Schlosser, P., 1999, Tracing and dating ground water in the middle Rio Grande basin, New Mexico-a progress report: U.S. Geological Survey, Middle Rio Grande basin study, Open-file Report 99-203, pp. 83-86.

Pollack, N. H., and Chapman, D. S., 1993, Underground records of changing climate: Scientific American, v. 268, no. 6, pp. 44-50.

Ramey, H. J., 1962, Well bore heat transmission: Journal of Petroleum Technology, v. 14, pp. 427-435.

Rawling, G. C., Goodwin, L. B., and Wilson, J. L., 2001, Internal architecture, permeability structure, and hydrologic significance of contrasting fault zone types: Geology, v. 29, no. 1, pp. 43-46.

Reiter, M., 1999, Hydrogeothermal studies on the southern part of

Sandia National Laboratories/Kirtland Air Force Basin-data regarding ground water flow across the boundary of an intermontane basin; *in* Haneberg, W. C., Mozley, P. S., Moore, J. C., and Goodwin, L. 13. (eds.), Faults and subsurface fluid flow in the shallow crust: American Geophysical Union, Geophysical Monograph 113, pp. 207-222.

Reiter, M., 2001a, Using precision temperature logs to estimate horizontal and vertical ground water flow components: Water Resources Research, v. 37, no. 3, pp. 663-674.

Reiter, M., 2001b, Precision temperature logging and ground water flow studies along the eastern side of the Albuquerque Basin; *in* Remote sensing and hydrology 2000: International Association of Hydrological Science, Publication 267, pp. 487-490.

Reiter, M., Costain, J. K., and Minier, J., 1989, Heat flow and vertical ground water movement, examples from southwestern Virginia: Journal of Geophysical Research, v. 94, no. 9, pp. 12,423-12,431.

Reiter, M., Eggleston, R. E., Broadwell, B. R., and Minier, J., 1986, Terrestrial heat-flow estimates from deep petroleum tests along the Rio Grande rift in central and southern New Mexico: Journal of Geophysical Research, v. 91, no. 6, pp. 6225-6245.

Reiter, M., Mansure, A. J., and Peterson, B. K., 1980, Precision continuous temperature logging and correlations with other types of logs: Geophysics, v. 45, no. 12, pp. 1857-1868.

Russell, L. R., and Snelson, S., 1994, Structure and tectonics of the Albuquerque Basin segment of the Rio Grande rift-insights from reflection seismic data; *in* Landon, S. (ed.), Basins of the Rio Grande rift-structure, stratigraphy, and tectonic setting: Geological Society of America, Special Paper 191, pp. 83-112.

Sawyer, D. A., 1999, Hydrologic barriers to regional ground water flow in the Albuquerque and Santo Domingo Basins, north-central New Mexico: U.S. Geological Survey, Middle Rio Grande basin study, Open-file Report, 99-203, pp. 56-58.

Sigda, J. M., Goodwin, L. B., Mozley, P. S., and Wilson, J. L., 1999, Permeability alterations in small-displacement faults in poorly lithified sediments: Rio Grande rift, central New Mexico; *in* Haneberg, W. C., Mozley, P. S., Moore, J. C., and Goodwin, L. B. (eds.), Faults and subsurface fluid flow in the shallow crust: American Geophysical Union, Geophysical Monograph 113, pp. 51-68.

Smith, D. A., 1996, Theoretical considerations of sealing and non-sealing faults: American Association of Petroleum Geologists, Bulletin, v. 50, pp. 363-374.

Stallman, R. W., 1963, Computation of ground water velocity from temperature data: U.S. Geological Survey, Water-supply Paper, 1544-H, pp. 36-46.

Thomas, C. L., and Thorn, C. R., 2000, Use of air-pressurized slug tests to estimate hydraulic conductivity of selected piezometers completed in the Santa Fe Group aquifer system, Albuquerque area, New Mexico: U.S. Geological Survey, Water-resources Investigation, Report 00-4253,19 p.

Titus, F. B., Jr., 1961, Ground water geology of the Rio Grande trough in north-central New Mexico, with sections on the Jemez caldera and the Lucero uplift; *in* Northrop, S. A. (ed.), Albuquerque country: New Mexico Geological Society, Guidebook 12, pp. 186-192. Wade, S. C., and Reiter, M., 1994, Hydrothermal estimation of vertical ground water flow, Cañutillo, Texas: Ground Water, v. 32, no. 5, pp. 735-742.

Woodside, W., and Messmer, J. H., 1961, Thermal conductivity of porous media, I. Unconsolidated sands: Journal of Applied Physics, v. 32, no. 9, pp. 1688-1698.

Ziagos, J. P., and Blackwell, D. D., 1986, A model for the transient temperature effects of horizontal fluid flow in geothermal systems: Journal of Volcanology and Geothermal Research, v. 27, pp. 371-397.

Appendix I

Tables

TABLE 1—Compilation of site-specific flow information listed as referenced in text and figure list. Water depth in winter from hydrographs were possible.

Site (map label)	EGS (m)	Location °W °N	Screen depth (m)	Water depth (m)	Flow zone (m)	Estimate[1] Γ_{xc} or Γ_{xw} (10^{-4} °C/m)		V_x[2] (m/yr)	V_x[3] (m/yr)	V_z[4] (m/yr)
Dome Road (DR)	1773.8	106.37 35.68	390.2–393.3	180.8	181–344	Γ_{xc} = ?			1–2	~0.02 (d)
Bernalillo (B)	1538.1	106.56 35.31	182.9–213.4	9.8	20–93	Γ_{xc} ~2.9	(after Montaño)[5]	~31	~26	0.04–2.2 (d)
			304.9–365.9	12.4	100–240	Γ_{xw} ~2.9	(after Montaño)	~10	~12	[6]
					240–360	Γ_{xc}~2.4	(after Rio Bravo Park)	4–6	3–4	0.02–0.03 (d)
Intel C (IC)	1525.3	106.63 35.22	9.1–15.2	3.0	20–62	Γ_{xc} ~5.4	(upgrade to Rio Grande, temp. from Paseo)[5]	38–39	~32	0.04 (d)
			27.4–33.5	4.1		"				
			67.1–79.3	9.2	140–187	Γ_{xc} ?			10–11	0.01–0.02 (d)
			106.7–118.9	11.1	222–439	Γ_{xc} ?			1–2	0.01–0.03 (d)
			216.5–240.9	16.5						
			414.6–445.1	17.6						
Paseo (P)	1521.6	106.65 35.18	3.0–6.1	2.1	30–99	Γ_{xc} ~2.5	(to Montaño)[5,7]	42–46	30–33	0.03–0.50 (d)
			41.2–44.2	6.0	100–179	Γ_{xw} ~5.4	(to Sandia Pueblo)[5,7]	~6	~10	[6]
			178.4–181.4	11.5						
West Mesa 3 (W3)	1522.6	106.67 35.18	106.7–173.8	7.0	23–49	Γ_{xc} ~1.1	(to Intel C)[5]	93–95	27–30	0.03–1.5 (d)
			216.5–240.9	8.5	215–237	Γ_{xc} ~3.8	(to Intel C)[5]	15	17	0.03 (d)
			265.2–301.8	8.8	252–276	Γ_{xc} ~4.7	(to Intel C)[5]	21–22	28	0.03–0.19 (d)
Montaño (M)	1515.2	106.67 35.14	52.5–54.0	6.3	20–154	Γ_{xc} ~2.9	(to Paseo)[5,7]			
			170.1–171.6	8.6	63–150	possible zone of reduced flow		33–36	27–30	0.03–0.47 (d)
			251.8–253.4	9.1	116–150	"				
			296.6–298.2	9.5	154–297	Γ_{xw} ~2.9	(to Nor Este)[5,7]	4	4	[6]
Garfield Park (G)	1513.4	106.65 35.12	13.1–25.3	14.0	30–104	Γ_{xc} ~6.4	(to Paseo)[5,7]	7–13	13–25	0.03–0.28 (d)
			168.3–174.4	14.7	146–184	Γ_{xc} ~8.4	(to Paseo)[5,7]	9–11	23–27	0.03–0.20(d)
			303.4–307.9	14.8	189–305	Γ_{xc} ~10.8	(to Montaño)[5,7]	~1	3–5	≤ 0.01–0.03 (d)
West Bluff (W)	1554.9	106.69 35.11	43.6–49.7	47.3	56–82	Γ_{xc} ~5.8	(after Paseo to Montaño)[5,7]	88–144	146–157	0.07–1.23 (d)
			97.0–98.5	47.5	82–130	Γ_{xw} ~3.9	(to Sierra Vista)[5,7]	12–44	26–49	0.08 (d)
			128.7–130.2	47.6	139–148[8]					
			207.0–208.5	50.4	148–160[8]					
			330.8–332.3	52.2	161–246	Γ_{xw} ~2.5	(to Paradise Road)[5]	~16	11	[6]

TABLE 1—Continued

Site (map label)	EGS (m)	Location °W °N	Screen depth (m)	Water depth (m)	Flow zone (m)	Estimate[1] Γ_{xc} or Γ_{xw} (10^{-4} °C/m)		V_x[2] (m/yr)	V_z[3] (m/yr)	V_z[4] (m/yr)
Rio Bravo (R)	1503.9	106.67 35.03	2.1–5.2	2.4	33–46	Γ_{xc} ~4.6	(Paseo temp., dist. north to Rio Grande)[5]	116	151	[6]
			41.2–44.2	2.2	46–152	Γ_{xw} ~2.2	(to West Bluff)[5,7]	41–87	26–55	≤ 0.12 (d)
			152.4–155.5	3.7						
Rio Bravo Park (RP)	1501.5	106.68 35.01	61.0–62.5	2.0	20–74	Γ_{xc} ~1.2	(to Rio Bravo)[5,7]	23–25	78–84	0.14 (d)
			178.4–179.9	3.4	75–121	Γ_{xc} ~2.4	(to Montaño)[5,7]	4–19	3–14	0.05–0.06 (d)
Black Mesa (BM)	1493.9	106.70 34.95	3.0–12.2	1.6	80–167	Γ_{xc} = ?			0–8	0.05–0.09 (d)
			53.4–54.9	2.1	167–380	Γ_{xc} = ?			1	0.01 (d)
			245.4–247.0	2.3						
			400.9–402.4	5.0						
Isleta Golf Course (I)	1500.6	106.67 34.94	32.0–41.2	7.2	42–50	Γ_{xc} ~3.1	(to Rio Bravo)[5,7]	~981	~867	NC [11]
			164.6–173.8	7.9	64–243	Γ_{xc} ~2.5	(to Montaño)	<4	<3	0.02
			234.3–243.4	8.5	169–200	"		≤ 60	≤ 43	≤ 0.03
West Mesa 2 (W2)	1747.0	106.78 35.18	243.9–291.0	233.9	248–400	Γ_{xc} ~0.9	(Lincoln Mid Sch.)[5,7]	6–9	~2	0.01–0.02 (d)
			388.8–430.0	239.0						
Hunter Ridge (H)	1538.1	106.67 35.20	45.1–69.5	44.6	52–327	Γ_{xc} = 6.3	(to Intel C)[5,7]	~2	3–4	0.01–0.07 (d)
			257.6–259.1	49.1	329–412	Γ_{xc} = 9.6	(to Intel C)[5,7]	~1	~4	0.02 (d)
			459.8–461.3	50.1						
Sierra Vista (SV)	1557.9	106.70 35.15	42.7–61.0	45.6	55–107	Γ_{xc} = 6.8	(to West Mesa 3)[5,7]	11–14	22–27	0.03–0.28 (d)
			279.9–281.4	46.6	202–322	Γ_{xc} = 7.4	(to West Mesa 3)[5,7]	1–2	2–4	0.01–0.03 (d)
			498.2–499.7	54.6						
Lincoln Mid. Sch. (L)	1661.6	106.68 35.25	149.4–179.9	148.5	151–164	Γ_{xc} = 3.0	(to Bernalillo)[5,7]	~47	~41	0.02 (d)
			247.0–253.0	150.4	180–222	Γ_{xc} = 3.9	(to Bernalillo)[5,7]	~9	~10	0.02 (d)
			365.9–378.0	150.5	251–259[9]					
					264–371	Γ_{xw} = ?			~2	[6]
Intel A (IA)	1585.0	106.65 35.23	67.1–73.2	65.3	97–131	Γ_{xw} = ?			~7	[6]
			83.8–89.9	68.2	135–190	Γ_{xc} = 4.2	(to Rio Grande, temp. from Paseo)[5]	1–3	2–3	0.01–0.56 (d)
			118.9–131.1	71.2						
			186.0–198.2	75.8	191–235	Γ_{xc} = 2.6	"	64–73	48–54	0.04–1.37 (d)
			282.0–306.4	77.5	250–360	disturbed zone				
			489.3–519.8	79.0	365–455	Γ_{xc} = ?			13–15	0.02–0.24 (d)

TABLE 1—Continued

Site (map label)	EGS (m)	Location °W °N	Screen depth (m)	Water depth (m)	Flow zone (m)	Estimate[1] Γ_{xc} or Γ_{xw} (10^{-4} °C/m)	V_x [2] (m/yr)	V_z[3] (m/yr)	V_z[4] (m/yr)
Paradise Rd. **(PR)**	1777	106.81 35.18	524.4–527.4	271.5	301–326 326–347 360–516	Γ_{xw} = ? Γ_{xw} = ? Γ_{xc} ~3.4 (to Lincoln Mid. Sch.)	1–3	~19 ~28 1–3	0.02–0.06 (d)
98th Street **(98)**	1618.9	106.75 35.09	118.3–132.0 225.3–226.8 336.0–337.5 467.7–469.2	119.4 126.5 128.4 128.1	137–396	Γ_{xw} = 6.2 (to West Mesa 1)[5] (Hydrograde. to West Mesa 2)	2–5	3–9	~0.06 (d)
Westgate Heights **(WG)**	1594.5	106.75 35.05	97.6–109.8 261.6–263.1 390.2–391.8	100.6 110.4 110.7	146–291 291–387	Γ_{xw} ~2.9 (to 98th Street)[5,7] Γ_{xw} ~3.8 (to 98th Street)[5,7]	3–11 2–7(8)	3–9 (10) 2–8 (9)	~0.06 (d) ~0.05 (d)
Niese **(NI)**	1573.2	106.74 34.97	73.8–89.0 289.6–291.2 440.5–442.1	74.4 75.0 79.3	182–362	Γ_{xc} ~1.2 (to Rio Bravo Pk.)[5]	3–8 (9)	1–3	(0.02) 0.03–0.04 (d)
Sandia Pueblo **(S)**	1655.5	106.54 35.23	147.9–160.1 309.5–311.0 394.8–396.3	146.5 148.5 148.5	158–179 191–220 312[10]	Γ_{xc} = 1.9 (to Bernalillo)[5,7] Γ_{xc} = 3.4 (to Bernalillo)[5,7]	78–124 34–55	43–68 33–54	0.18–0.23 (d) ~0.20 (d)
Nor Este **(N)**	1664.6	106.55 35.19	164.0–182.3 360.7–362.2 461.9–463.4	165.7 164.9 164.3	165–189 201–276 200	Γ_{xc} = 4.6 (to Sandia Pueblo)[5,7] Γ_{xc} = 4.8 (to Sandia Pueblo)[5,7] Possible warm (up?) flow zone	24–34 8–14	31–45 11–19	[6] ≤ 0.16 (u)
Sister Cities **(SC)**	1597.6	106.58 35.15	106.7–137.2 240.5–242.1 395.7–397.3	104.4 105.8 105.5	109–309 348[12]	Γ_{xc} ~3.0 (to Intel C)[5,7]	5–10	5–9	0.02–0.15 (d)
Del Sol Divider **(D)**	1588.4	106.60 35.09	96.0–126.5 253.7–255.2 474.7–476.2	105.9 103.5 100.5	150–200 376–404	Γ_{xc} ~1.9 (to Sister Cities)[5,7] Γ_{xw} ~4.2 (to Matheson Park)[5]	14–102 24	8–55 28	≤ 0.73 (u) NC[11]
Matheson Park **(MAP)**	1696.6	106.52 35.11	182.9–213.4 311.0–317.1 445.1–457.3	177.4 218.6 217.4	222–371 372–455 372–455	Γ_{xc} ~1.3 (to Nor Este)[5] Γ_{xw} ~4.2 (to Del Sol Divider)[5] Γ_{xc} ~1.6 (to Nor Este)[5]	~5 ~5 ~11	~2 ~6 5	~0.02 (d) ≤ 0.07 (u) 0.15 (u)

TABLE 1—Continued

Site (map label)	EGS (m)	Location °W °N	Screen depth (m)	Water depth (m)	Flow zone (m)	Estimate[1] Γ_{xc} or Γ_{xw} (10^{-4} °C/m)	V_x[2] (m/yr)	V_z[3] (m/yr)	V_z[4] (m/yr)
Montesa Park	1554.9	106.62	79.3–97.6	65.3	67–86	Γ_{xc} ~2.4 (to Del Sol Div.)[5]	74–120	51–82	0.03–0.47 (d)
(MP)		35.02	212.8–214.3	65.4	113–141	Γ_{xc} ~3.9 (to Del Sol Div.)[5]	18–20	20–22	≤ 0.17 (d)
(second log)			493.3–494.5	65.2	310–370	Γ_{xw} = ?		~5	~0.82 (u)
Mesa del Sol	1615.9	106.61	128.0–158.5	126.4	126–174	Γ_{xc} ~12 (to PL2)[5]	2–4	8–15	0.06 to 0.13 (d)
(MS)		34.97	301.8–307.9	128.6	213–316	Γ_{xw} = ?		1–5	~0.07 (d)
			481.7–493.9	124.8	316–490	"		3	0.02 (u)
Tomé	1530.5	106.66	68.6–80.8	59.0	60–215	Γ_{xc} = ?		2–6	0.04–0.07 (d)
(T)		34.74	211.9–214.9	59.2	280–350	Γ_{xw} = ?		3	[6]
			361.3–364.3	58.3					
Nancy Lopez	1501.5	106.72	205.8–208.8	40.1	50–106	[6]			≤ 0.04 (d)
(NL)		34.63	329.6–332.6?	40.2	142–207	Γ_{xw} ?		9	[6]
					269–314	Γ_{xw} ?		20	[6]

[1] Γ_{xc} is the horizontal temperature gradient estimate when cooling is suggested from the T log; Γ_{xw} is the horizontal temperature gradient when warming is suggested from the T log.
[2] V_x, horizontal component of specific discharge calculated from present estimates given for Γ_{xc} or Γ_{xw}.
[3] V_x calculated from general horizontal temperature gradient estimate by Stallman (3.5 x 10^{-4} °C/m, 1963).
[4] V_z is vertical specific discharge component, if vertical flow is down (d), upflow (u).
[5] Brief description of how Γ_x was estimated.
[6] V_x or V_z fits (F statistic) poorer than straight line.
[7] Site data used also for estimate of hydrologic head.
[8] Possible warm flow upward along fault, see Fig. 8.
[9] Possible water circulation around screen.
[10] Downward fluid flow along steeply dipping fault at approximately 312 m (see Appendix 2–19).
[11] NC implies not calculated, typically for reasons such as: T log curvature and piezometer data are inconsistent; horizontal flow only model fits significantly better than 2d models (F statistic an order of magnitude greater); piezometer data indicate no vertical flow; or V_z estimate very small (<10^{-4} m/yr).
[12] Possible upflow along a fault or zone at ~348 mm.
Note: Specific discharge estimates for Westgate Heights and Niese sites that are in parentheses are for the second log; see Appendix 2-20b and 2–21b.

TABLE 2—Hydraulic conductivity estimates for sites in the study.

Site	Depth interval (m)	K_x[1] (m/sec)	K_y[2] (m/sec)	K_z[3] (m/sec)	Depth[10] interval (m)	K[10] (m/sec)
Dome Road	181–344	[4]	[4]	[11]		
Bernalillo	20–93	[4]	8.2×10^{-4}	[12]		
	100–240	[4]	2.6×10^{-4}	[12]		
	240–360	[4]	1.3×10^{-4}	4.0×10^{-8}		
Intel C	20–62	[5]	3.3×10^{-3}	1.3×10^{-8}		
	140–187	[4]	0.9×10^{-4}	1.4×10^{-8}		
	223–439	[4]	1.2×10^{-4}	1.3×10^{-7}		
Paseo	30–99	1.1×10^{-3}	1.6×10^{-3}	9.5×10^{-8}		
	100–179	[6]	5.9×10^{-4}	[12]		
West Mesa 3	23–49	[6]	3.8×10^{-3}	1.1×10^{-6}		
	215–237	[6]	6.1×10^{-4}	3.6×10^{-8}		
	252–276	[6]	8.2×10^{-4}	6.9×10^{-7}		
Montaño	20–154	2.8×10^{-3}	1.2×10^{-3}	4.1×10^{-7}		
	154–297	[6]	2.6×10^{-4}	[12]		
Garfield Park	30–104	1.6×10^{-4}	3.4×10^{-4}	1.1×10^{-6}	303–308	2.0×10^{-4}
	146–184	2.3×10^{-4}	3.4×10^{-4}	7.6×10^{-7}		
	189–305	3.6×10^{-5}	7.7×10^{-5}	9.9×10^{-7}		
West Bluff	56–82	4.8×10^{-3}	4.9×10^{-3}	4.9×10^{-6}	74–76	4.6×10^{-5}
	82–130	1.1×10^{-3}	2.6×10^{-3}	6.7×10^{-7}	97–98	2.4×10^{-5}
	161–246	[6]	[7]	[5]	207–209	4.3×10^{-5}
					331–332	2.5×10^{-5}
Rio Bravo	33–46	[6]	4.0×10^{-3}			
	46–152	3.4×10^{-3}	2.2×10^{-3}	2.9×10^{-7}		
Rio Bravo Park	20–74	7.8×10^{-4}	6.8×10^{-4}	3.6×10^{-7}		
	75–121	6.7×10^{-4}	3.2×10^{-4}	1.5×10^{-7}		
Black Mesa	80–167	[6]	1.1×10^{-4}	2.2×10^{-6}	53–55	$(6.8–24) \times 10^{-5}$
	167–380	[6]	2.8×10^{-5}	3.5×10^{-8}	245–247	6.4×10^{-5}
					401–402	5.0×10^{-4}
Isleta Golf Course	42–50	4.1×10^{-2}	4.1×10^{-2}	[5]		
	64–243	2.0×10^{-4}	1.6×10^{-4}	1.1×10^{-7}		
	169–200	3.5×10^{-3}	2.5×10^{-3}	1.2×10^{-7}		
West Mesa 2	248–400	4.2×10^{-3}	4.1×10^{-4}	1.1×10^{-8}		
Hunter Ridge	52–327	1.2×10^{-5}	4.4×10^{-5}	5.6×10^{-8}	90–91	4.6×10^{-5}
	329–412	1.0×10^{-5}	3.4×10^{-5}	1.3×10^{-7}	106–108	1.5×10^{-4}
					258–259	7.1×10^{-5}
					460–461	1.5×10^{-5}
Sierra Vista	55–107	6.5×10^{-4}	3.5×10^{-4}	1.1×10^{-6}	280–281	2.9×10^{-5}
	202–322	8.8×10^{-5}	4.1×10^{-5}	1.4×10^{-7}	498–500	1.3×10^{-5}
Lincoln Middle School	151–164	1.4×10^{-3}	1.1×10^{-3}	1.9×10^{-8}		
	180–222	2.9×10^{-4}	2.3×10^{-4}	2.2×10^{-8}		
	264–371	[4]	[4]	[5]		

TABLE 2—Hydraulic conductivity estimates for sites in the study.

Site	Depth interval (m)	K_X[1] (m/sec)	K_X[2] (m/sec)	K_Z[3] (m/sec)	Depth[10] interval (m)	K[10] (m/sec)
Intel A	94–131	[4]		[12]		
	135–190	[6]	6.0×10^{-5}	1.3×10^{-7}		
	191–235	[6]	2.0×10^{-3}	1.4×10^{-6}		
	365–455	[4]	4.1×10^{-4}	6.0×10^{-7}		
Paradise Road	360–516	2.4×10^{-4}	2.2×10^{-4}	[11]	336–338	9.6×10^{-5}
					468–469	2.1×10^{-5}
98th St.[9]	137–396	9.0×10^{-5}	3.3×10^{-4}	5.4×10^{-8}		
Westgate Heights	146–291	2.4×10^{-4}	2.4×10^{-4}	3.1×10^{-8}		
	291–387	1.3×10^{-4}	1.6×10^{-4}	7.2×10^{-7}		
Niese	182–362	[6]	1.7×10^{-4}	7.9×10^{-8}		
Sandia Pueblo	158–179	1.7×10^{-3}	2.4×10^{-3}	5.2×10^{-7}	309–311	3.3×10^{-4}
	195–220	7.3×10^{-4}	1.1×10^{-3}	4.9×10^{-7}	395–396	1.3×10^{-5}
Nor Este	165–189	4.1×10^{-4}	1.2×10^{-3}	[12]	462–463	2.1×10^{-4}
	201–276	2.8×10^{-4}	5.3×10^{-4}	1.1×10^{-6}		
Sister Cities	109–309	1.2×10^{-4}	3.4×10^{-4}	2.2×10^{-7}	241–242	2.3×10^{-5}
					396–397	6.1×10^{-5}
Del Sol Divider	150–200	2.0×10^{-3}	2.8×10^{-3}	1.2×10^{-6}	254–255	6.8×10^{-4}
	376–404	[6]	5.9×10^{-4}	[5]	475–476	5.4×10^{-4}
Matheson Park	222–371	[6]	[7]	1.8×10^{-8}		
	372–454	[6]	[7]	$(2.6–5.6) \times 10^{-7}$		
Montesa Park	67–86	[6]	6.2×10^{-3}	9.2×10^{-6}	213–214	6.8×10^{-5}
	113–141	[6]	1.2×10^{-3}	6.4×10^{-6}	493–495	5.4×10^{-7}
	310–370	[4]	2.2×10^{-4}	1.1×10^{-6}		
Mesa del Sol	126–174	[6]	1.0×10^{-4}	2.0×10^{-7}		
	213–316	[4]	[4]	1.6×10^{-7}		
	316–490	[4]	[4]	3.9×10^{-8}		
Tomé	60–215	[4]	[4]	1.2×10^{-6}		
Nancy Lopez		[4]	[4]	[11]		

[1] Horizontal hydraulic conductivity calculated using head difference from piezometer data and piezometer nest indicated for horizontal temperature gradient estimate in Table 1.
[2] Horizontal hydraulic conductivity calculated using head difference estimated from water table contours by Titus (1961), Bexfield and Anderholm (2000).
[3] Vertical hydraulic conductivity calculated from piezometer data (Table 1).
[4] Cannot estimate flow path.
[5] V_Z not calculated in Table 1.
[6] Piezometer data not compatible with consistent horizontal hydrologic gradient calculation.
[7] Water table contours not compatible with consistent horizontal hydrologic gradient calculation.
[8] See Table 1.
[9] Horizontal hydraulic gradient calculated to West Mesa 2.
[10] Estimated in Thomas and Thorn (2000).
[11] Don't know the vertical hydraulic gradient.
[12] V_X or V_Z is a poorer fit to the data than a straight line.

Appendix II

T logs represented to show ground water effects, date logged indicated.

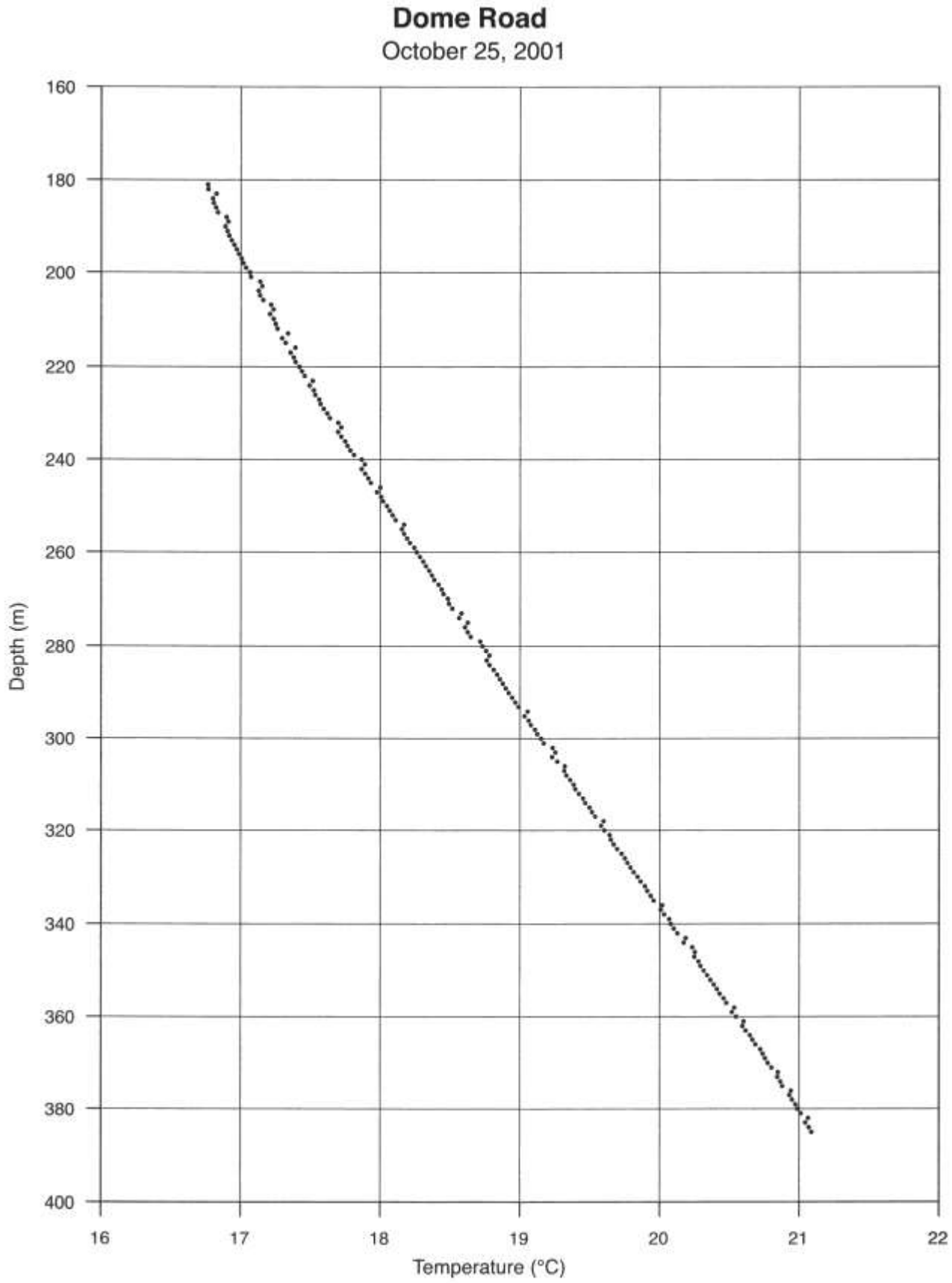

FIGURE 2–1—Temperature log (T log) at Dome Road site. T log made with same electronics as Westgate Heights, first log (Appendix 2–20a).

FIGURE 2–2—T log at Bernalillo site.

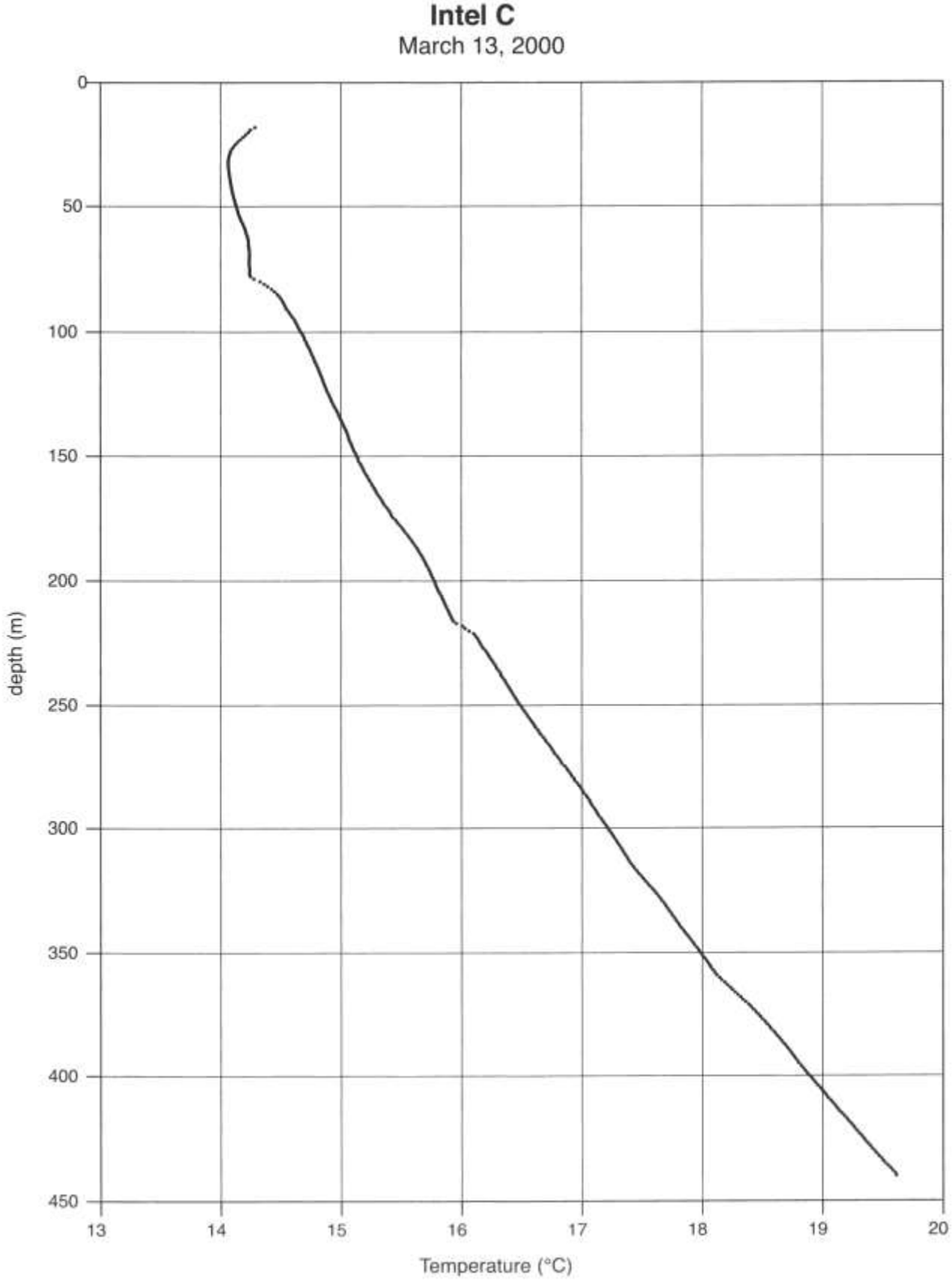

FIGURE 2–3—T log at Intel C site.

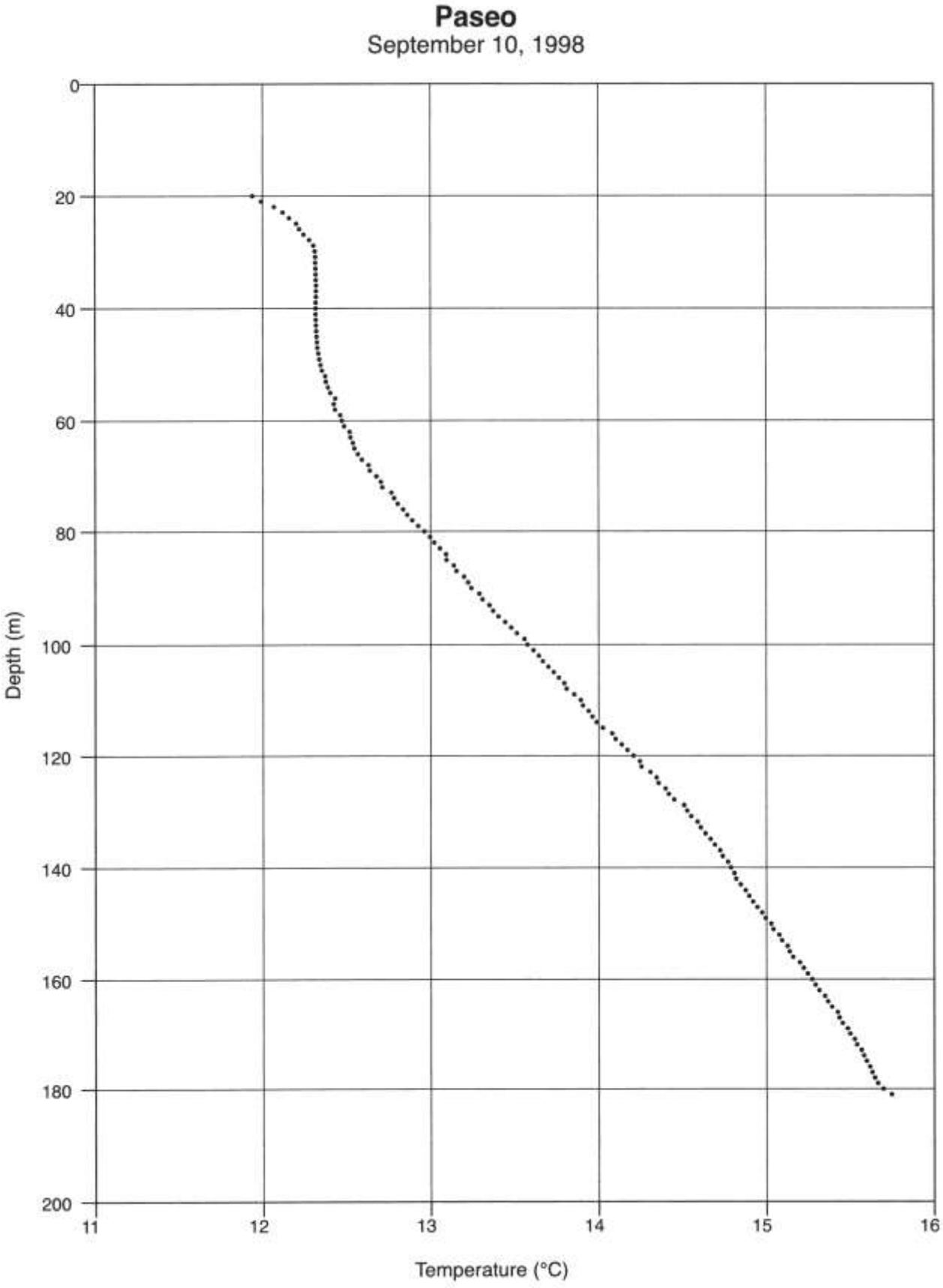

FIGURE 2–4—T log at Paseo site.

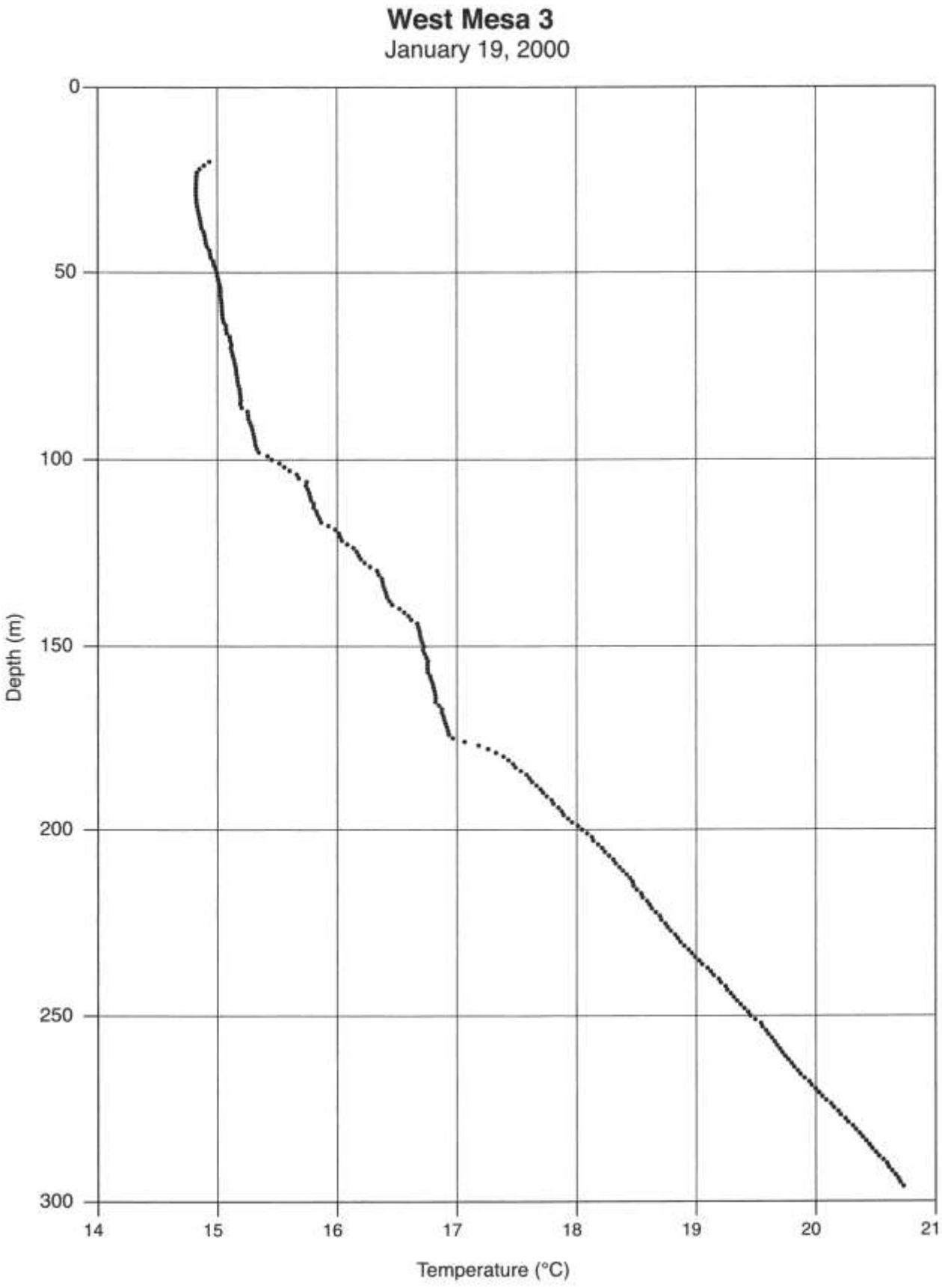

FIGURE 2–5—T log at West Mesa 3 site. Disturbances in T log to ~175 m probably caused to some extent by circulation near screens.

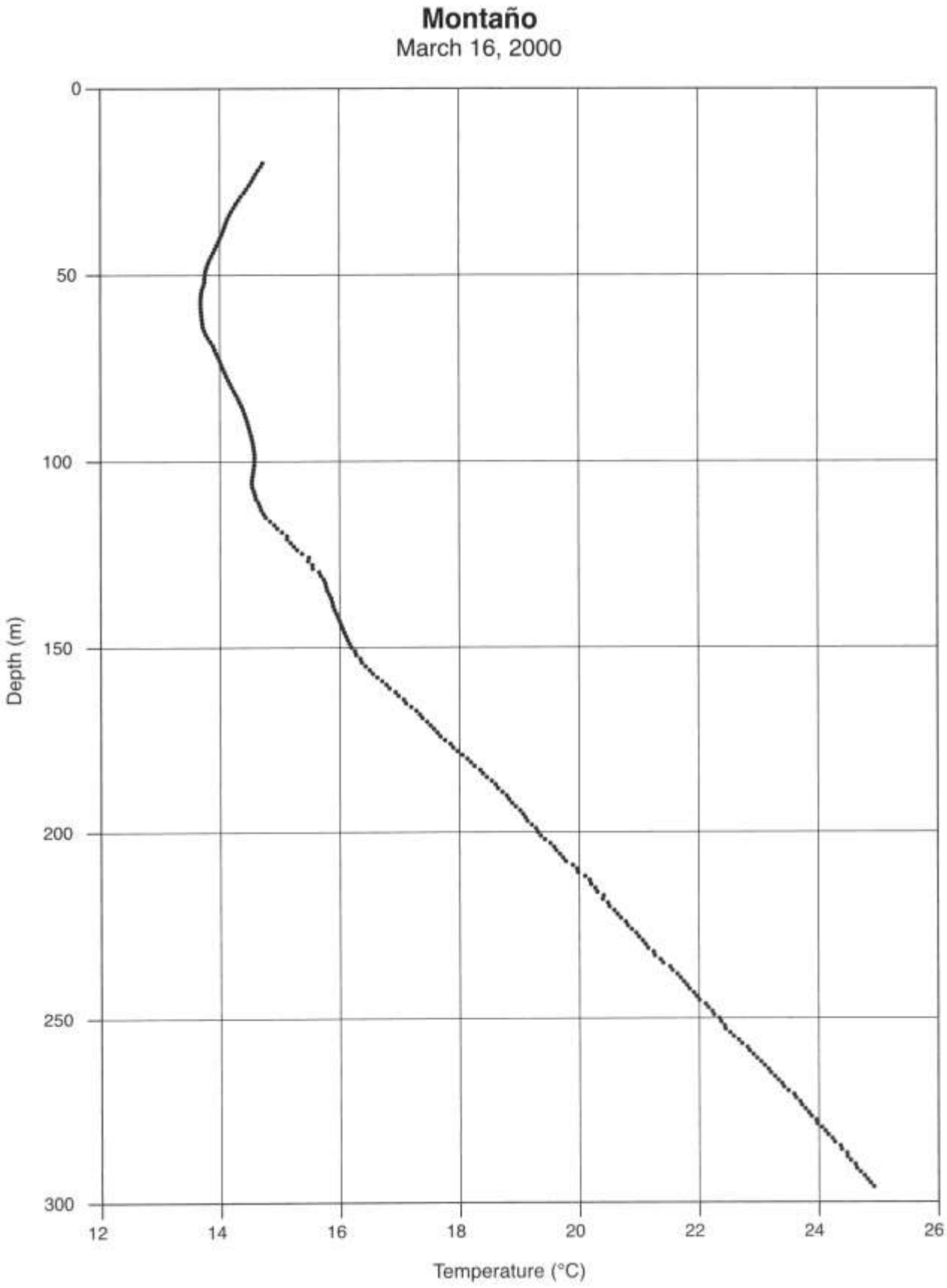

FIGURE 2–6—T log at Montaño site.

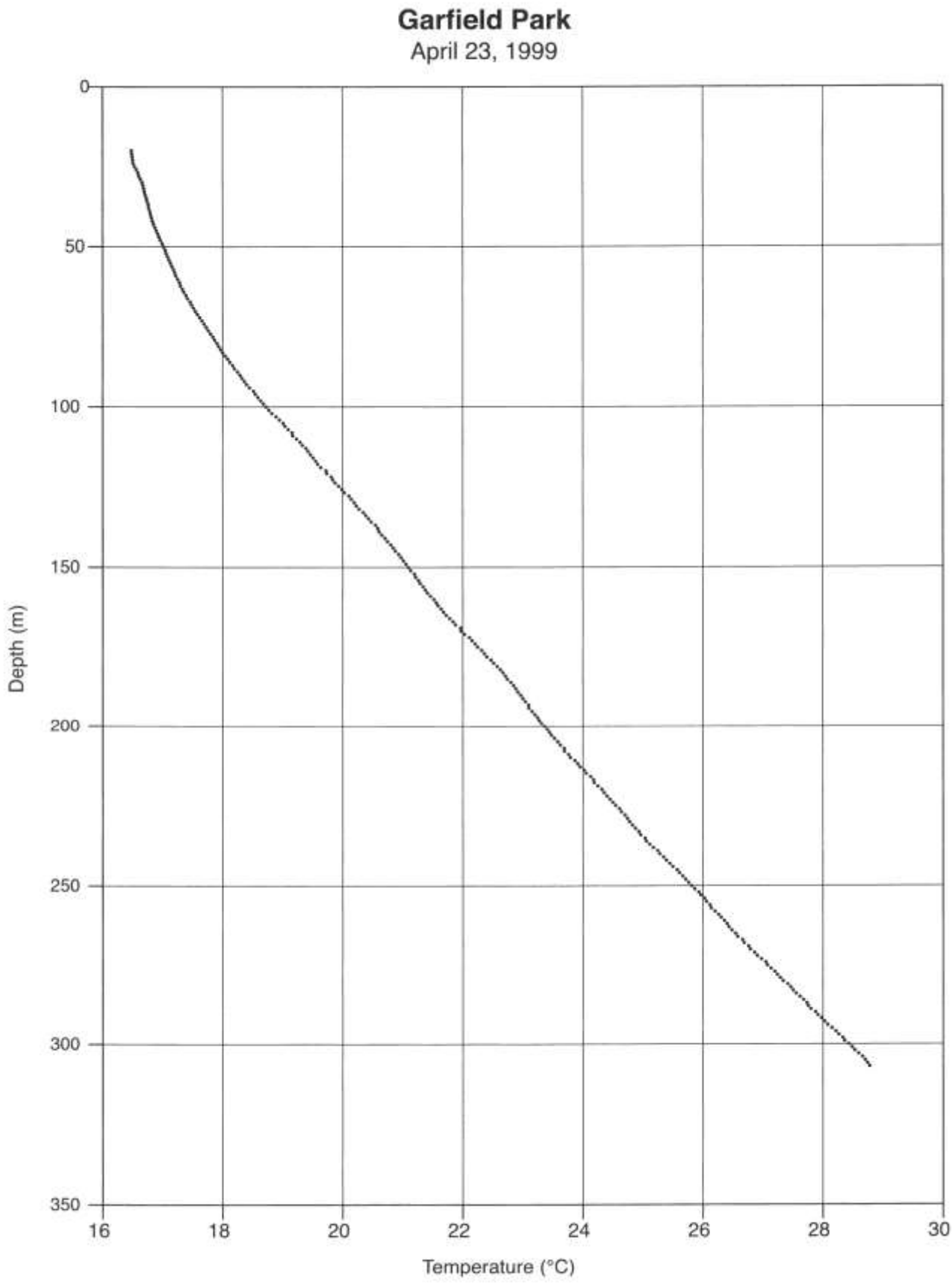

FIGURE 2–7—T log at Garfield Park site.

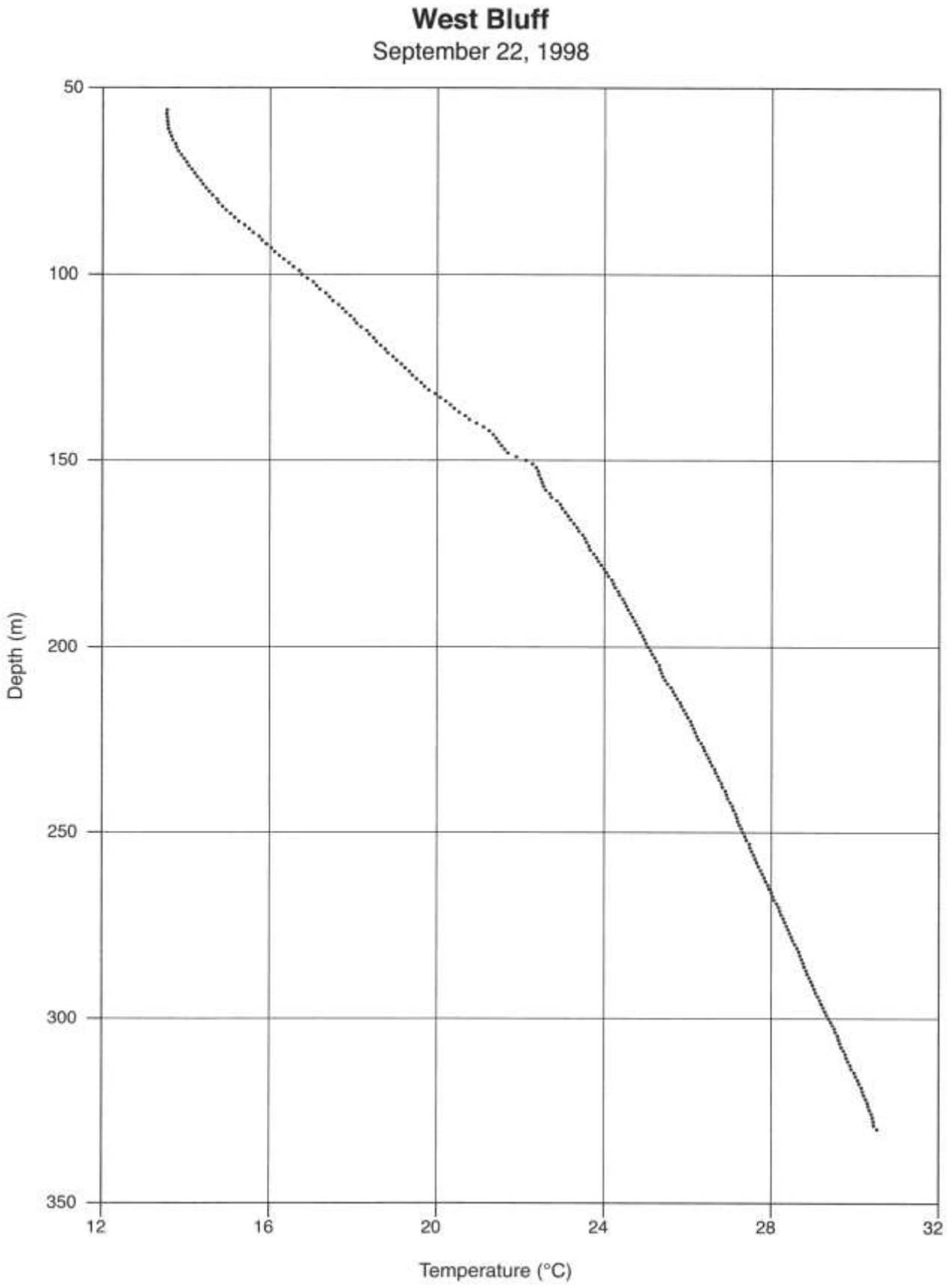

FIGURE 2–8—T log at West Bluff site. Temperature gradient increases at ~140 m and ~150 m may indicate warm flow along a thin zone, perhaps a fault.

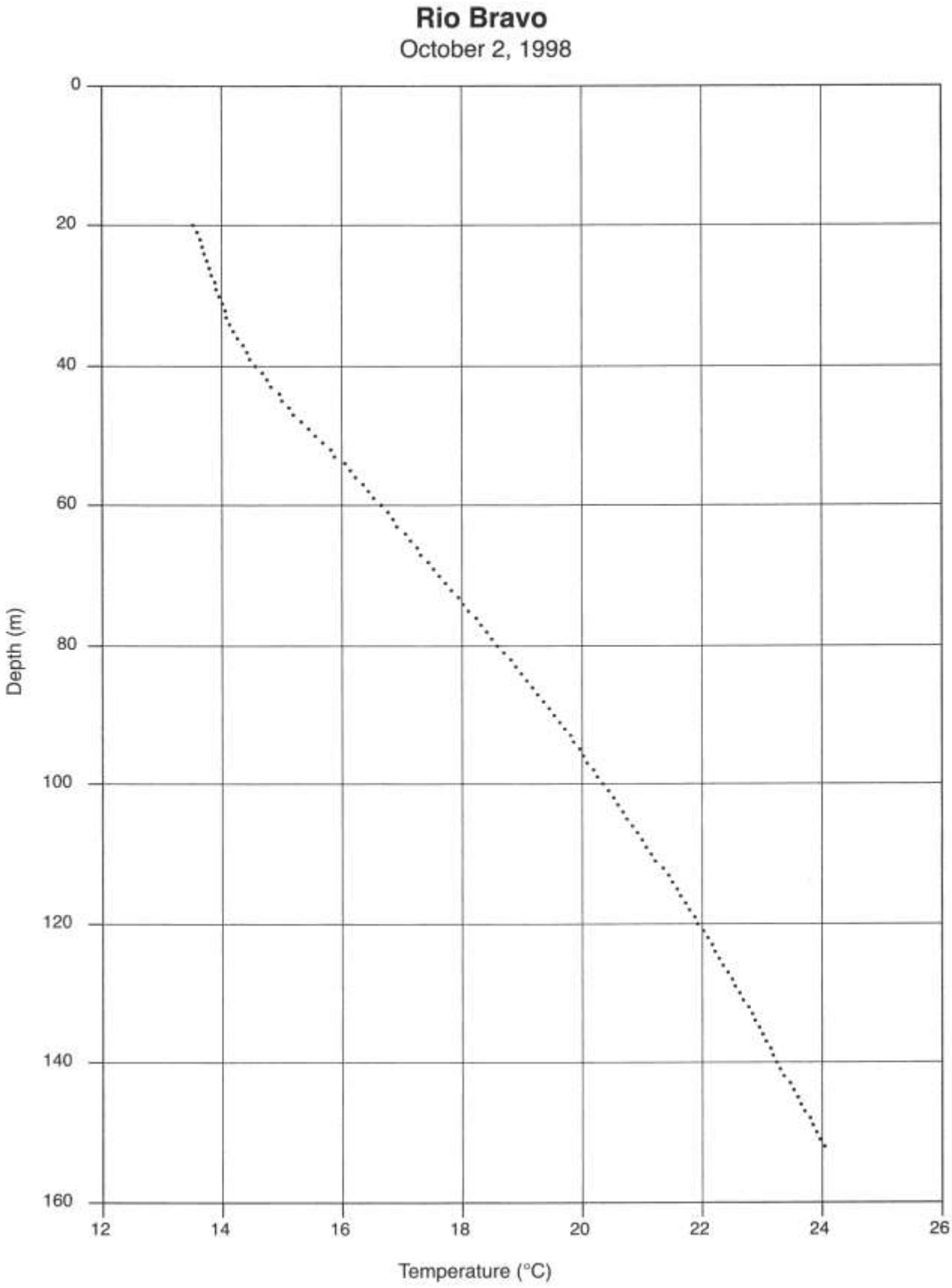

FIGURE 2-9—T log at Rio Bravo site.

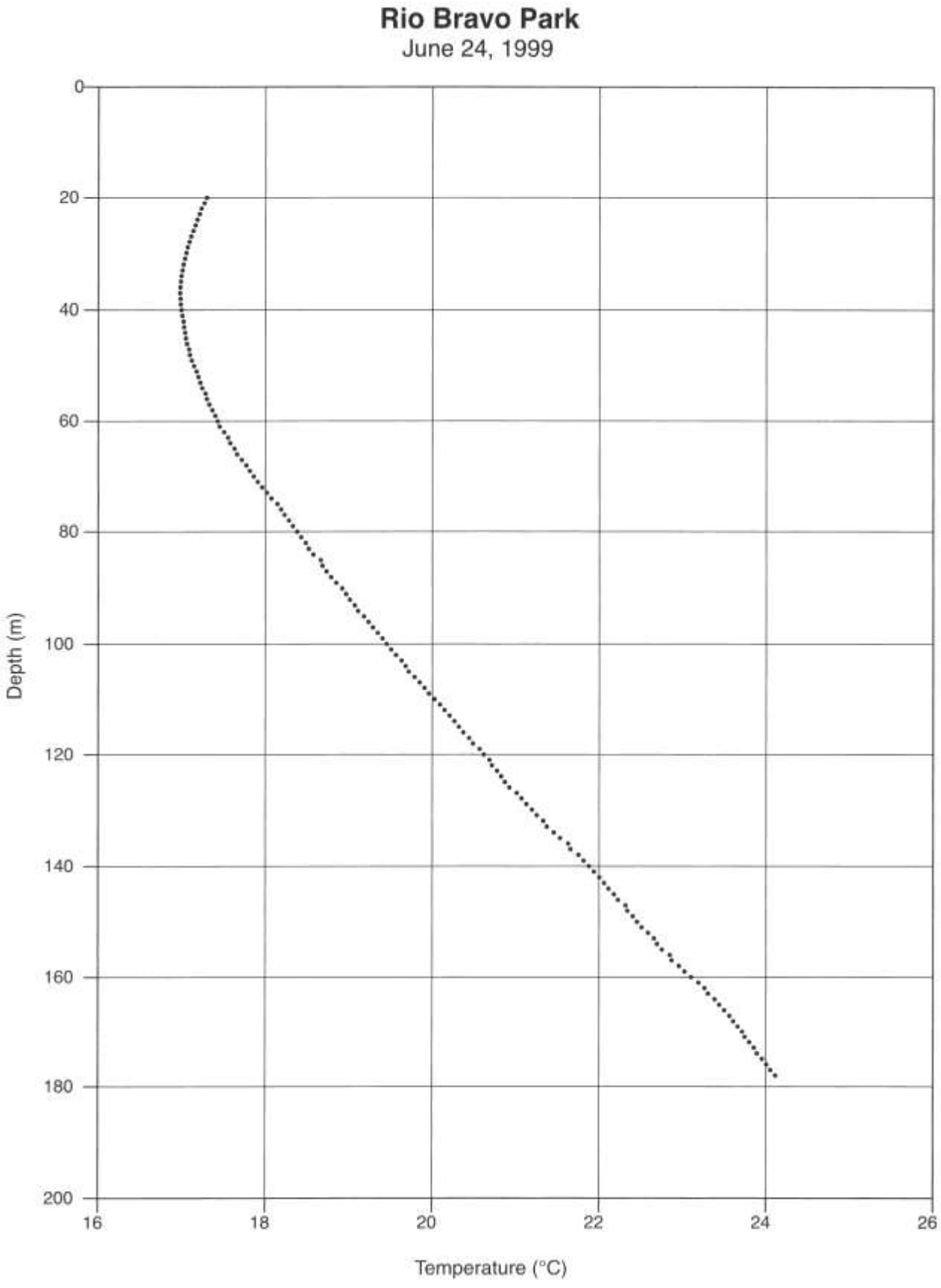

FIGURE 2–10a—First T log at Rio Bravo Park site, modified from Reiter (2001a).

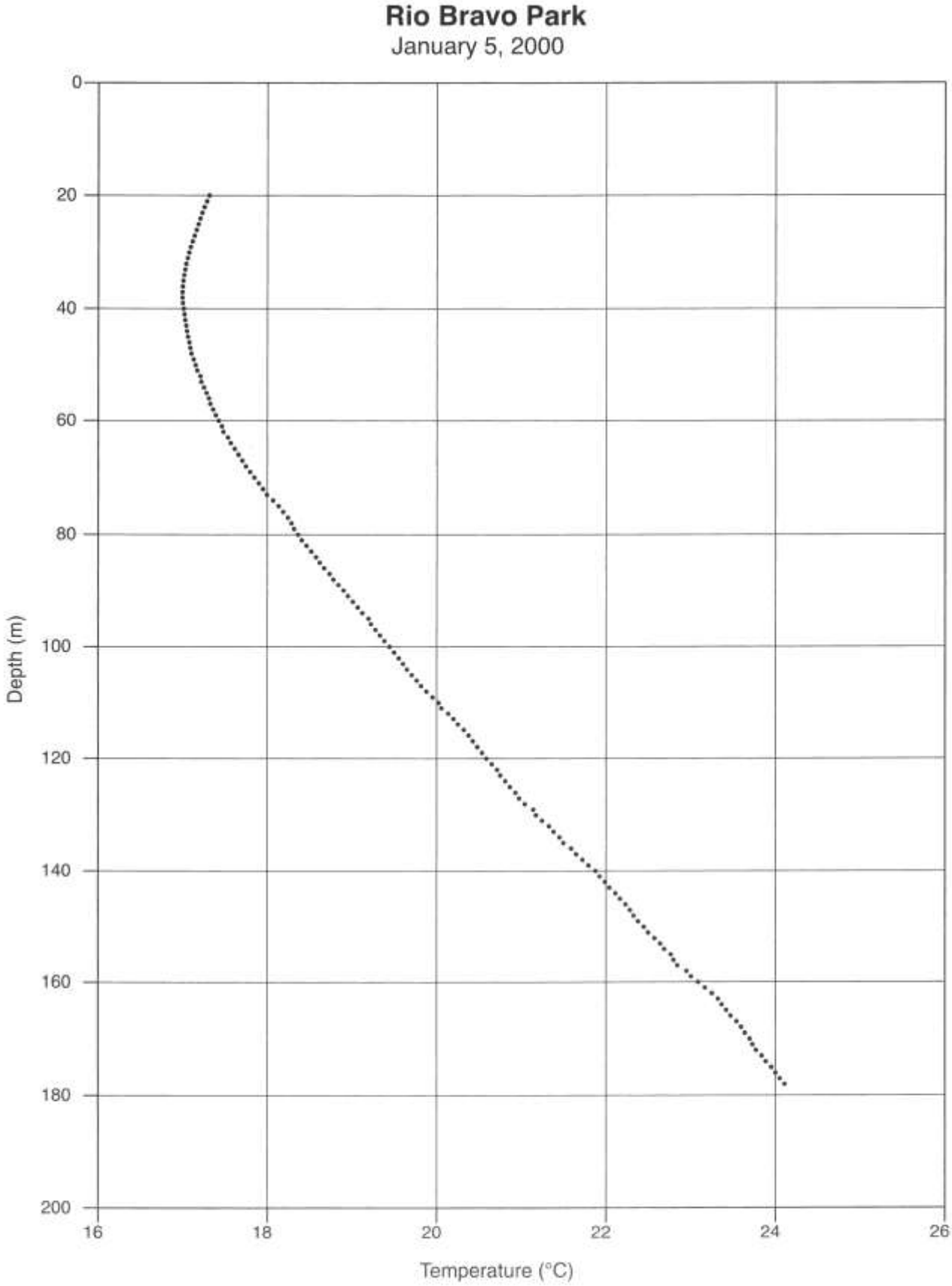

FIGURE 2–10b—Second T log at Rio Bravo Park site.

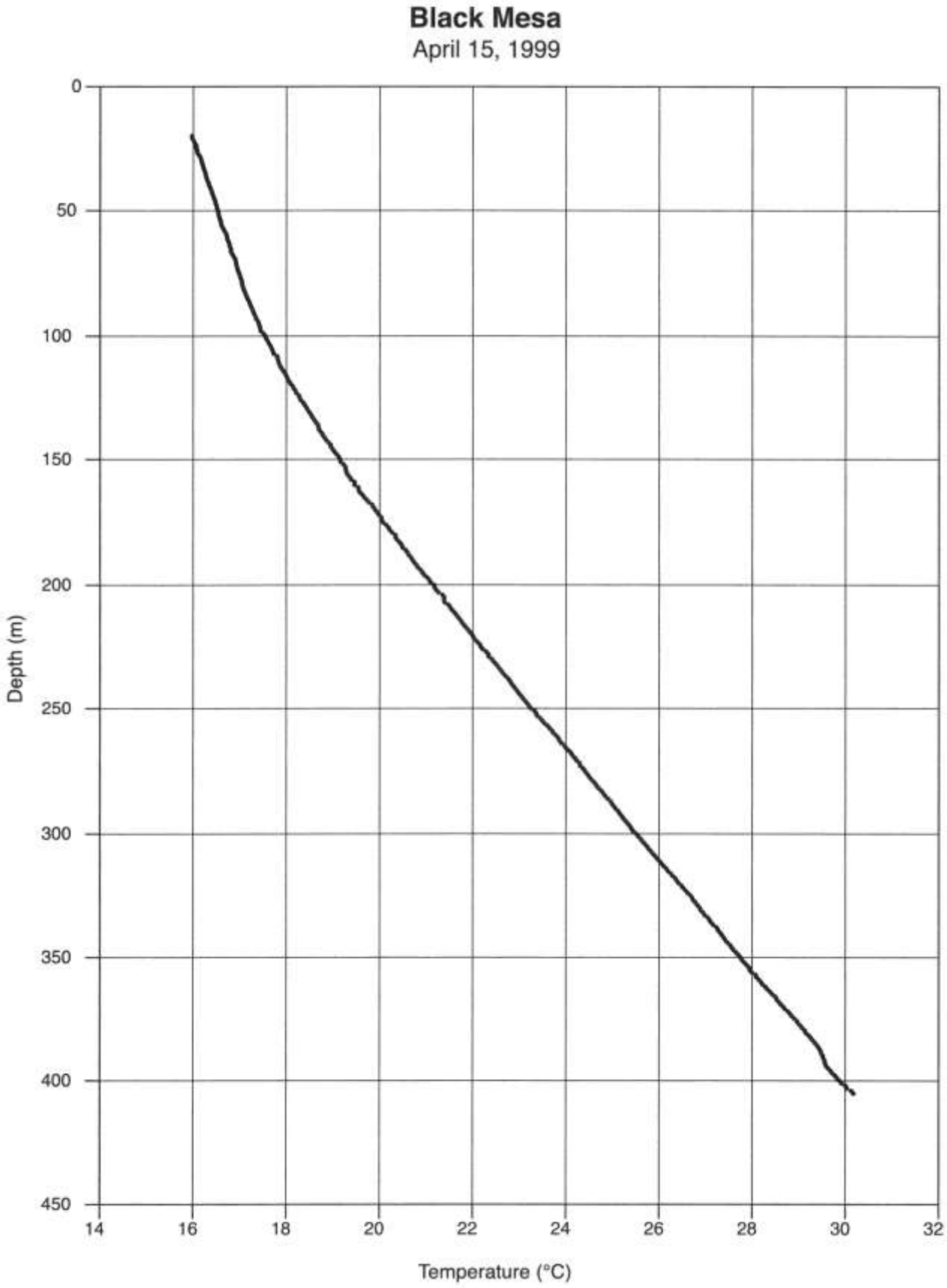

FIGURE 2–11—T log at Black Mesa site.

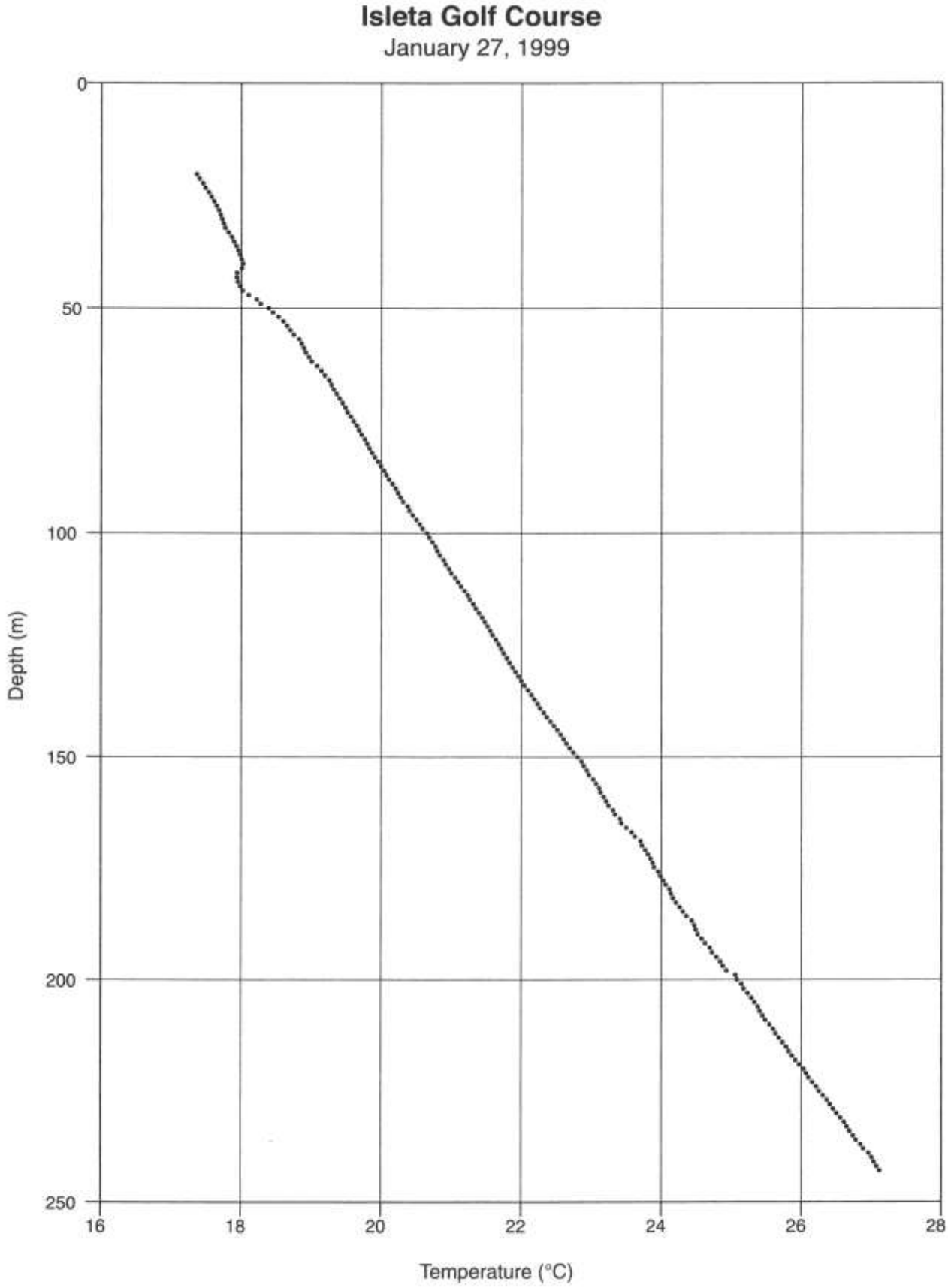

FIGURE 2–12—T log at Isleta Golf Course site.

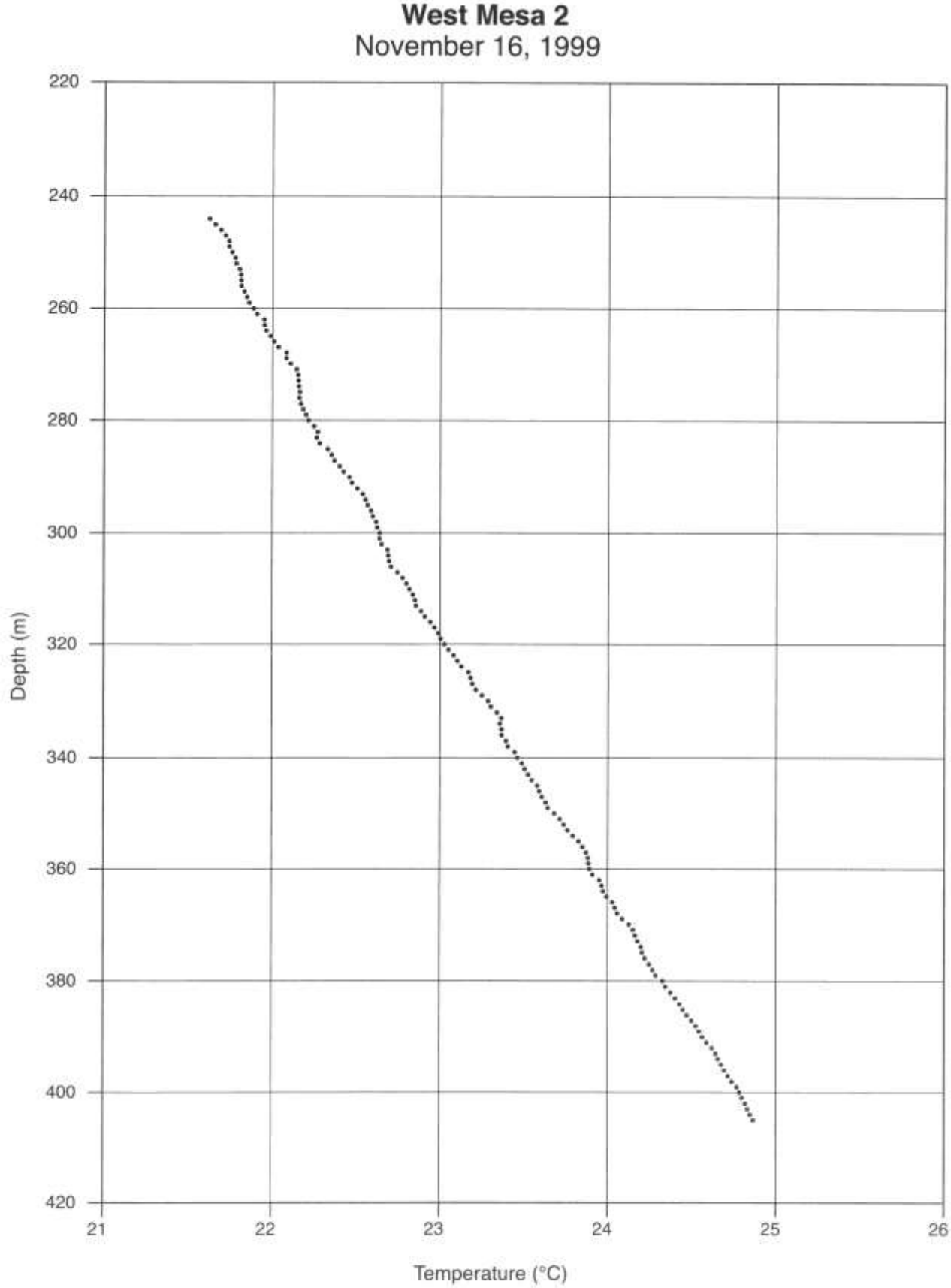

FIGURE 2–13—T log at West Mesa 2 site. Much of the erratic nature of the T log results because of the casing pinching the temperature sensor connection.

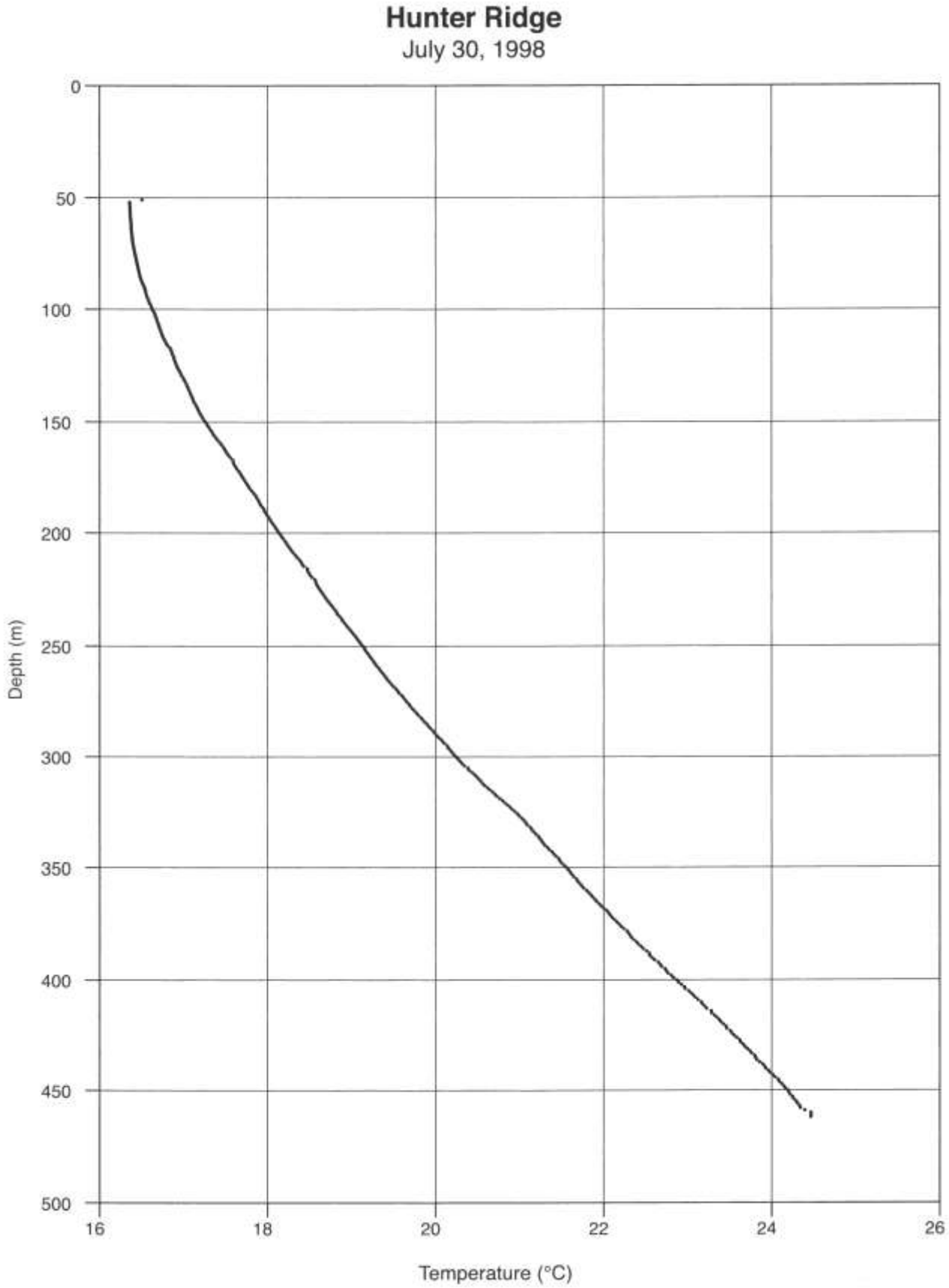

FIGURE 2–14—T log at Hunter Ridge site.

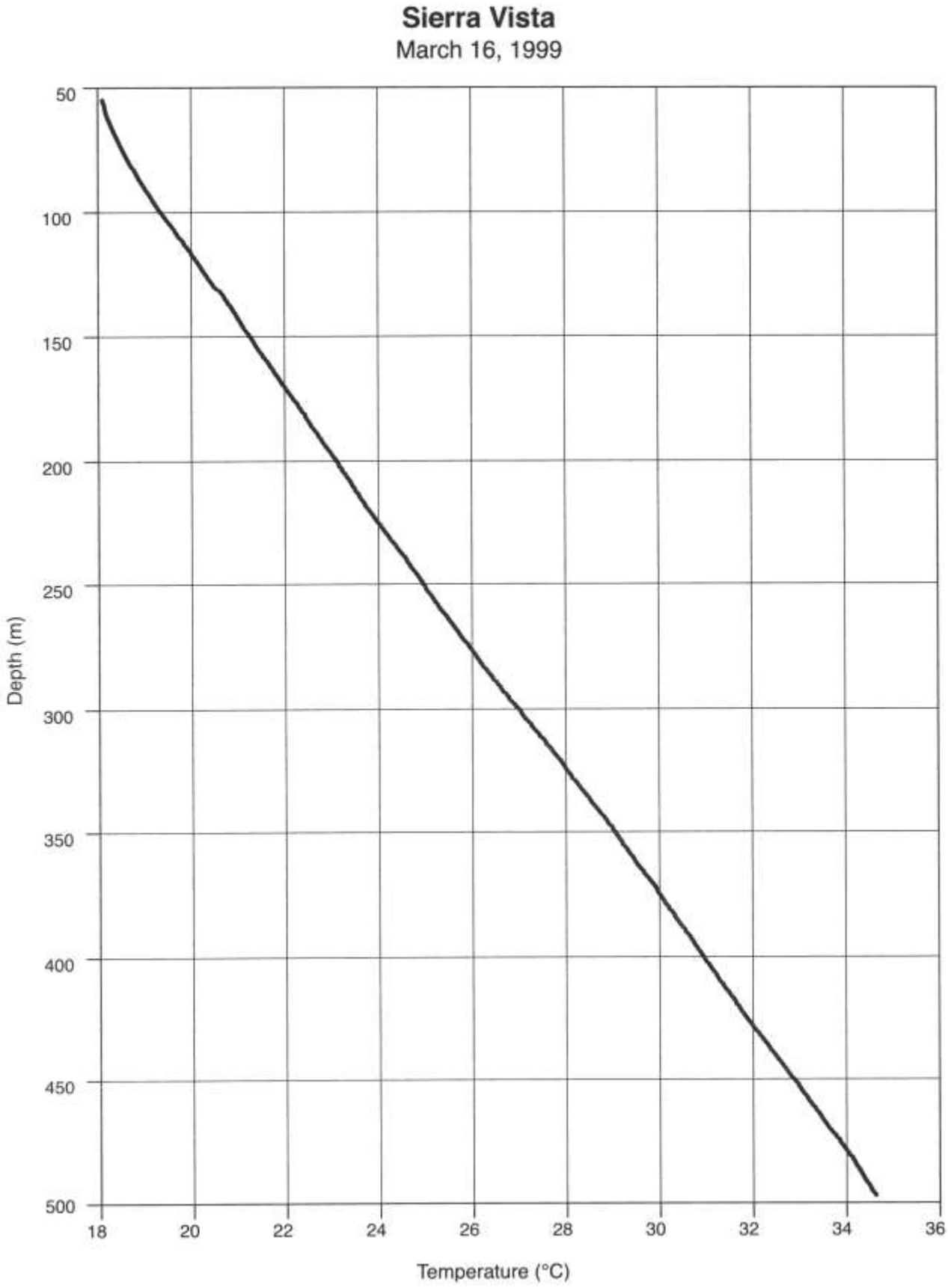

FIGURE 2–15—T log at Sierra Vista site.

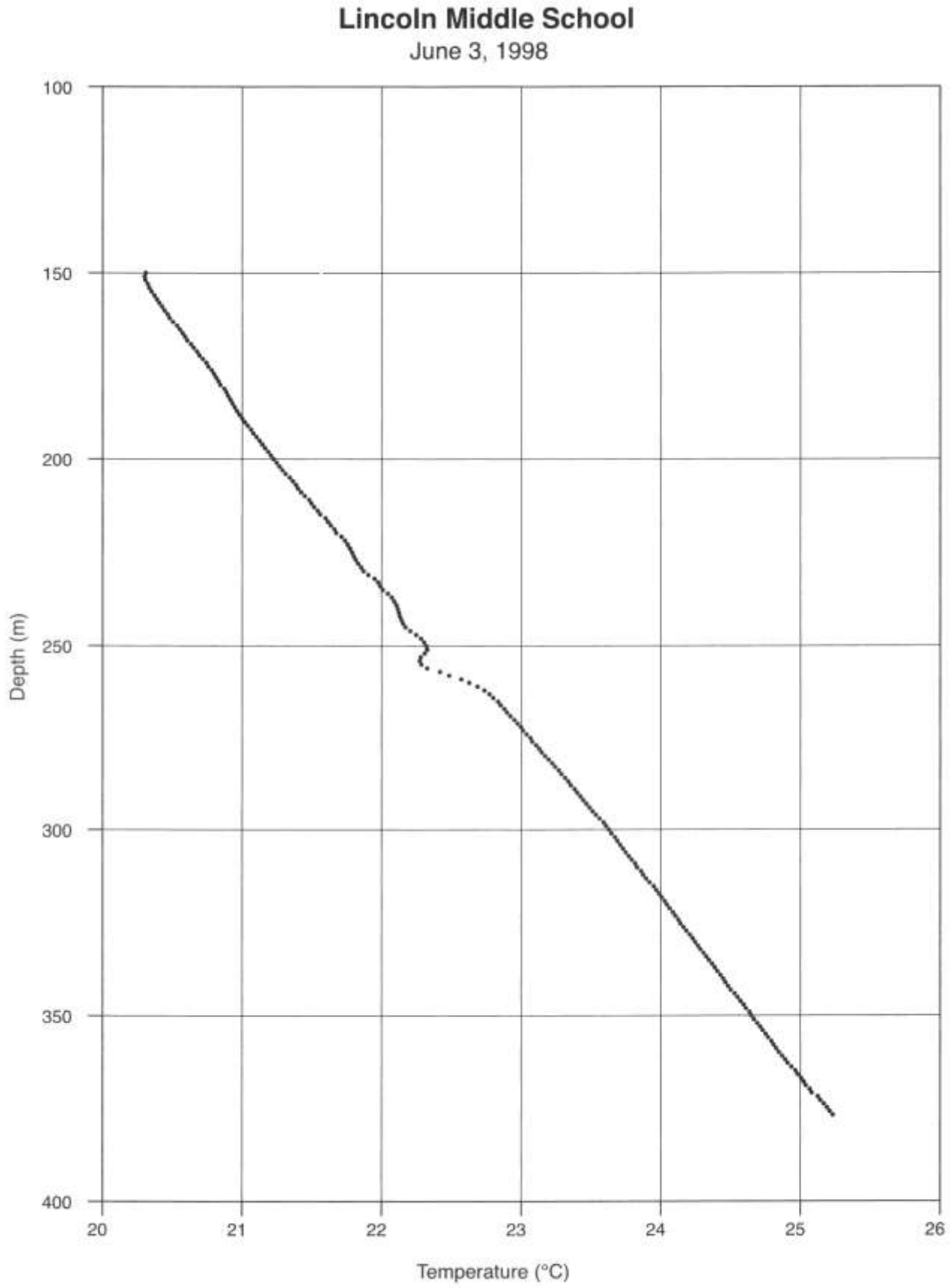

FIGURE 2–16—T log at Lincoln Middle School site. Temperature data at ~225 m probably influenced by water circulation around screen.

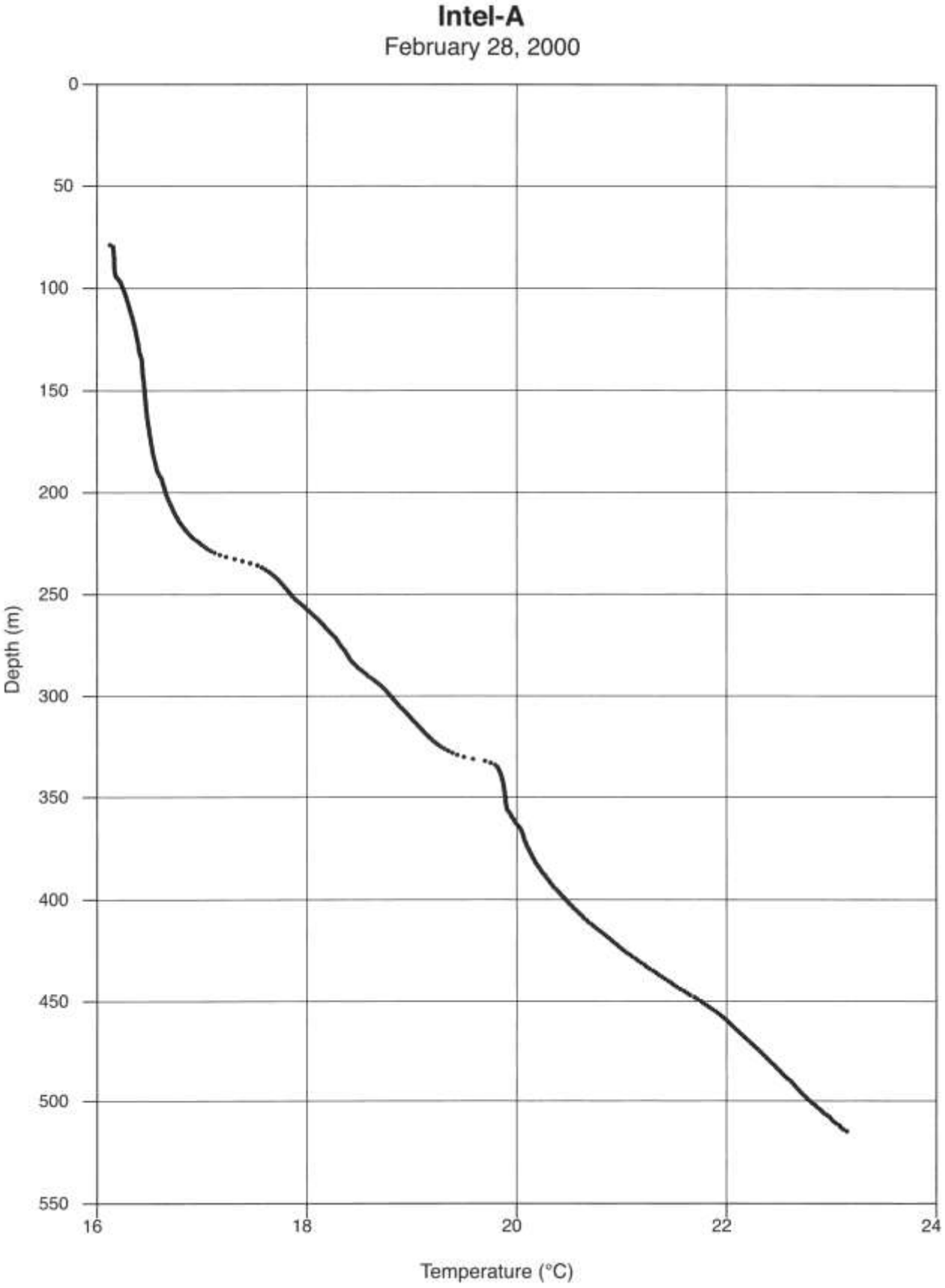

FIGURE 2-17—T log at Intel A site.

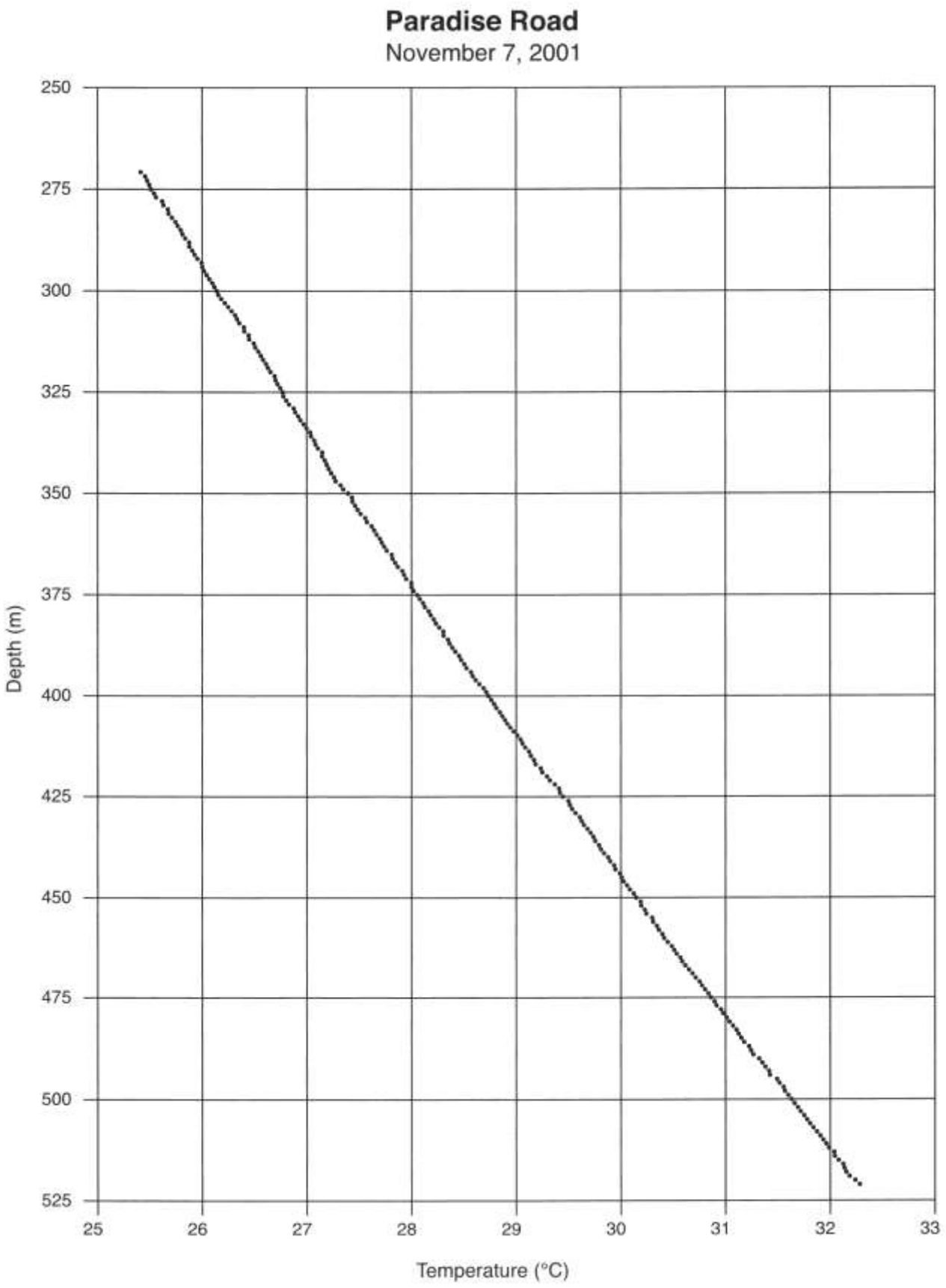

FIGURE 2–18—T log at Paradise Road site. T log made with same electronics as Westgate Heights, first log; see Appendix 2–20a.

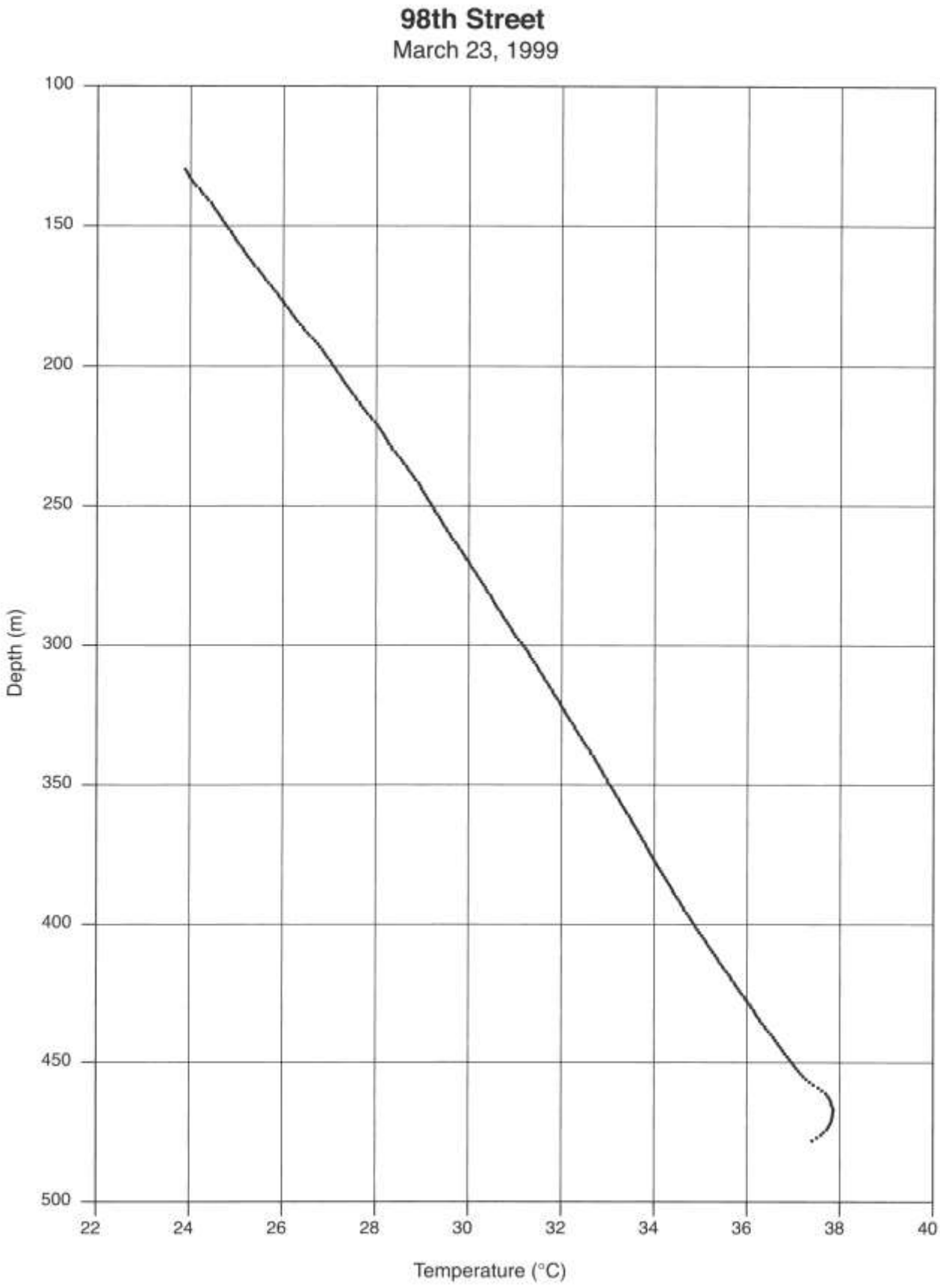

FIGURE 2–19—T log at 98th Street site. Temperature data from ~460 m to ~475 m probably influenced by circulation around screen.

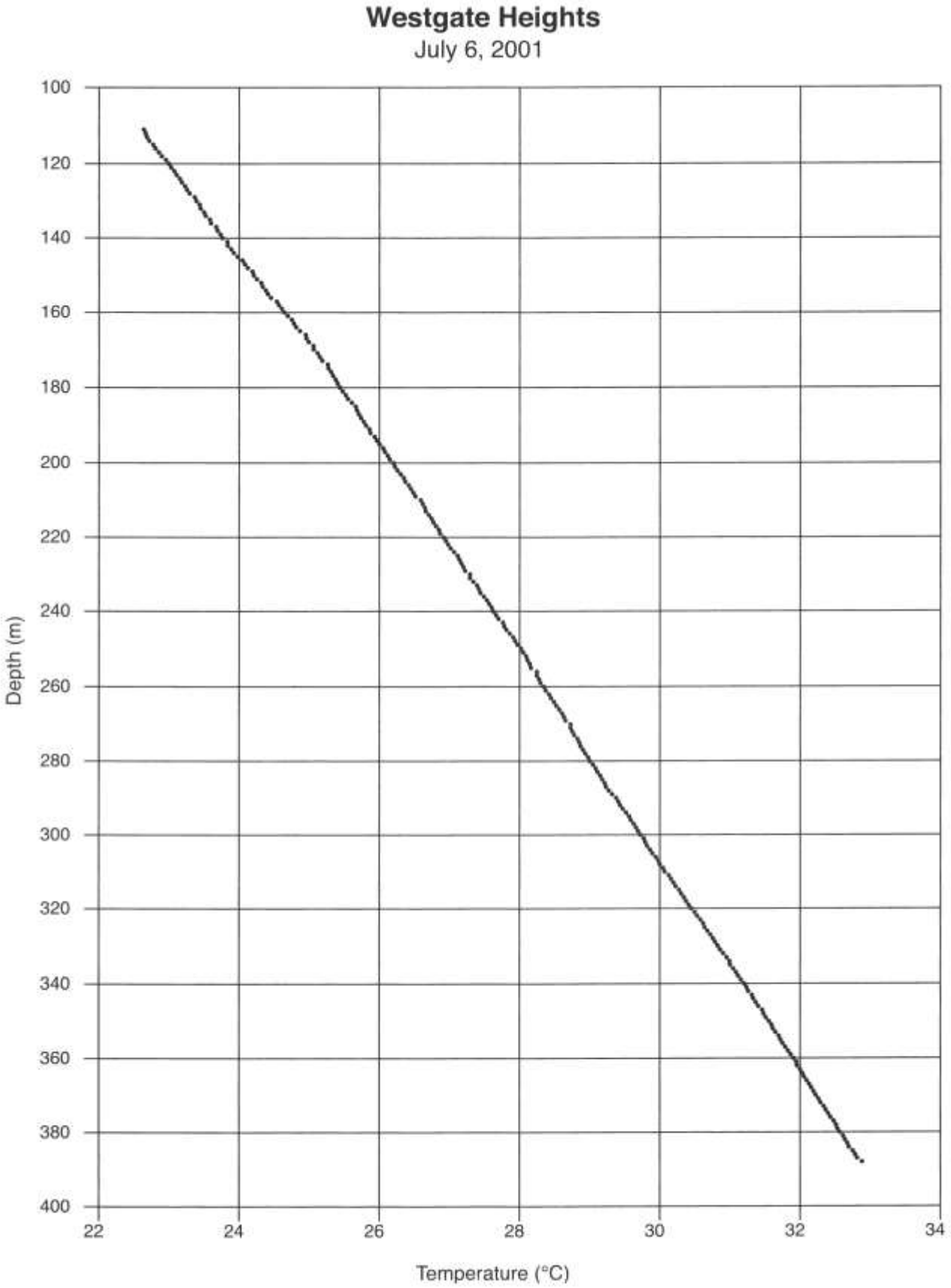

FIGURE 2–20a—T log at Westgate Heights site. Note: first T log at Westgate Heights and Niese made with sensing electronics set at lower accuracy level, second T log made using sensing electronics with higher accuracy, the same as for most sites. See Appendix 1, Table 1, for slight differences in results.

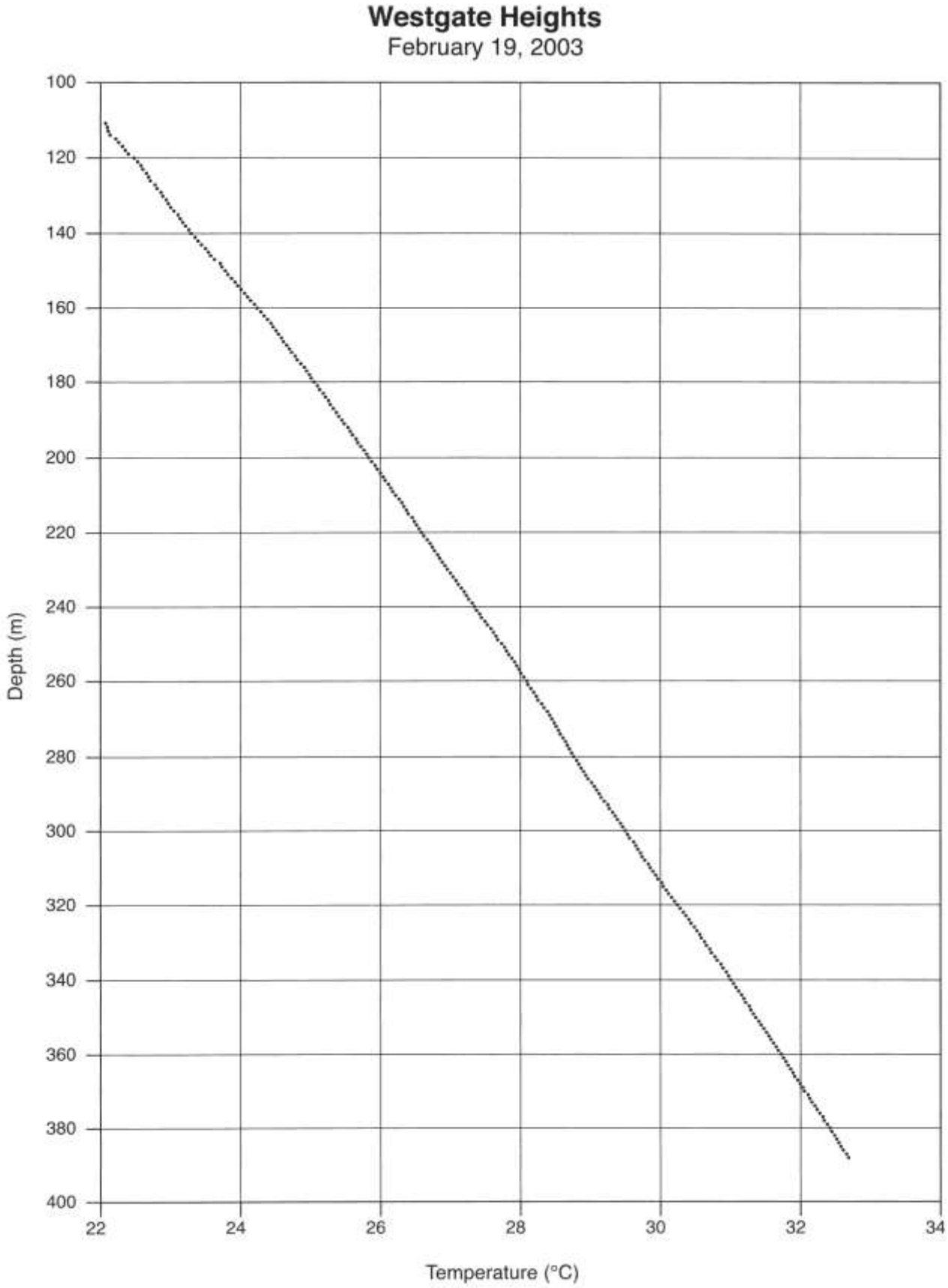

FIGURE 2–20b—Second T log at Westgate Heights site; see Appendix 2–20a.

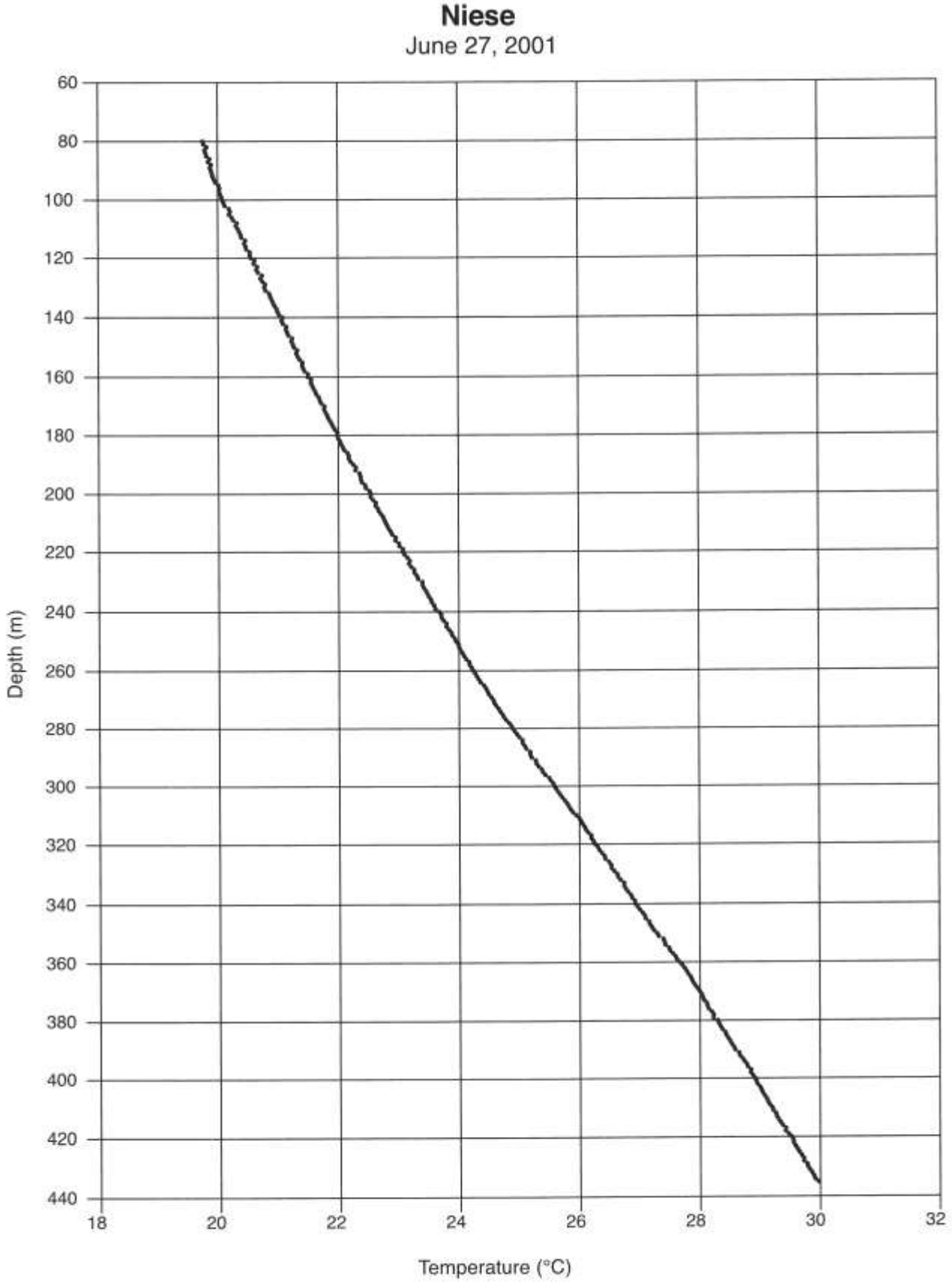

FIGURE 2–21a—T log at Niese site. See Appendix 2–20a for explanation of electronics.

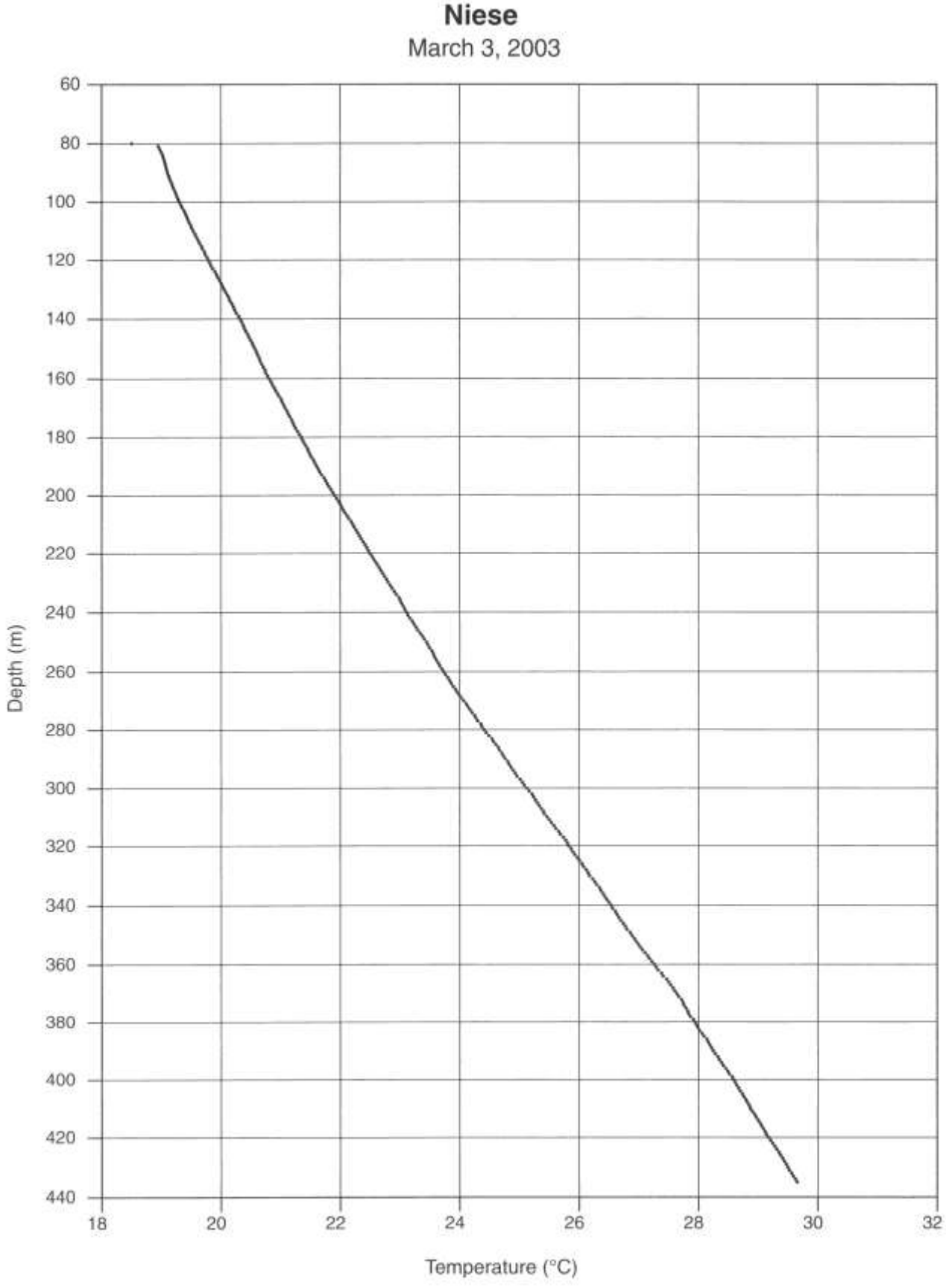

FIGURE 2–21b—Second T log at Niese site; see Appendix 2–20a.

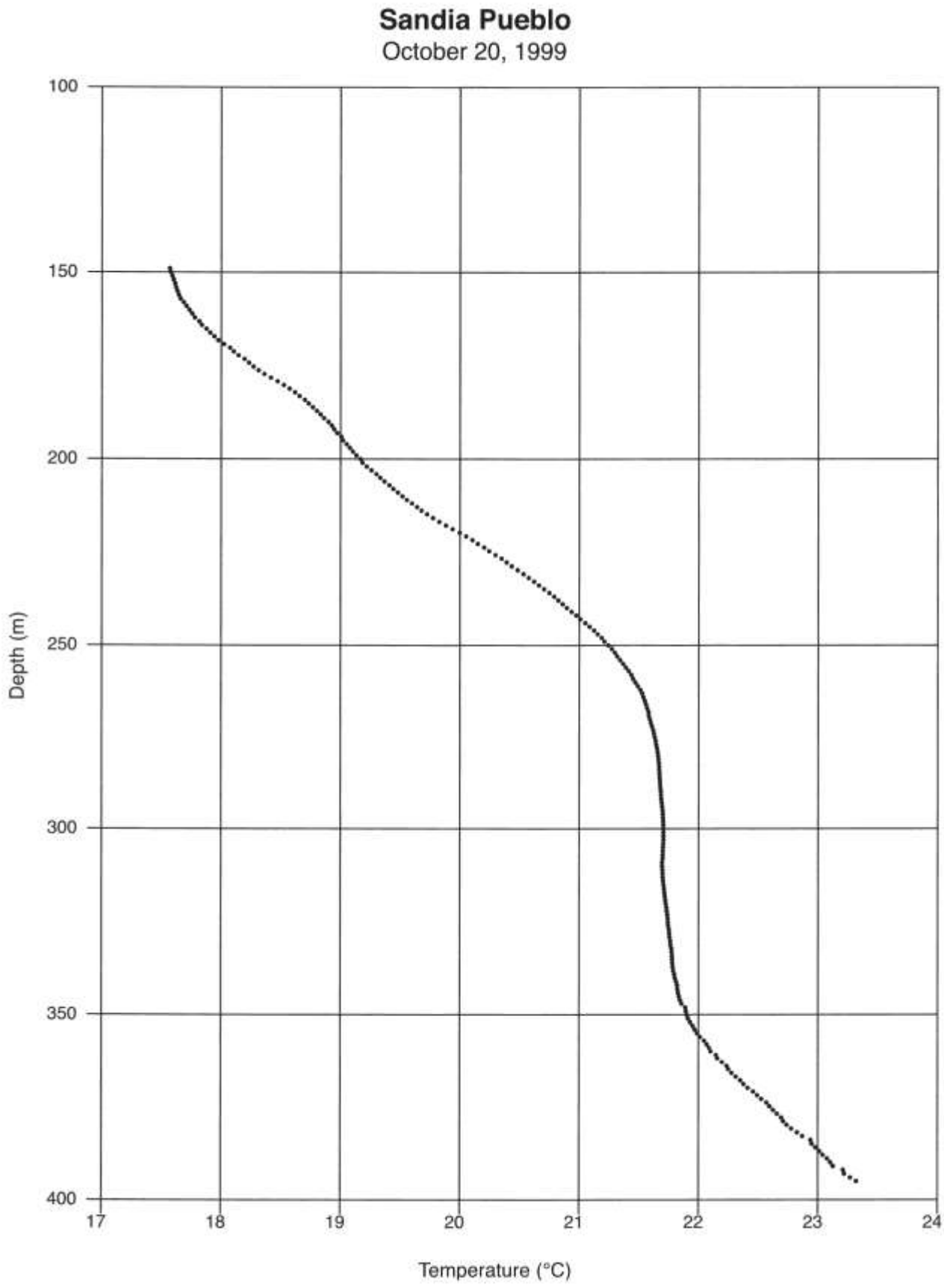

FIGURE 2–22—T log at Sandia Pueblo site. (Fault crossing piezometer estimated to be at 312 m, with cool down flow.)

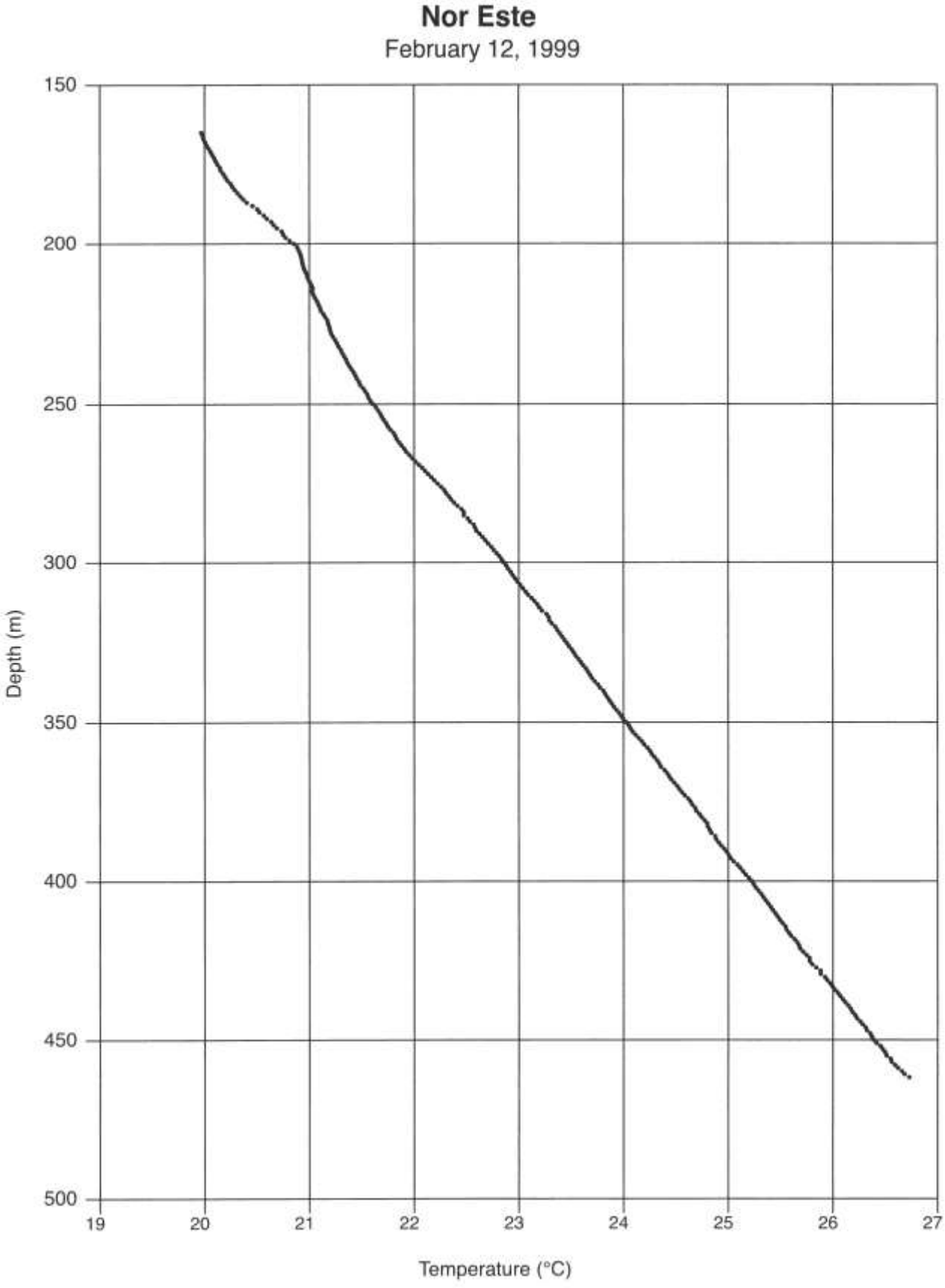

FIGURE 2–23—T log at Nor Este site.

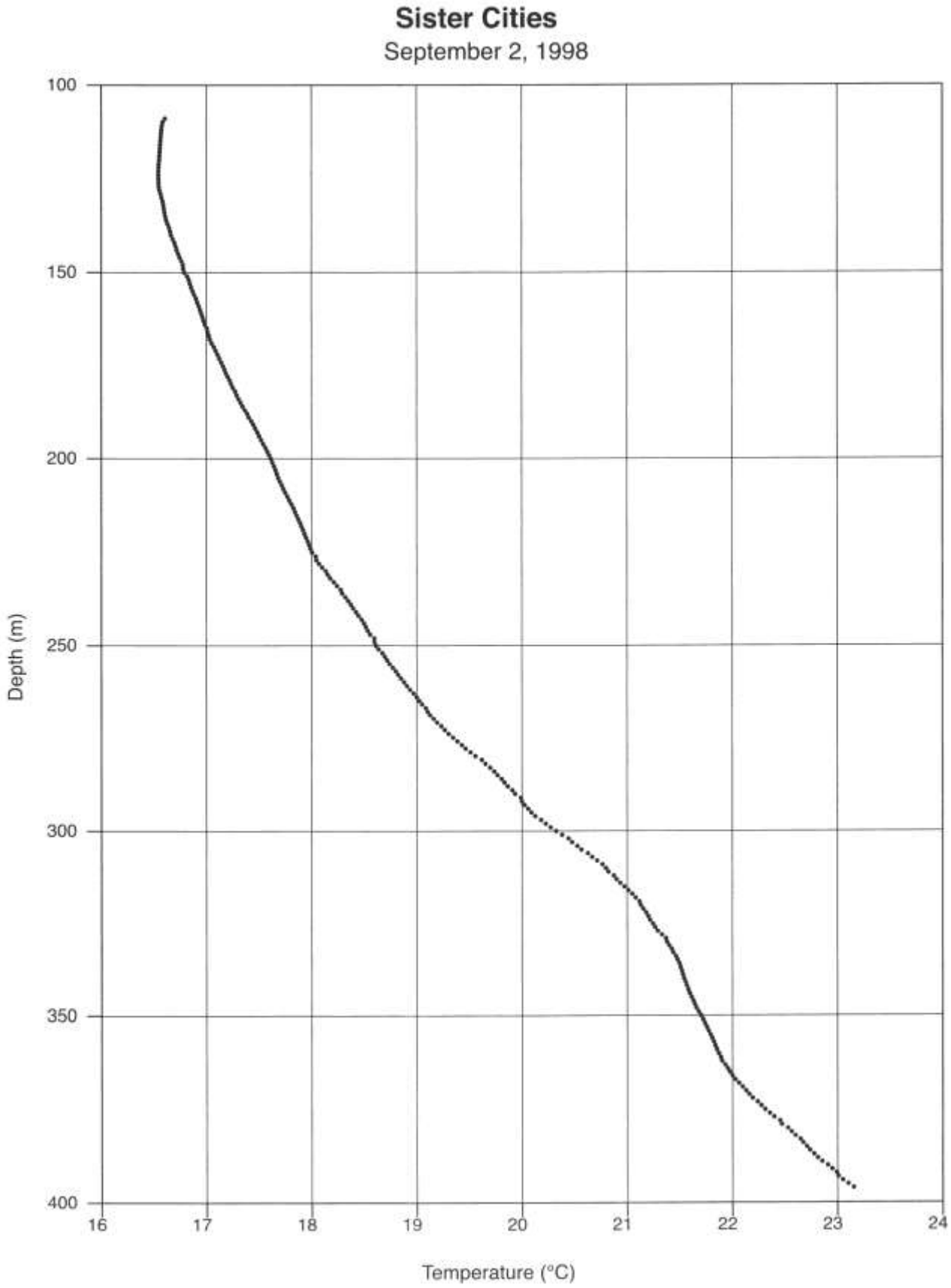

FIGURE 2–24—T log at Sister Cities site.

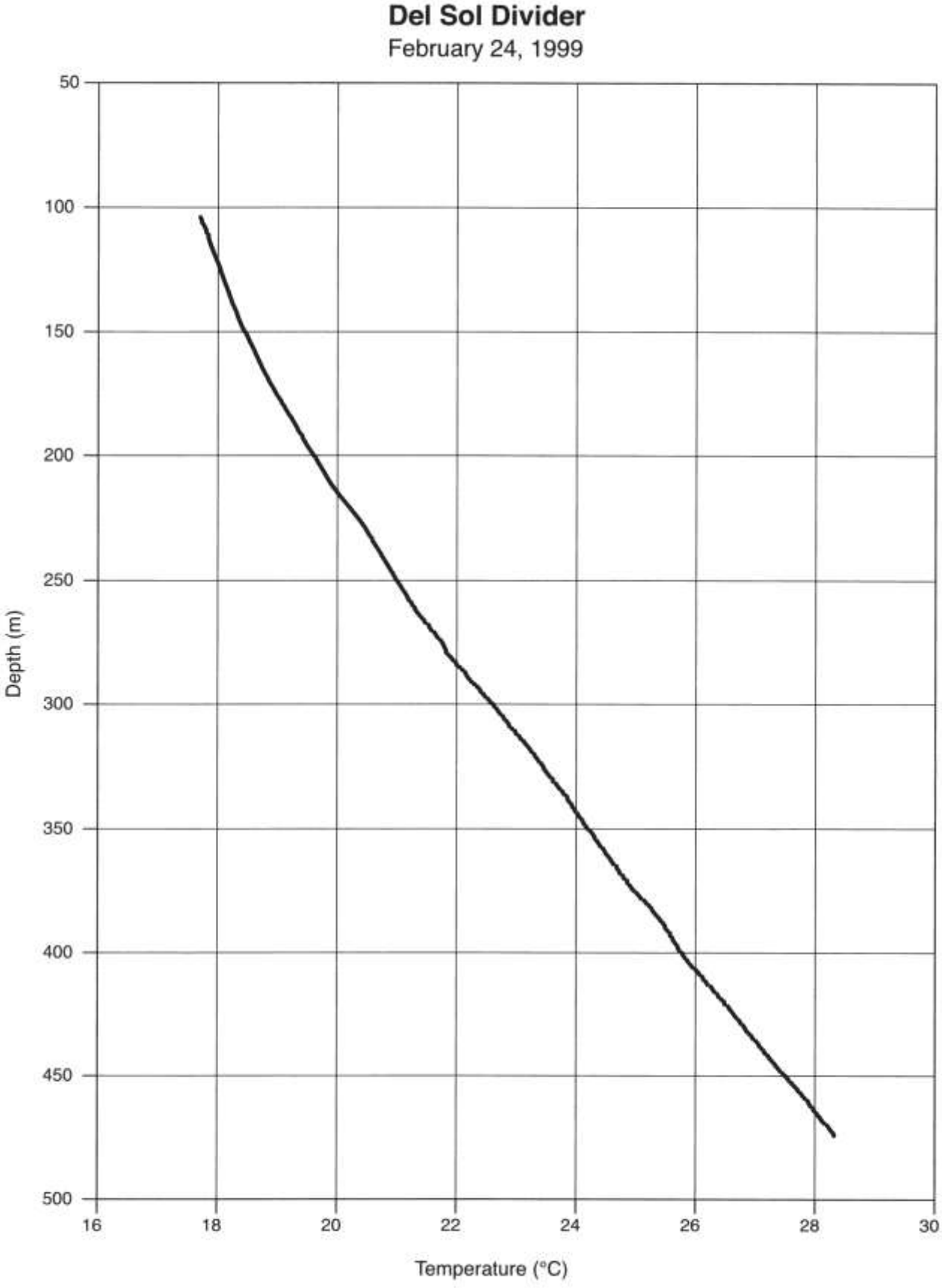

FIGURE 2–25—T log at Del Sol Divider site.

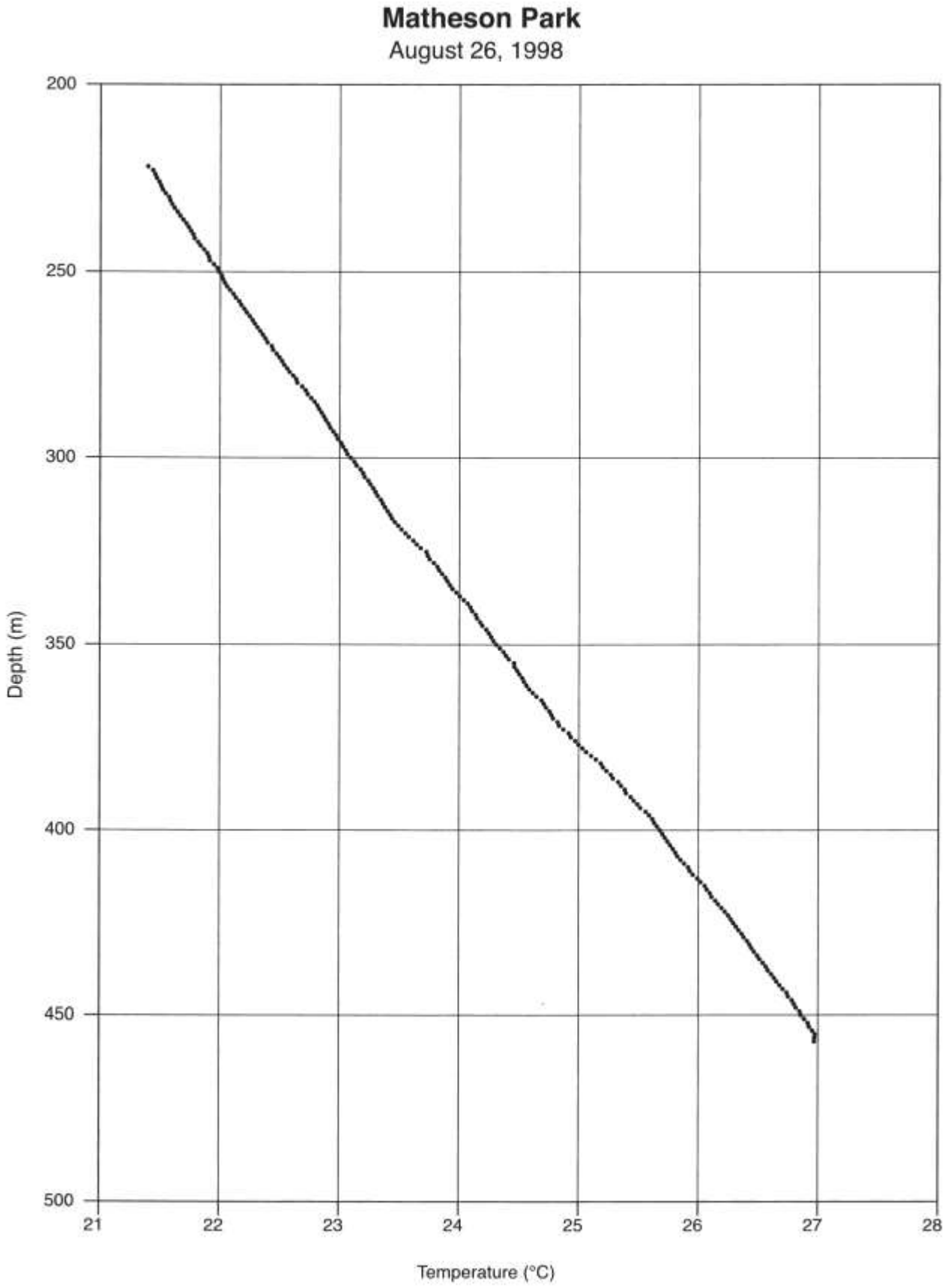

FIGURE 2–26–T log at Matheson Park site.

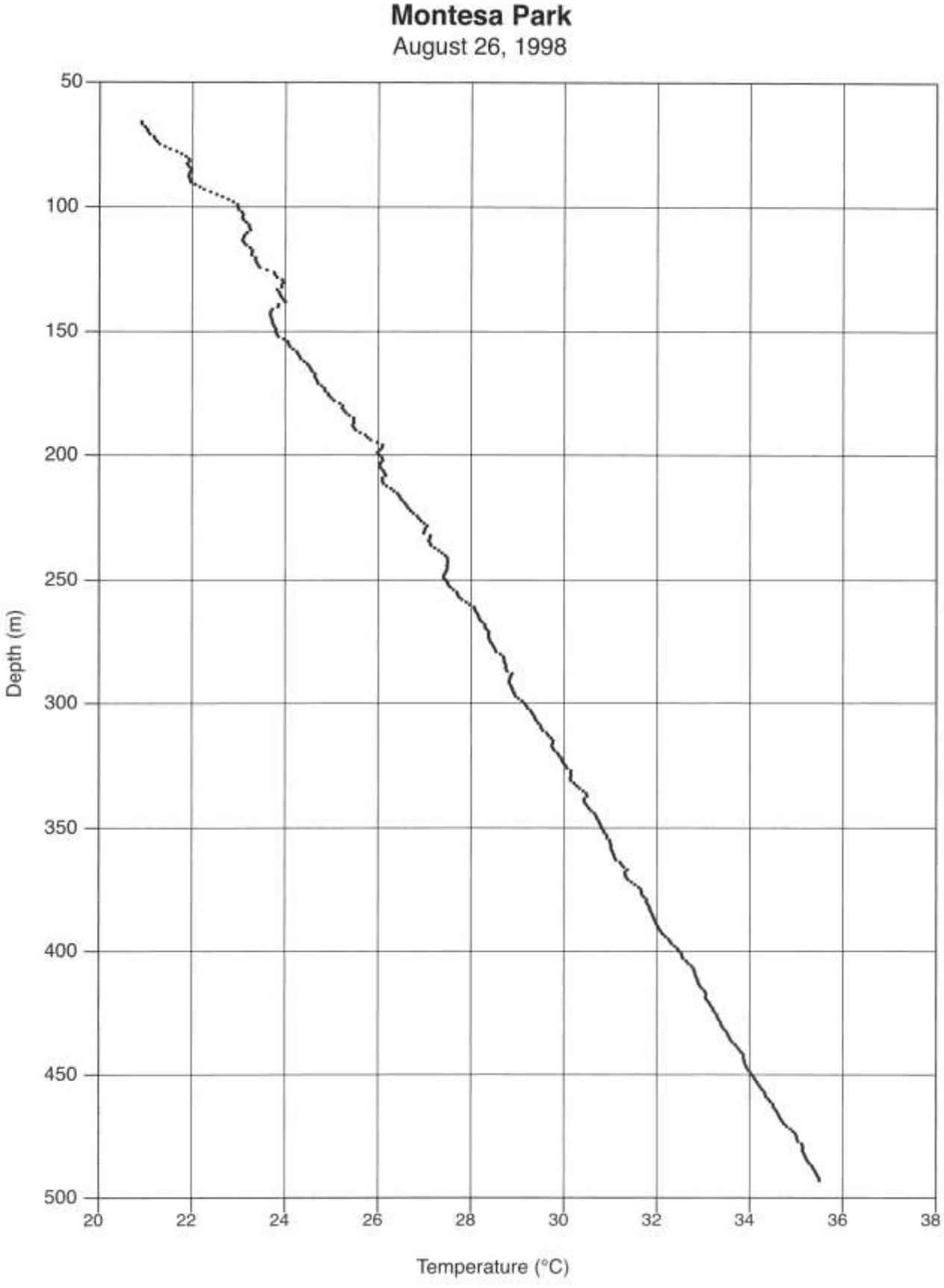

FIGURE 2–27a—T log at Montesa Park site, modified from Reiter (2001b).

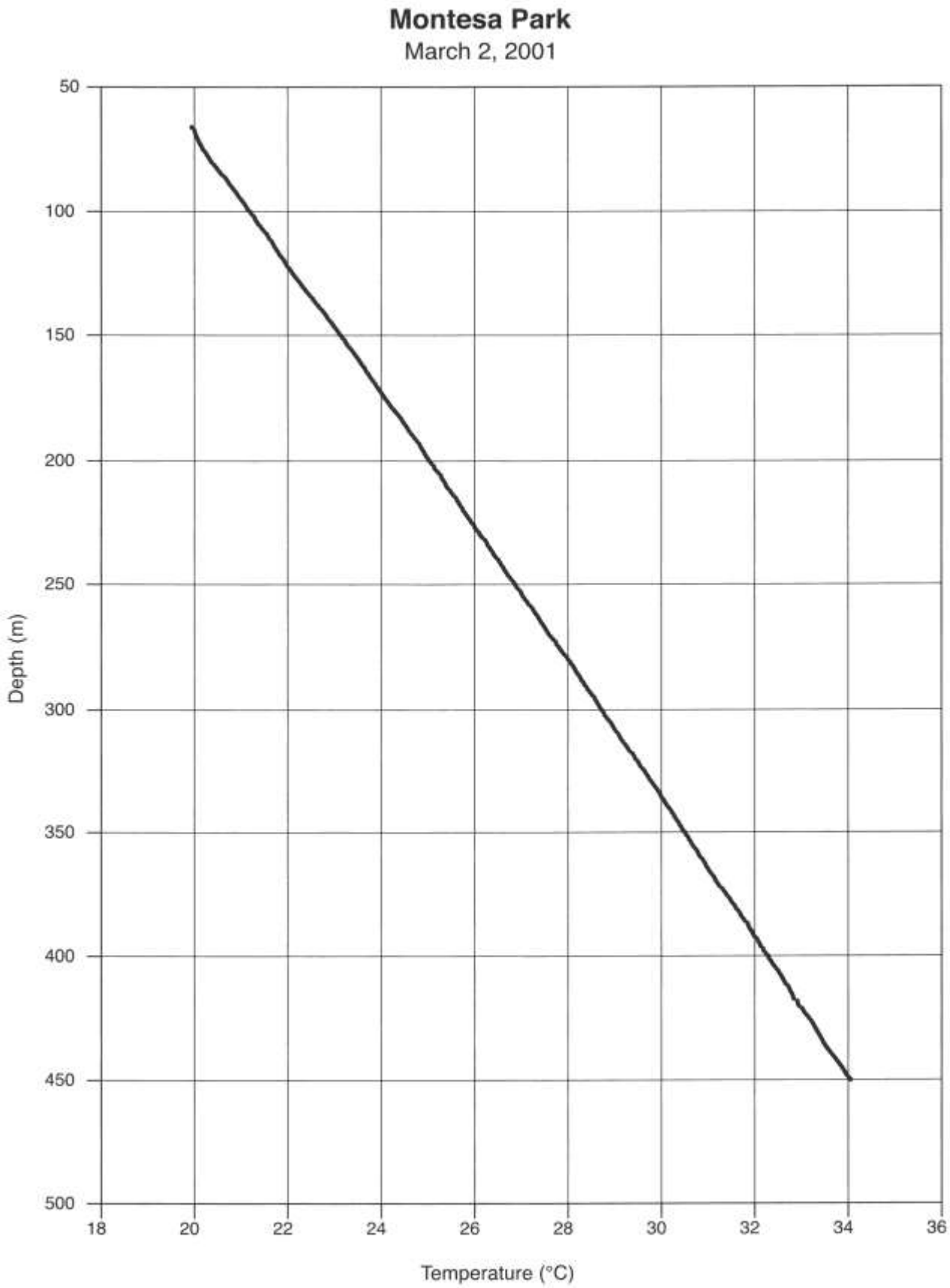

FIGURE 2–27b—Second T log at Montesa Park site.

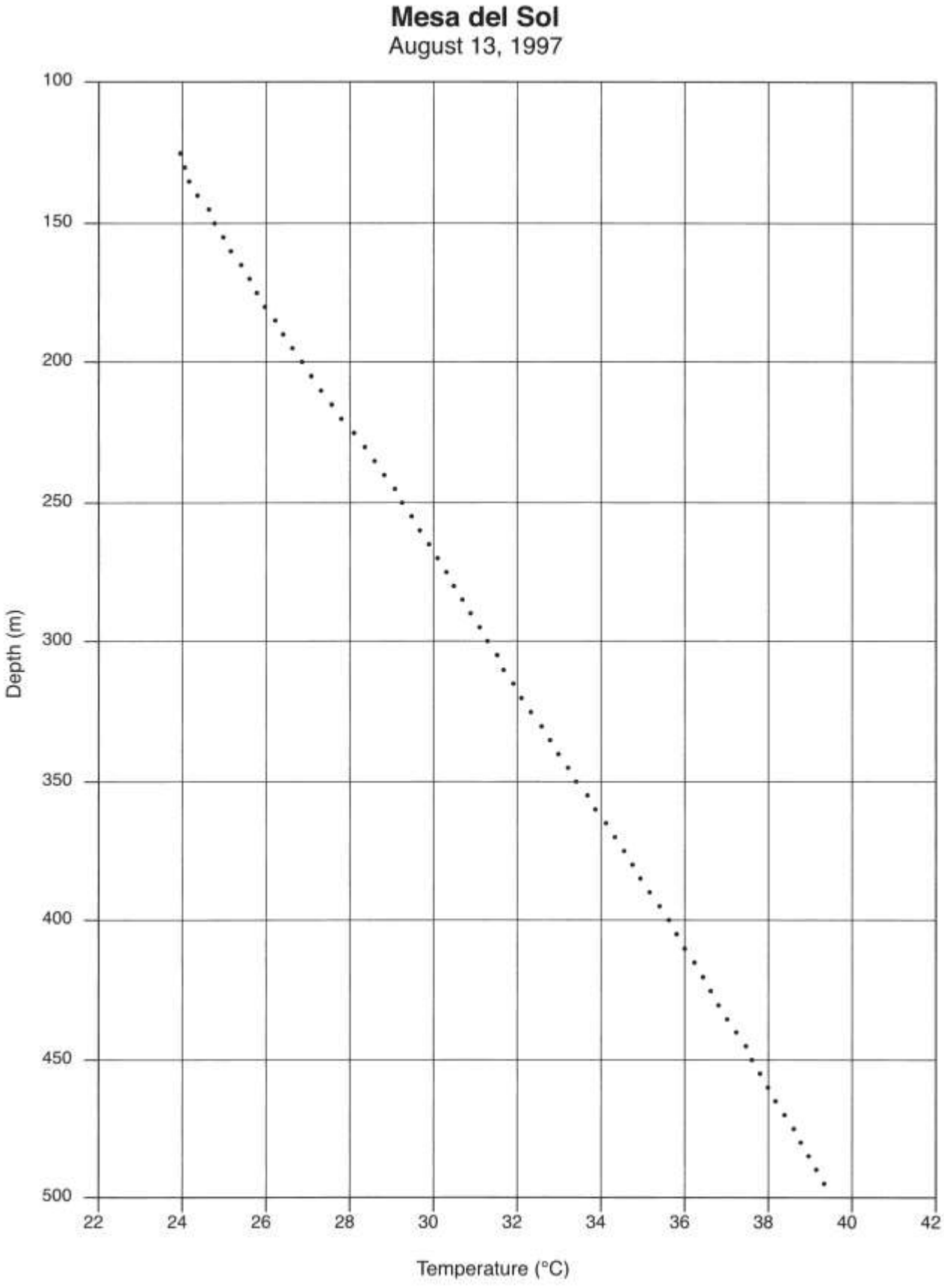

FIGURES 2–28a—First T log at Mesa del Sol site, modified from Reiter (1999, 2001b).

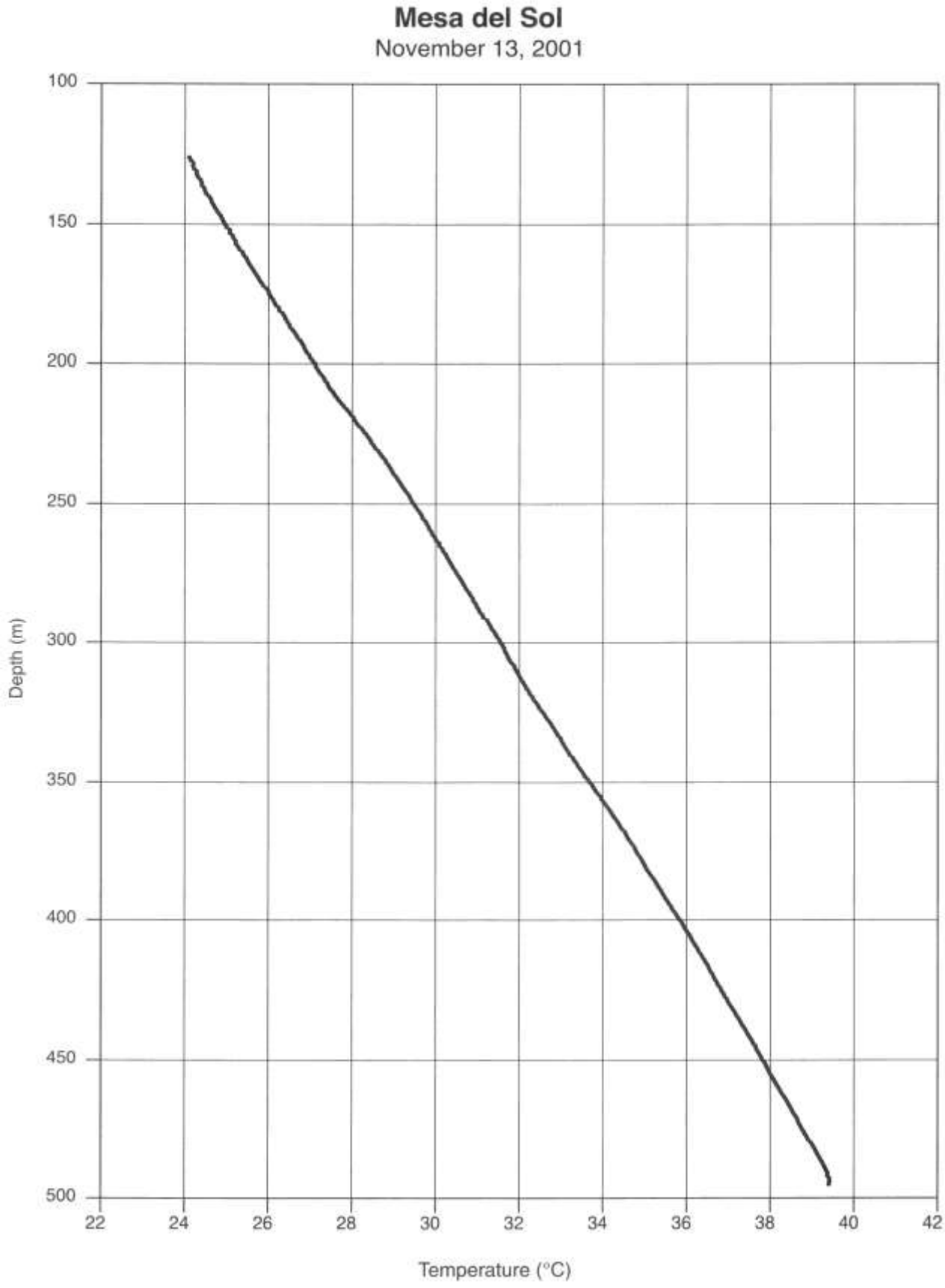

FIGURE 2–28b—Second T log at Mesa del Sol site.

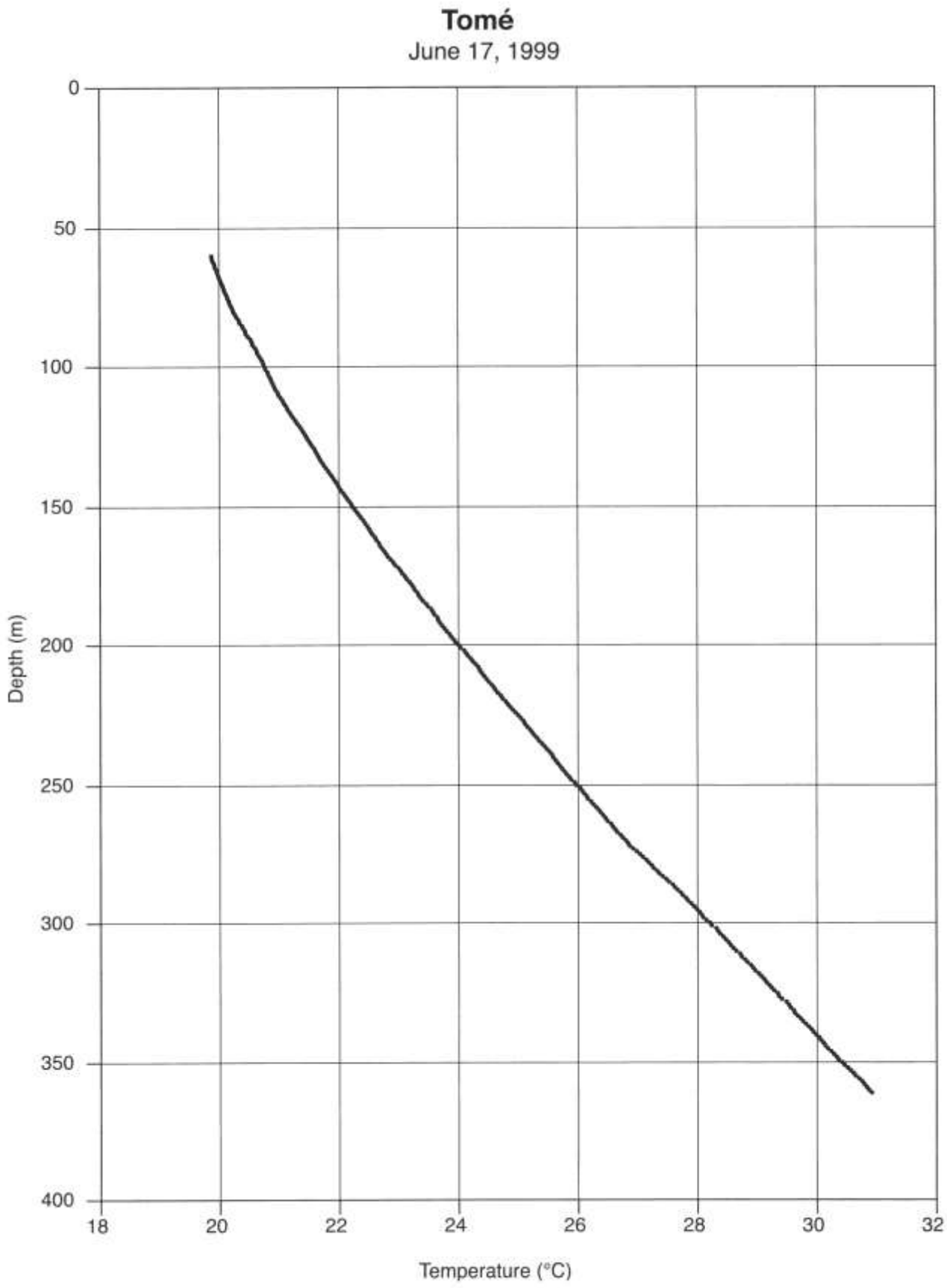

FIGURE 2–29—T log at Tomé site, modified from Reiter (2001a, 2001b).

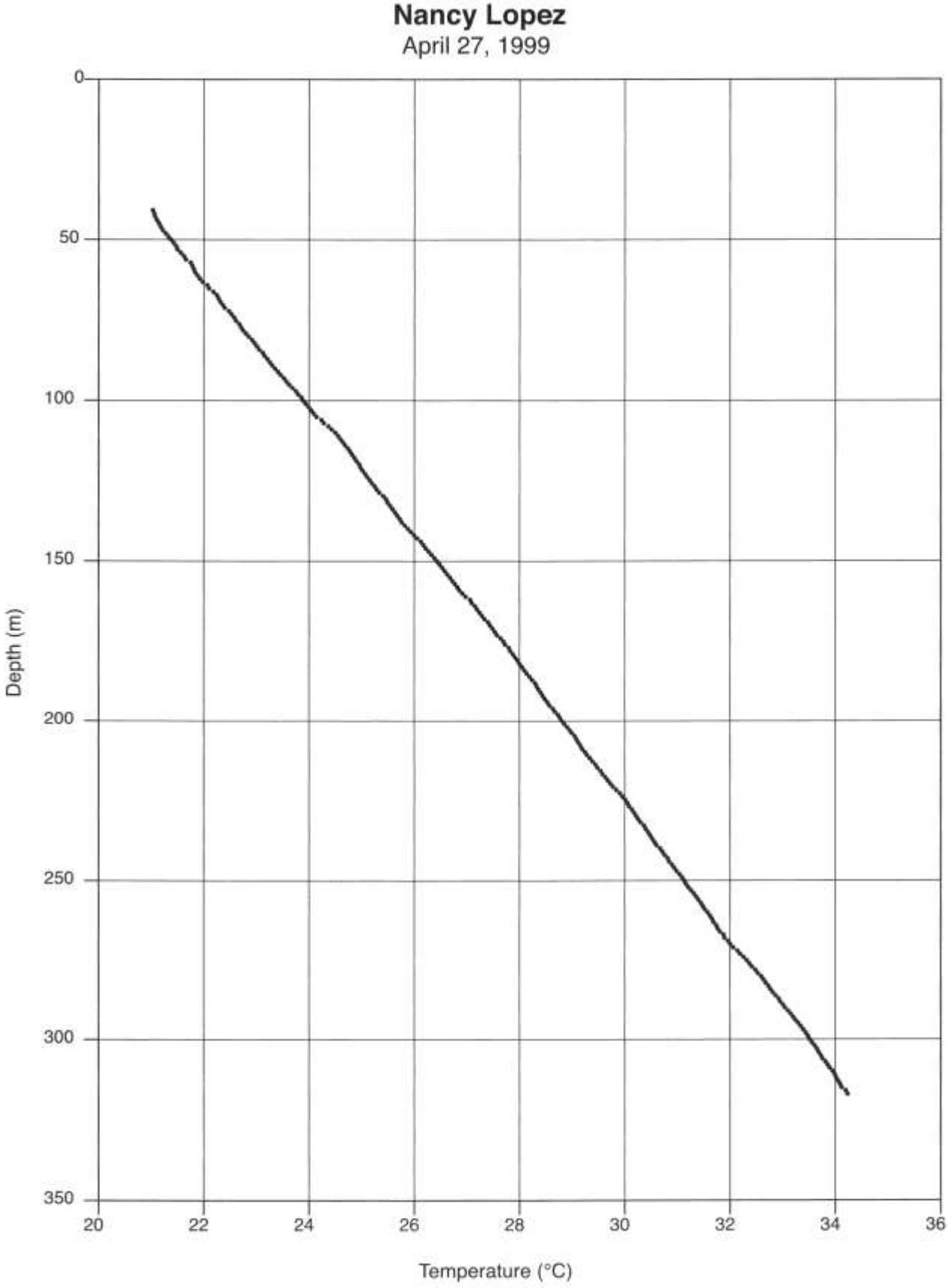

FIGURE 2–30—T log at Nancy Lopez site, modified from Reiter (2001b).

Appendix III

T logs on same scale for comparison; date logged indicated.

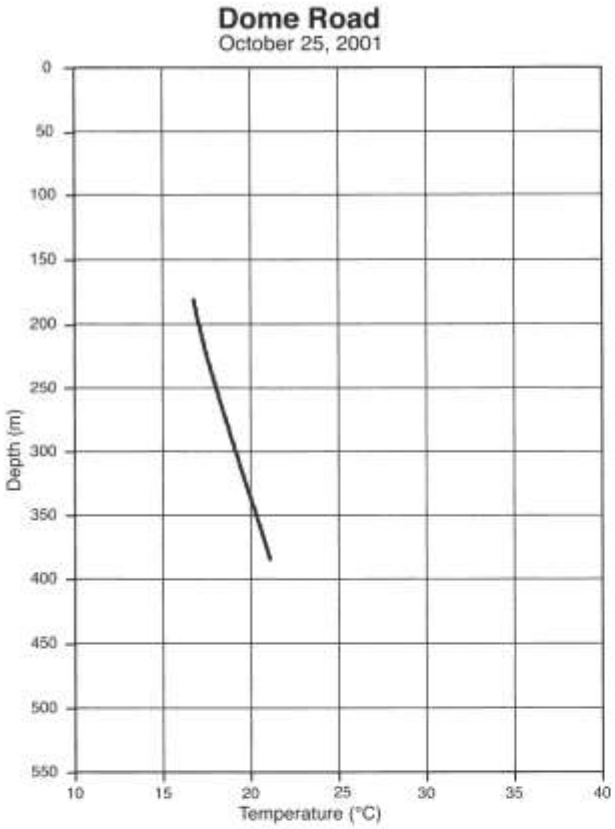

FIGURE 3–1—Temperature log (T log) at Dome Road site.

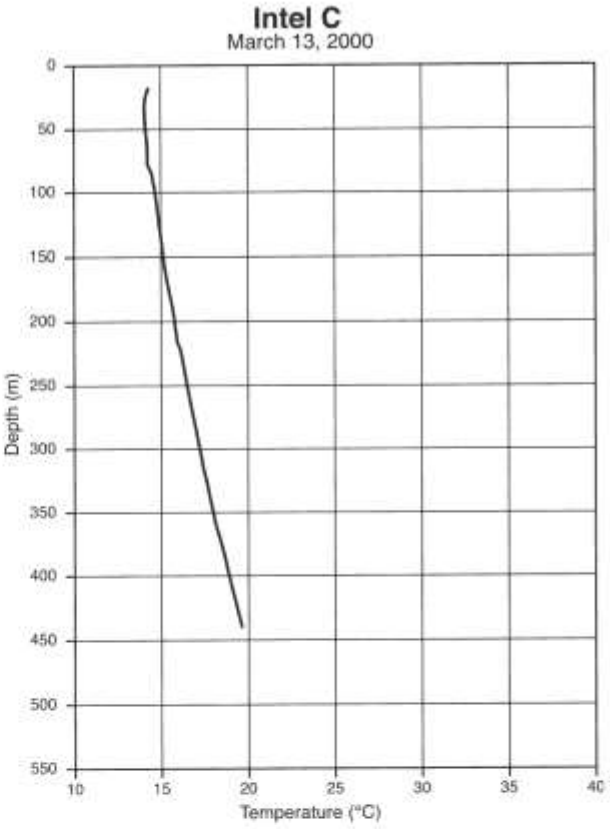

FIGURE 3–3—T log at Intel C site.

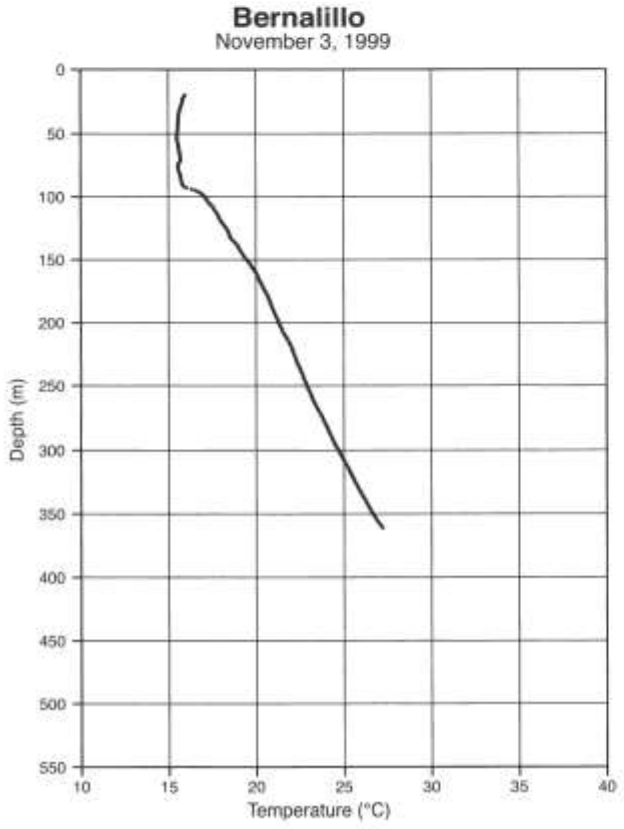

FIGURE 3–2—T log at Bernalillo site.

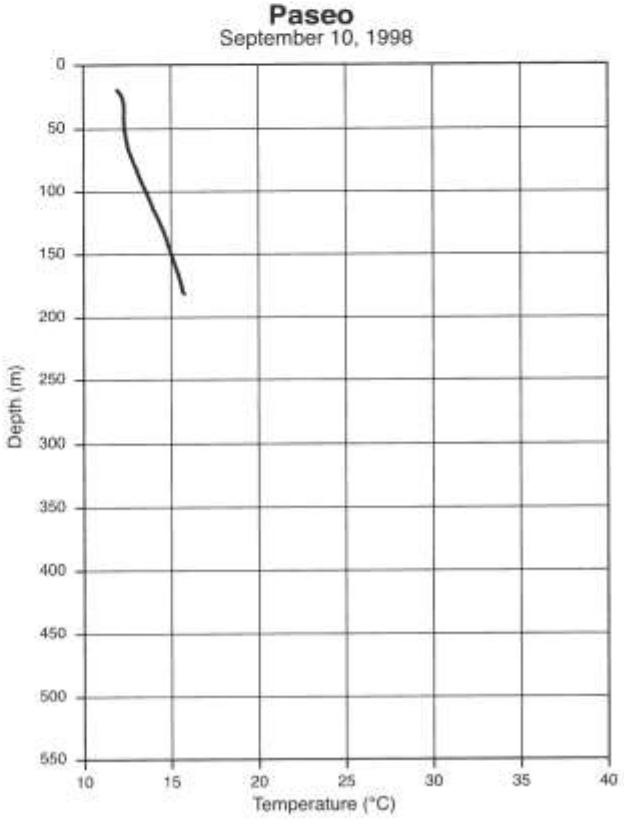

FIGURE 3–4—T log at Paseo site.

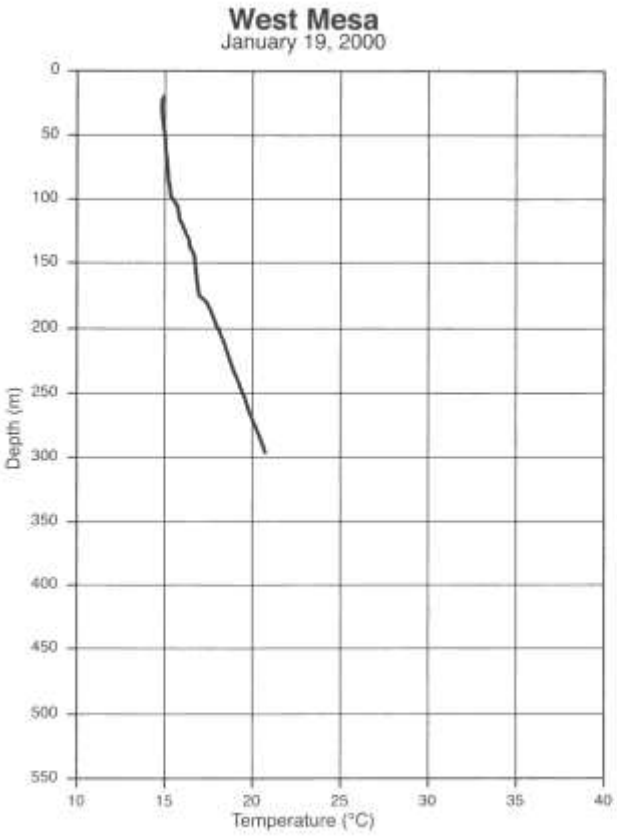

FIGURE 3–5—T log at West Mesa 3 site. Disturbances in T log to ~175 m caused to some extent by circulation near screens.

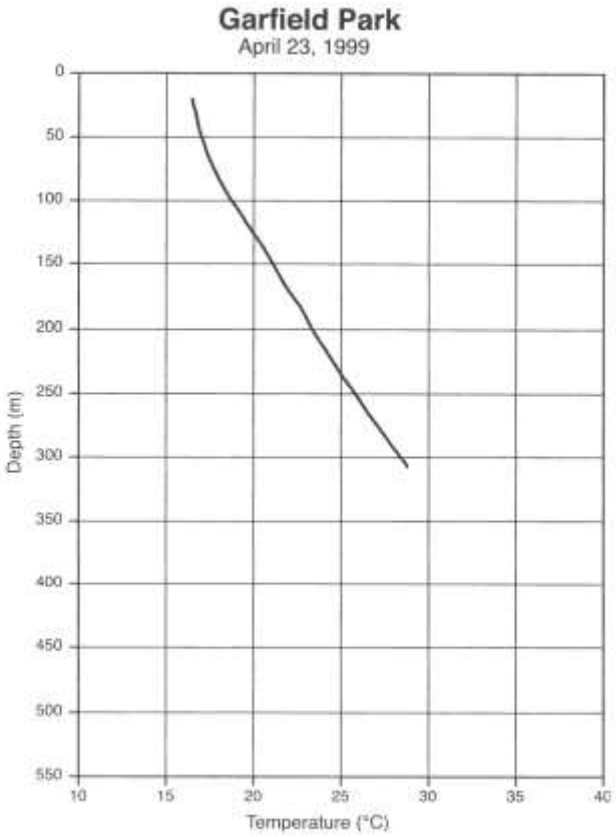

FIGURE 3–7—T log at Garfield Park site.

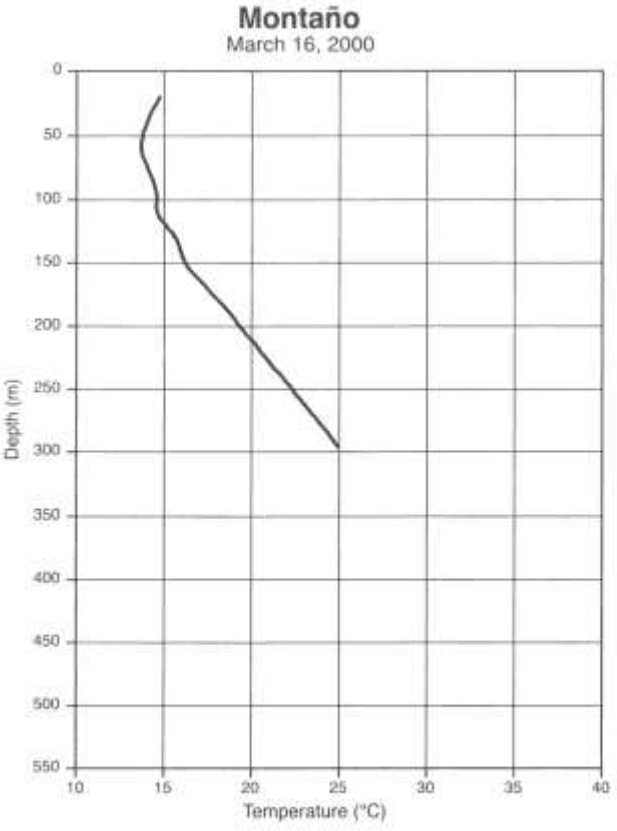

FIGURE 3–6—T log at Montaño site.

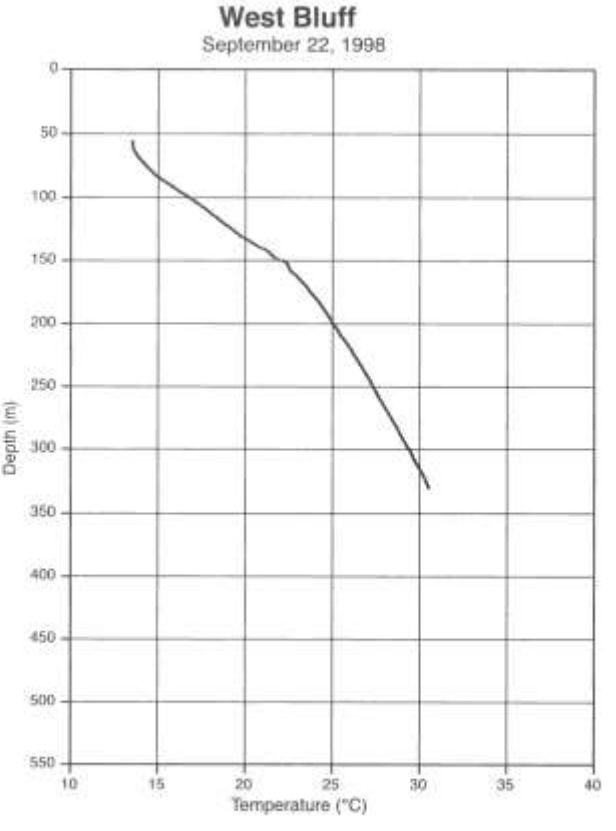

FIGURE 3–8—T log at West Bluff site. Temperature gradient increases at –140 m and –150 m may indicate warm flow along a thin zone, perhaps a fault.

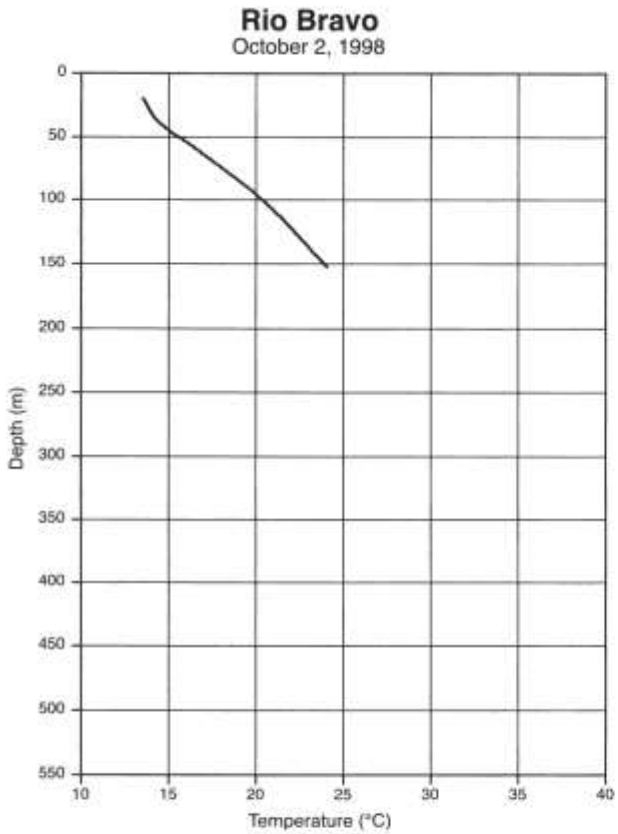

FIGURE 3–9—T log at Rio Bravo site.

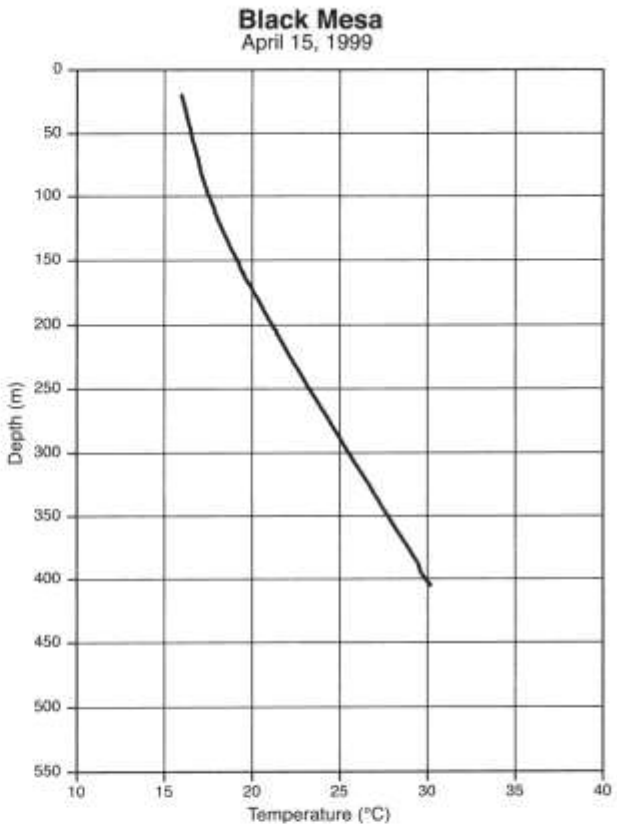

FIGURE 3–11—T log at Black Mesa site.

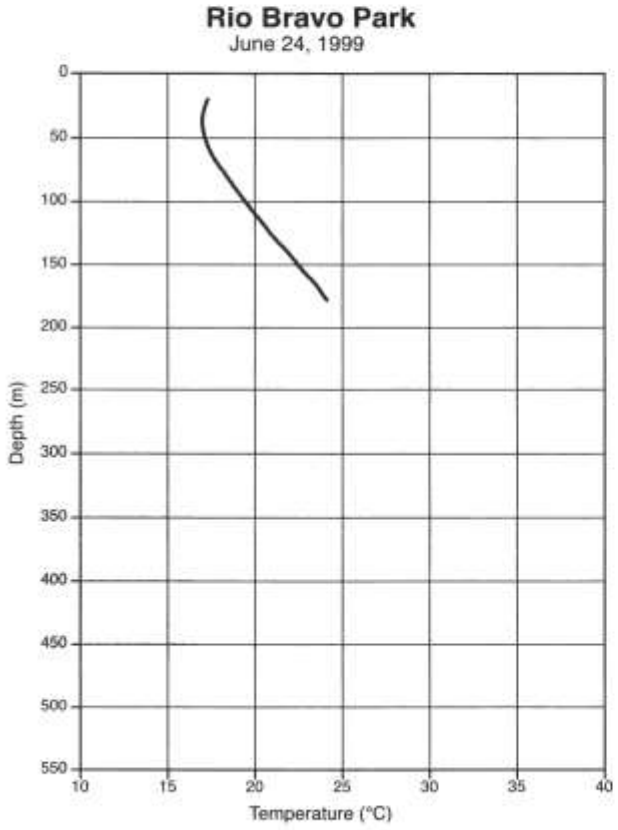

FIGURE 3–10—T log at Rio Bravo Park site, modified from Reiter (2001a).

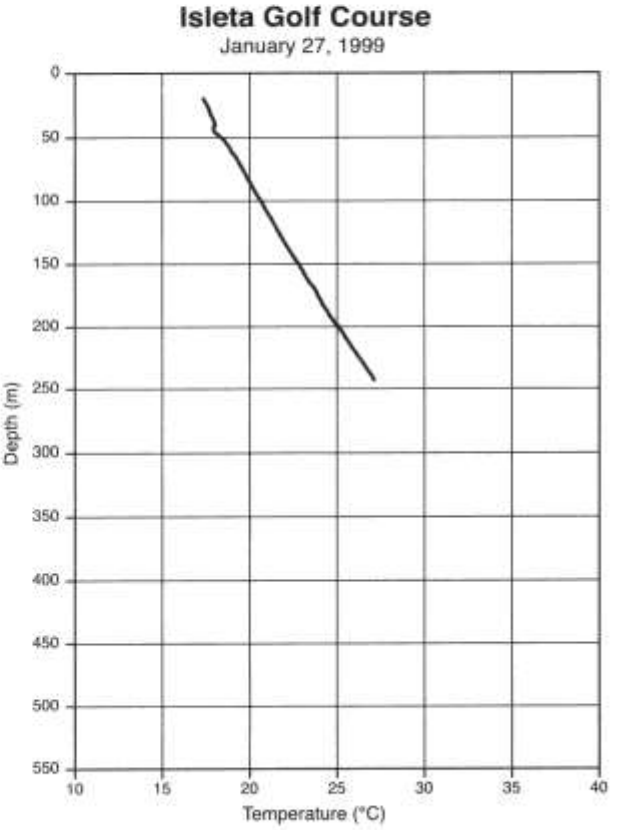

FIGURE 3–12—T log at Isleta Golf Course site.

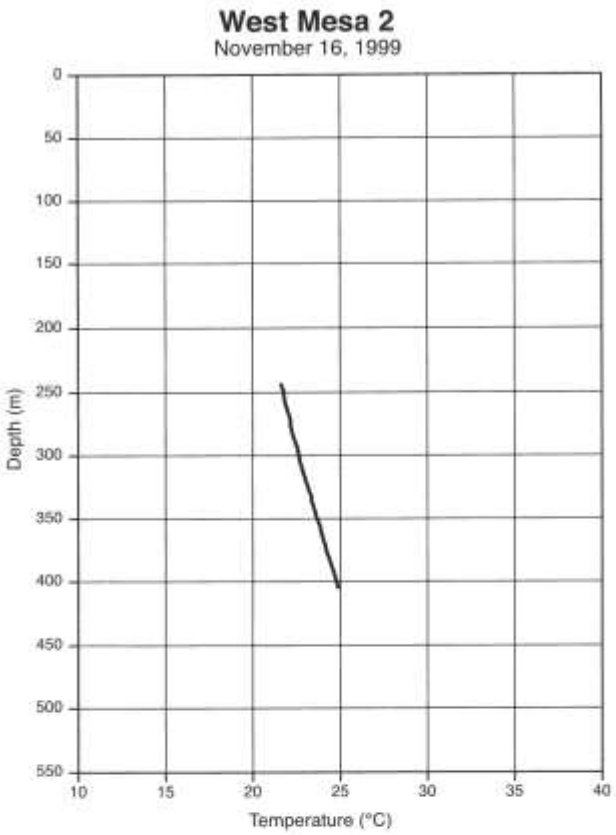

FIGURE 3–13—T log at West Mesa 2 site. Much of the erratic nature of the T log results because of the casing pinching the temperature sensor connection. See Appendix 2–13.

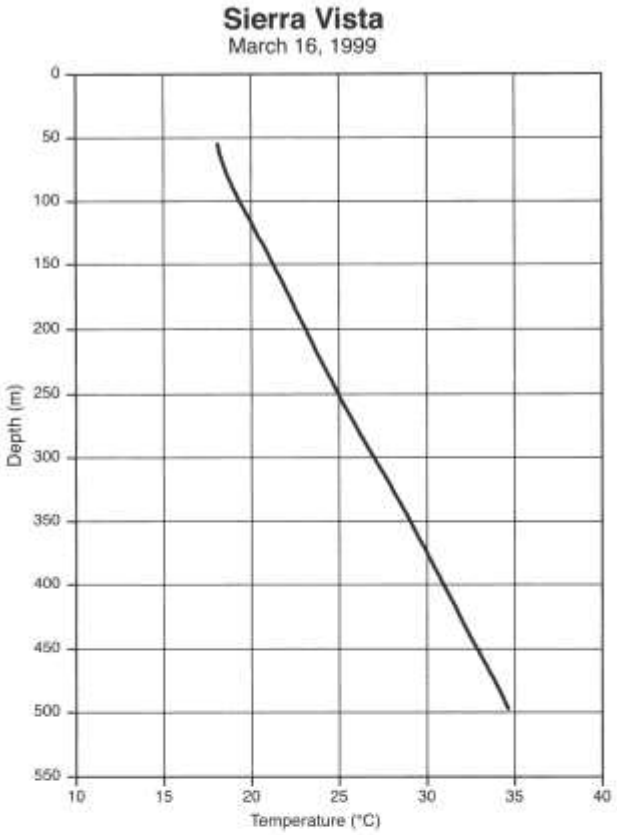

FIGURE 3–15—T log at Sierra Vista site.

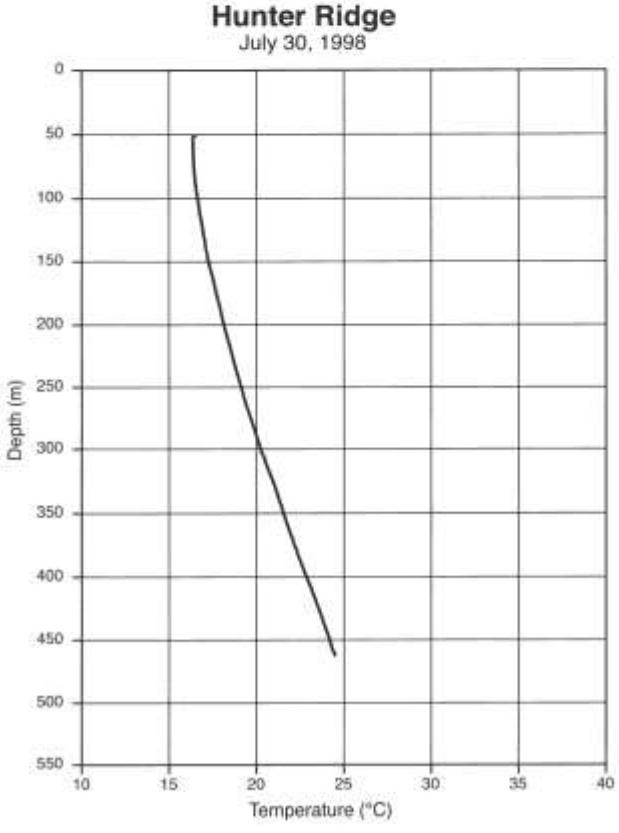

FIGURE 3–14—T log at Hunter Ridge site.

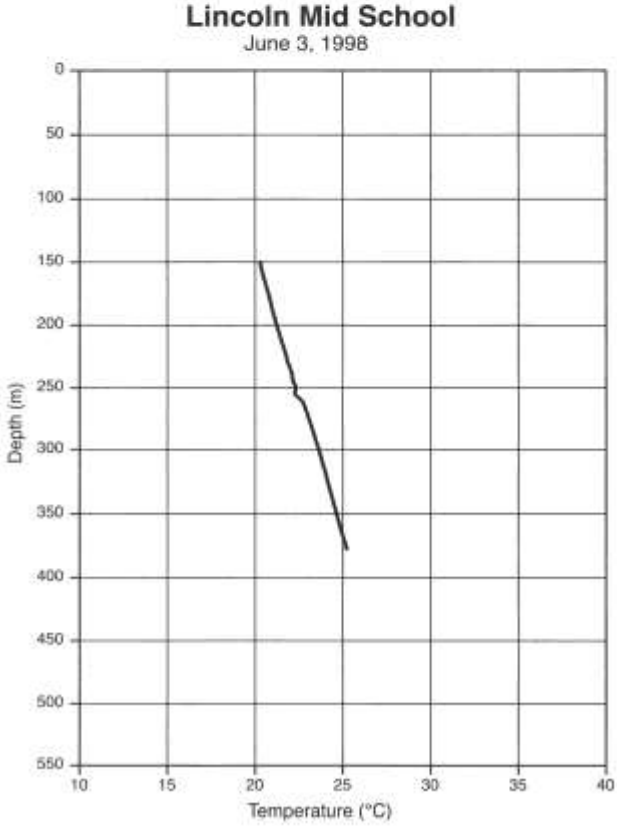

FIGURE 3–16—T log at Lincoln Middle School site. Temperature data at ~225 m probably influenced by water circulation around screen.

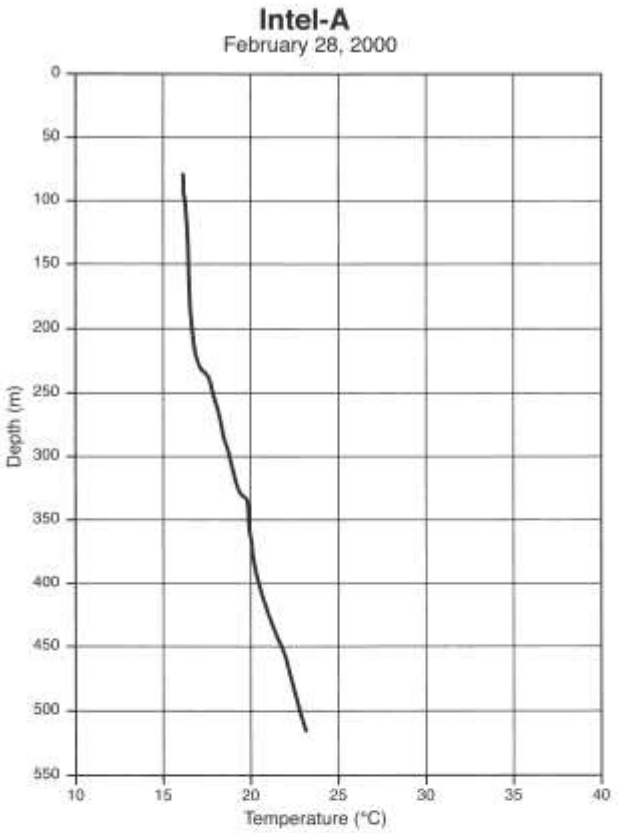

FIGURE 3–17—T log at Intel A site.

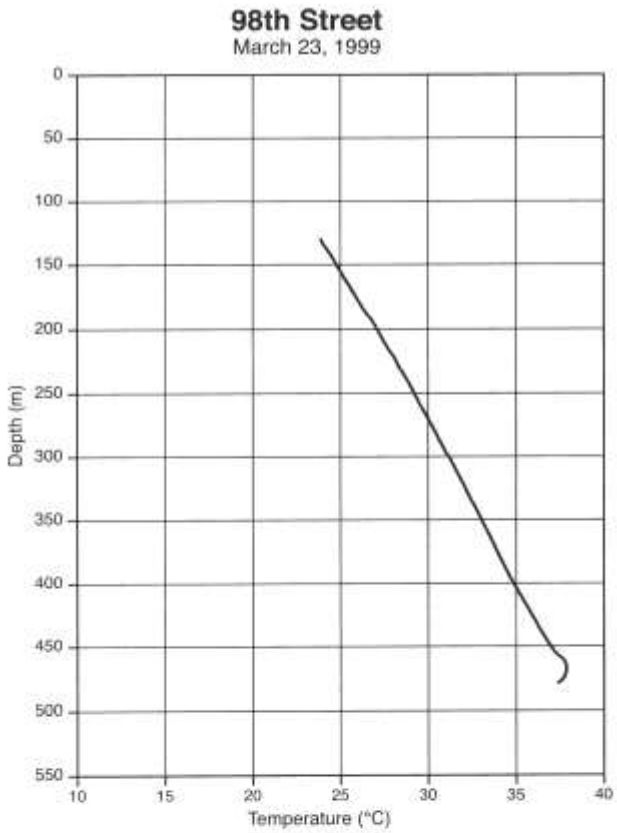

FIGURE 3–19—T log at 98th Street site. Temperature data from –460 m to approximately 475 m probably influenced by circulation around screen.

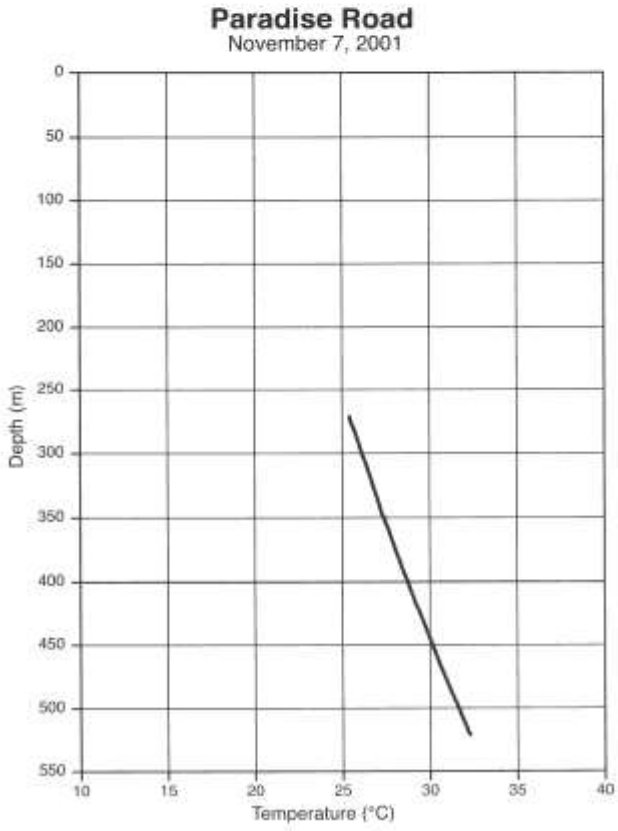

FIGURE 3–18—T log at Paradise Road site.

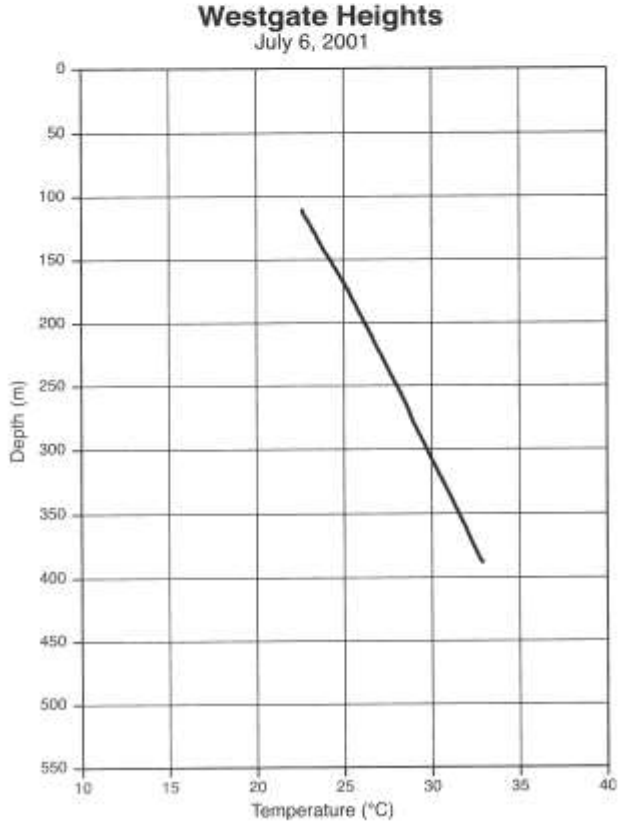

FIGURE 3–20—T log at Westgate Heights site.

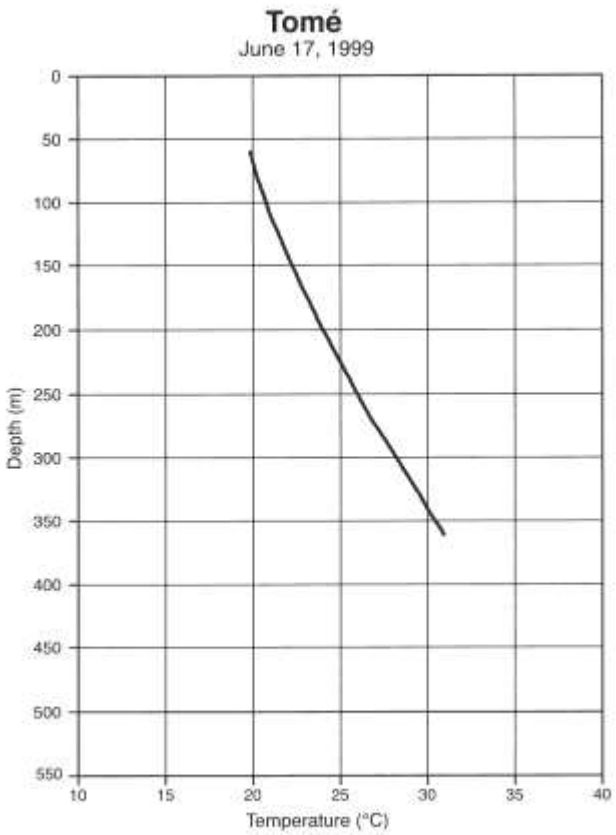

FIGURE 3–29—T log at Tomé site, modified from Reiter (2001a, 2001b).

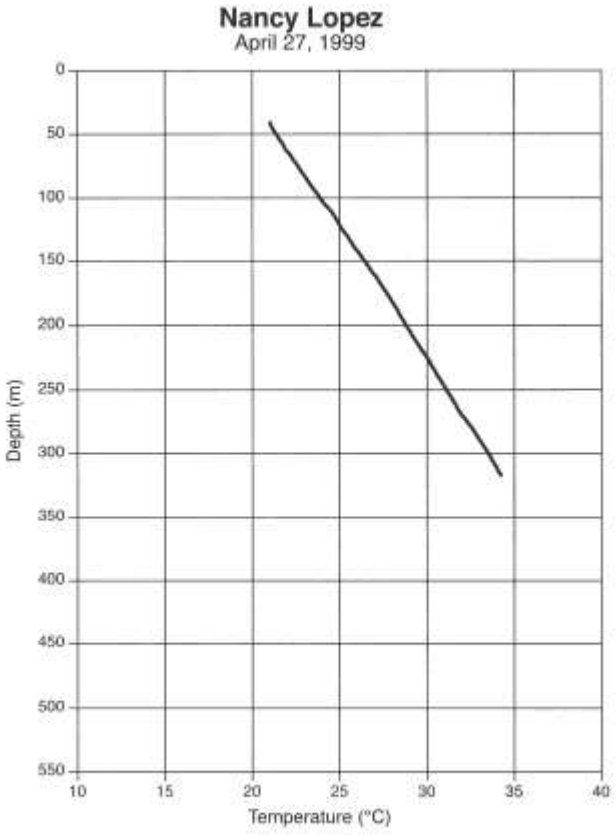

FIGURE 3–30—T log at Nancy Lopez site, modified from Reiter (2001b).

Selected conversion factors*

TO CONVERT	MULTIPLY BY	TO OBTAIN
Length		
inches, in	2.540	centimeters, cm
feet, ft	3.048×10^{-1}	meters, m
yards, yds	9.144×10^{-1}	m
statute miles, mi	1.609	kilometers, km
fathoms	1.829	m
angstroms, Å	1.0×10^{-8}	cm
Å	1.0×10^{-4}	micrometers, μm
Area		
in^2	6.452	cm^2
ft^2	9.29×10^{-2}	m^2
yds^2	8.361×10^{-1}	m^2
mi^2	2.590	km^2
acres	4.047×10^{3}	m^2
acres	4.047×10^{-1}	hectares, ha
Volume (wet and dry)		
in^3	1.639×10^{1}	cm^3
ft^3	2.832×10^{-2}	m^3
yds^3	7.646×10^{-1}	m^3
fluid ounces	2.957×10^{-2}	liters, l *or* L
quarts	9.463×10^{-1}	l
U.S. gallons, gal	3.785	l
U.S. gal	3.785×10^{-3}	m^3
acre–ft	1.234×10^{3}	m^3
barrels (oil), bbl	1.589×10^{-1}	m^3
Weight, mass		
ounces avoirdupois, avdp	2.8349×10^{1}	grams, gr
troy ounces, oz	3.1103×10^{1}	gr
pounds, lb	4.536×10^{-1}	kilograms, kg
long tons	1.016	metric tons, mt
short tons	9.078×10^{-1}	mt
oz mt^{-1}	3.43×10^{1}	parts per million, ppm
Velocity		
ft sec^{-1} (= ft/sec)	3.048×10^{-1}	m sec^{-1} (= m/sec)
mi hr^{-1}	1.6093	km hr^{-1}
mi hr^{-1}	4.470×10^{-1}	m sec^{-1}
Pressure, stress		
lb in^{-2} (=lb/in^2), psi	7.03×10^{-2}	kg cm^{-2} (kg/cm^2)
lb in^{-2}	6.804×10^{-2}	atmospheres, atm
lb in^{-2}	6.895×10^{3}	newtons (N)/m^2, N m^{-2}
atm	1.0333	kg cm^{-2}
atm	7.6×10^{2}	mm of Hg (at 0°C)
inches of Hg (at 0°C)	3.453×10^{-2}	kg cm^{-2}
bars, b	1.020	kg cm^{-2}
b	1.0×10^{6}	dynes cm^{-2}
b	9.869×10^{-1}	atm
b	1.0×10^{-1}	megapascals, MPa
Density		
lb in^{-3} (= lb/in^3)	2.768×10^{1}	gr cm^{-3} (= gr/cm^3)
Viscosity		
poises	1.0	gr cm^{-1} sec^{-1} *or* dynes cm^{-2}
Discharge		
U.S. gal min^{-1}, gpm	6.308×10^{-2}	l sec^{-1}
gpm	6.308×10^{-5}	m^3 sec^{-1}
ft^3 sec^{-1}	2.832×10^{-2}	m^3 sec^{-1}
Hydraulic conductivity		
U.S. gal day^{-1} ft^{-2}	4.720×10^{-7}	m sec^{-1}
Permeability		
darcies	9.870×10^{-13}	m^2
Transmissivity		
U.S. gal day^{-1} ft^{-1}	1.438×10^{-7}	$m^2 sec^{-1}$
U.S. gal min^{-1} ft^{-1}	2.072×10^{-5}	l sec^{-1} m^{-1}
Magnetic field intensity		
gausses	1.0×10^{5}	gammas
Energy, heat		
British thermal units BTU	2.52×10^{1}	calories, cal
BTU	1.0758×10^{2}	kilogram-meters, kgm
BTU lb^{-1}	5.56×10^{-1}	cal kg^{-1}
Temperature		
°C + 273	1.0	°K (Kelvin)
°C + 17.78	1.8	°F (Fahrenheit)
°F - 32	5/9	°C (Celsius)

**Divide by* the factor number to reverse conversions.
Exponents: for example 4.047×10^{3} (see acres) = 4,047; 9.29×10^{-2} (see ft^2) = 0.0929

Colophon

Typeface: Palatino
Presswork: Cottonwood Printing Company, Inc.
Binding: perfect bound with softbound cover
Paper: Cover on Kivar®4-12 Linenweave. Text on 70-lb white matte.
Ink: Cover—PMS 320, four color process. Text—Black.
Print run: 1000


ISBN 1-883905-14-2
90000
781883 905194